2016

Investigation Of Parameters Enabling Admicellar Reversible Addition-Fragmentation Chain Transfer (Raft) Polymerization

Poh Lee Cheah
University of Mississippi

INVESTIGATION OF PARAMETERS ENABLING ADMICELLAR REVERSIBLE ADDITION-FRAGMENTATION CHAIN TRANSFER (RAFT) POLYMERIZATION

A Dissertation
presented in partial requirements
for the degree of Doctor of Philosophy
in the Department of Chemical Engineering
The University of Mississippi

by

POH LEE CHEAH

August 2016

ABSTRACT

To date, enormous studies on admicellar polymerization have been recorded since the initial reports in the 1980's. This technique which offered the advantage of using inexpensive materials and facile procedures, proven to be a successful surface modification technique. Nevertheless, one has to tailor every particular case due to the contribution of various factors in the process. Therefore, understanding the fundamentals parameters affecting the characteristics of polymer formed by admicellar polymerization have become a great interest.

The effect of oxygen on the requisite amount of initiator and the polymer formed through the admicellar polymerization of styrene on silica particles was studied using cetyltrimethylammonium bromide (CTAB) as the adsorbed surfactant bilayer template, 2,2′-azobisisobutyronitrile (AIBN) as a water-insoluble initiator or 4, 4'-azobis (4-cyanovaleric acid) (V-501) as a water-soluble initiator. We demonstrated that deoxygenated admicellar polymerization via purging the headspace with nitrogen prior to the initiation of the admicellar polymerization of styrene on the surface of porous silica substrates produced satisfactory yield (high apparent conversion) and higher molecular weight polymer even at low initiator loading (ie. M/I 1000). Meanwhile insufficient polymer can be collected from control samples performed without deoxygenation at the same ratio. At moderate initiator loading (ie. M/I 150), we observed lower molecular weight polymer with slightly lower conversion when performed in the presence of oxygen. This can be explained by the mechanism of initiator consumption by oxygen causing the early termination and increases the rate of dead chain formation. Admicellar polymerizations

using the water-soluble initiator exhibited higher M_w polymer compared to the systems using the water-insoluble initiator due to less degree of partitioning of water-soluble initiator in the admicelle compared to water-insoluble initiator, resulting in fewer polymerization sites and higher molecular weight polymer.

Results from deoxygenated admicellar polymerization offers a potential to implement oxygen sensitive technique such as reversible addition-fragmentation chain transfer (RAFT) polymerization in admicellar polymerization in order to obtain more advanced thin films. Our initial investigation focuses on admicellar RAFT polymerization of styrene, 4-methylstyrene, and 4-methoxystyrene inside cetyltrimethylammonium bromide (CTAB) admicelles on the surface of silica particles using AIBN and 2,2'-Azobis(2-methylpropionamidine) dihydrochloride (V-50) as the free radical initiator and 4-cyano-(dodecylsulfanylthiocarbonyl)sulfanyl pentanoic acid (CDP) and 2-phenyl-2-propyl benzothioate (CDB) as the chain transfer agent. The preliminary results demonstrate the ability to reduce the molecular weight of the formed polymer films and suggest the living characteristics of RAFT polymerization inside admicelles compared to the traditional admicellar polymerization technique though there were poor control on the molecular weight distribution.

DEDICATION

This thesis is dedicated to my beloved parents and family members, as well as my friends who gave me the strength and courage during my journey to achieve this dream.

LIST OF ABBREVATIONS

(Listed in Tables)

ADEP	Acryloyloxyethyldiethyl phosphate
AIBN	2,2′-azobisisobutyronitrile
AOT	Sodium bis[2-ethylhexil]sulfosuccinate
BC	Benzalkonium chloride
BEM	2-[3-(2H-benzotriazol-2-yl)-4- hydroxyphenyl]ethyl methacrylate
CPC	Cetylpyridinium chloride
C_{12}TAB	Dodecyltrimethylammonium bromide
C_{14}TAB	Tetradecyltrimethylammonium bromide
C_{16}TAB	Cetyl trimethylammonium bromide
EDTA	Ethylenediaminetetraacetic acid
HAB	2-hydroxyl-4-acryloyloxybenzophenone
$K_2S_2O_8$	Potassium persulfate
MMA	Methylmethacrylate
MDSi	Methacryloxypropylpenta-methyldisiloxane
MG	Malachite Green
Msi	Methacryloxymethyltrimethyl-silane
$(NH_4)_2S_2O_8$	Ammonium persulfate
PFC	Perfluorinated compounds
SDBS	Sodium dodecylbenzenesulfonate
SDS	Sodium dodecylsulfate
SFS	Sodium formaldehyde sulfoxylate
SPS, $Na_2S_2O_8$	Sodium persulfate
TBH	Tertbutylperoxide

ACKNOWLEDGEMENTS

I express my deepest appreciation to both of my advisor, Dr. John O'Haver and Dr. Adam E. Smith for their patience, encouragement and guidance throughout my graduate studies. I would like to thank my committee member, Dr. Paul Scovazzo and Dr. Hunain Alkhateb for reviewing and advising my work.

Special thanks are extended to Dr. Chun Hwa See for providing me the inspiration and professional advice. I would like to also thank the faculty in Department of Chemical Engineering, our former chair Dr. Clint Williford, Dr. Peter Sukanek, Dr. Wei Yin Chen, Dr. Ajit Sadana, Dr. Sasan Nouranian, Dr. Taskin Karim and Ms. Anne Pringle for making my experience at OleMiss worthwhile.

Lastly, I would like to thank Caty Bhikha, Evalyn Holman, Julia Santos Rocha, Chuck Rainey, Jakin Bryce Delony, Sherman Jones and David Knox Langford for being great team members in Dr. O' and Dr. Smith group.

TABLE OF CONTENT

LIST OF TABLES

LIST OF FIGURES

1. BACKGROUND AND LITERATURE REVIEW

1.1 Admicellar polymerization

The first literature publication of admicellar polymerization was dated back in 1987 by J. Wu et. al. where a polystyrene ultrathin film was successfully formed on alumina.[1,2] Since the initial report, admicellar polymerization technique has proven to be an effective way to engineer the surface characteristics of solid substrates for various applications. Admicellar polymerization is called the surface analog to emulsion polymerization, but there are a few major differences.

Emulsion polymerization utilizes surfactant concentrations that are more than one order of magnitude above the critical micelle concentration (CMC).[3] The presence of micelles enable the suspension of hydrophobic monomer droplets up to 1-100 μm in a continuous aqueous medium and polymerization takes place mainly in the core of micelles. The mechanism of emulsion polymerization can be explained by progression of three stages according to Smith-Ewart theory.[4] Interval I is the formation of particles (micelle aggregates with the solubilizates) in equilibrium in the aqueous system. At Interval II, particles continue to grow as more monomer diffuses from monomer-saturated droplets and bulk solution into the micelles. Polymerization proceeds until all monomer is converted to polymer in the micelles at Interval III (Figure 1.1).

Meanwhile, admicellar polymerization systems utilize surfactant concentrations just below the CMC where surfactant aggregates on the surface close to the maximum surface coverage. Monomer adsolubilization takes place by the addition of hydrophobic monomers that preferentially partition into the admicelle. Further detailed discussions on surfactant type/ concentration, organic monomers and other parameters affecting adsolubilization can be found in

Chapter 3. Polymerization in the admicelle on the solid surface is initiated by thermal decomposition of a free radical initiator or a redox system. Following polymerization, the surfactant forming the admicelle is removed by repeated washings. Overall process of admicellar polymerization can be summarized into 4 steps: (i) surfactant adsorption, (ii) monomer adsolubilization, (iii) polymerization and, (iv) surfactant removal. (Figure 1.2).

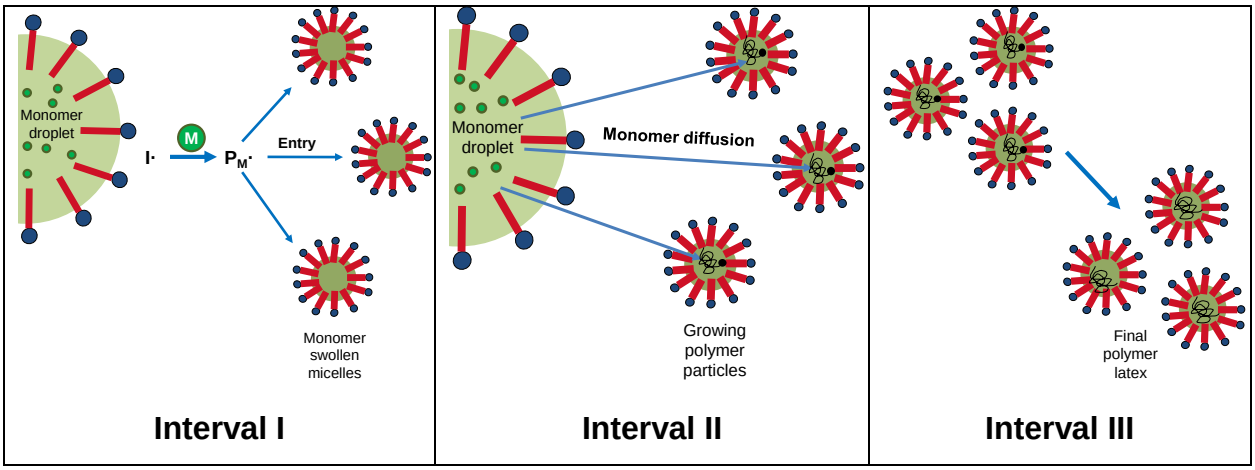

Figure 1.1 Mechanism of emulsion polymerization.

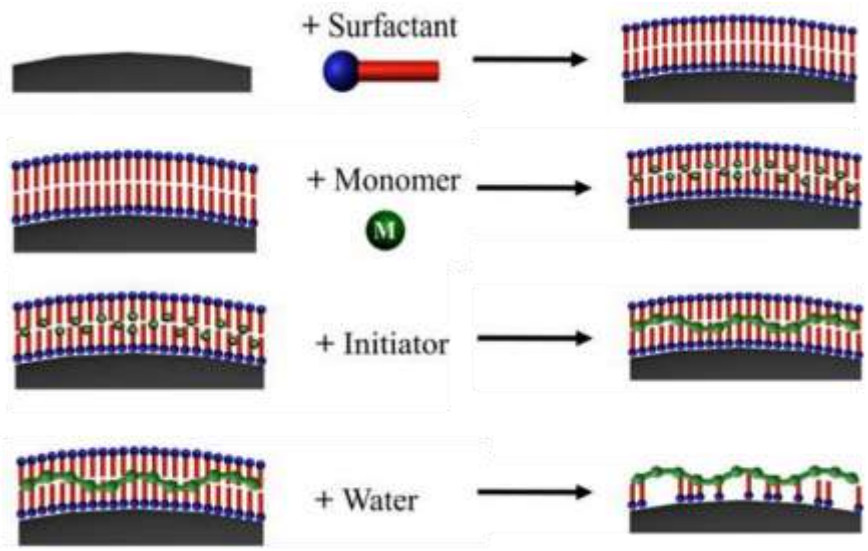

Figure 1.2 Admicellar polymerization 4 steps process.

Example of admicellar polymerization studies demonstrated that low M/I values (below 15) were needed in order to achieve effective conversion of monomer to polymer. A few examples are listed in Table 1.1.

Table 1.1 Parameters in admicellar polymerization

Substrate	Surfactant (S)	Monomer (M)	Initiator (I)	M/I mol ratio	Ref
Silica	C_{12}TAB, C_{14}TAB, C_{16}TAB	Isoprene	$K_2S_2O_8$	10:1, 5:1 to 1:1	Yooprasert et. al.[5] Pongprayoon et. al.[6]
Silica	C_{16}TAB, octylphenoxypoly-(ethoxy) ethanol, methyltri(C_8-C_{10}) ammonium chloride	Styrene (S/M ≈ 2)	(Thermal) AIBN, (REDOX) TBH, EDTA	(Thermal) <6 (REDOX) 100-300	O'Haver et. al.[7]
Aluminium plate	SDS	Styrene, MMA	AIBN	20:1, 10:1, 5:1, 2:1	Matarredona et. al.[8]
Boron nitride	CPC	Styrene, MMA	$K_2S_2O_8$	10:1	Wattanakul et. al.[9]
Polyester/ cotton fabric	SDBS (anionic), Corning®949 (cationic), Sylgard®309 (non-ionic)	MMA, ADEP, Msi, MDSi, HAB, BEM, Styrene	AIBN, $(NH_4)_2S_2O_8$, SPS	10:1, 5:1, 2:1, 1:1	Siriviriyanun et. al.[10,11] Tragoonwichian et. al.[12–14] Pongprayoon et. al.[15]
Glass Fibers	C_{12}TAB, CPC	Styrene	SPS	0.3:1	Sakhalkar et. al.[16]

1.1.1 Various application of admicellar polymerization

Admicellar polymerization has been utilized in different area of applications such as rubber reinforcement,[6,17,18] corrosion control,[8,19] formation of conducting films,[20–23] surface modification of cotton fibers,[12,14,24–28] and composite fillers.[29,30]

1.1.1.1 Admicellar polymerization on fillers for rubber reinforcement:

T. Pongprayoon et. al.[6] compared different methods of admicellar polymerization to modify silica surface for the rubber reinforcement application, thermal or radiation-induced admicellar polymerization. Cationic surfactant C_{12}-, C_{14}-, C_{16}- trimethyl ammonium bromide (DTAB, TTAB, C_{16}TAB) were used to obtain admicelle layer and isoprene was used as the monomer. It was reported that 40phr (phr = parts per hundred rubber) of silica was the optimum ratio for the reinforcement of a model rubber compound. Rubber compound with modified silica showed improved mechanical properties. Among the systems tested, modification of silica with C_{16}TAB via radiation-induced admicellar polymerization had the best performance, which is consistent with previous work done by N. Yooprasert et.al. in 2010.[5] C_{16}TAB has the longest hydrophobic chain length with closer packing and adsolubilized the highest amount of monomer and hence had the best film formation. Scanning electron microscopy (SEM) images further confirmed the better dispersion in rubber compound with modified silica.

In 2005, P.Nontasorn et. al. successfully performed admicellar polymerization in a continuous stirred tank reactor to produce modified silicas.[17] Reinforcement into rubber proved to improve the physical properties and rubber testing results were consistent with those obtained from batch systems.

V. Thammathadanukul et. al. compared properties of rubber after reinforcement of two different surface-modified silicas, one silane-coupled and the other modified by admicellar polymerization.[18] Cetyltrimethyl ammonium bromide (C_{16}TAB) was used to form the admicelle, styrene–isoprene or styrene-butadiene were used as co-monomers for thin film formation. Overall, rubber properties were improved after reinforcement of modified silicas with both techniques especially for admicellar polymerized silicas which provided a better flex-cracking resistance.

They observed that the higher the surface area of admicellar polymerized silicas, the better the rubber physical properties.

1.1.1.2 Admicellar polymerization for corrosion control:

Matarredona et.al. were able to form polystyrene (PS) and polymethyl methacrylate (PMMA) films on the aluminum plate via admicellar polymerization using SDS surfactant and AIBN initiator.[8] The thickness of films formed were above 100 nm. Modified aluminum showed improved hydrophobicity with higher advancing contact angle compare to the bare aluminum before modification. PS reported to be a better water barrier which delayed the water penetration up to 4 hours. However PMMA acted as a good chemical barrier against chloride attack via hydrogen bonding of COO^- with water molecules and showed a better corrosion inhibition compared to PS. D.V. Le et. al. later performed admicellar polymerization of poly(2,2,2-trifluoroethyl acrylate) (PTFEA) and polymethyl methacrylate (PMMA) thin film on aluminum and found that PTFEA showed higher hydrophobicity and better corrosion control over PMMA.[19] PTFEA film formed was ranged from 10-50 nm and delayed water uptake up to 6 hours. The results showed that PTFEA-modified sample has higher hydrophobicity and higher corrosion control than PMMA-modified samples.

1.1.1.3 Formation of conducting film:

Salgaonkar group successfully make a polyaniline film-coated zirconia via admicellar polymerization with either anionic (SDS, pH 2, 0.15 M NaCl)[20] or cationic (ie. C_{16}TAB, pH 9, 0.05 M NaCl)[21] surfactant to effectively form the admicelle at the optimized pH and NaCl concentration. Polyaniline-coated zirconia showed to improve the conductivity by 3-order of magnitude compared to the bare zirconia. Pojanavaraphan et. al. were able to performed electrolytic admicellar polymerization of pyrrole onto natural rubber particle.[22,23] Electrical

conductivity of the natural rubber improved by 8 or 9 orders of magnitude after electropolymerized with pyrrole. Addition of layered-silicates clay further enhanced the electrical conductivity of polypyrrole modified-natural rubber when polypyrrole concentration is low. However, modification of nanocomposite with high concentration of pyrrole and layered-silicates does not necessary enhanced electrical conductivity due to the confinement of the conducting polypyrrole chains within the layered silicates which can delocalized the charge carriers.

1.1.1.4 Admicellar polymerization on cotton fibers:

X. Ren et. al. used admicellar polymerization to obtain antimicrobial N-halamines polymer coatings on cotton fibers.[24] FTIR and SEM proved the presence of N-halamines polymer coatings on the fabrics. The polymer-coated cotton after chlorination showed high efficiency in inactivating Staphylococus aureus and Escherichia coli. They also proved that the polymer coating was stable and chlorine can be rechargeable after 50 machine washing cycles.

A. Siriviriyanun et. al. utilized admicellar polymerization to make a flame retardant cotton fabric coated with phosphorus-containing thin film poly(acryloyloxyethyldiethyl phosphate) (PADEP).[25] Cationic surfactant hexadecyl/dodecyltrimethylammonium bromide (C_{16}TAB or C_{12}TAB) were used for admicelle layer. C_{16}TAB has larger hydrophobic core hence more ADEP adsolubilized and showed higher phosphorous content. FTIR further confirmed the formation of thin film PAEDP. They observed the higher the ADEP concentration, the lower the degradation temperature and the higher the char formation. All PADEP-coated cotton fabrics have less intense burning compared to untreated cotton. In addition, PADEP-coated cotton treated with C_{16}TAB has a self-extinguishing feature due to higher phosphorous coating.

J. Maity et. al. admicellar polymerized fluoropolymer thin layers on cotton fabric and compared with direct fluorination method.[26] Both methods successfully showed cotton surface

with great hydrophobicity after modification. They discussed that the advantages of direct fluorination is the reaction via covalent bonds without using initiator or catalyst. However, the method required control of exothermic reaction when using fluorine gas and the cellulose is susceptible to degradation. On the other hand, admicellar polymerization is performed in the aqueous system and may be more compatible with the existing textile processing methods.

S. Tragoonwichian et. al. produced cotton fabric with water repellent properties by admicellar polymerization silicon compounds as the hydrophobic surface.[12] Point of zero charge was reported to affect surfactant adsorption while structure of silicon-based monomer had affected monomer adsolubilization. Hydrophobic coatings were proven by analysis from wetting time, Scanning Electron Microscopy (SEM), Fourier Transform Infrared Spectroscopy (FTIR), Energy Dispersive Spectroscopy (EDS), X-ray Photoelectron Spectroscopy (XPS) and contact angle. Cotton fabric with better water repellency was produced by using cationic surfactant and less bulky silicon compound to form a thick and uniform hydrophobic film. In 2008, they worked on polymerizing UV-absorbing agent 2-hydroxy-4-acryloxybenzophenone (HAB) on cotton fabric.[14] They observed closer packing of adsorbed surfactant sodium dodecylbenzene sulfate (DBSA) in the presence of NaCl electrolytes. Increase in temperature increased adsorption rate but slightly decreased adsorption amount of surfactant. In the monomer adsolubilization study, adsolubilized HAB constrained and hence reduced surfactant adsorption. It was reported that mole ratio of HAB to DSAB was about 1:2. FTIR and SEM images showed the presence of poly(HAB) and the fabric exhibited great UV protection properties with stability up to 24 hours. In his paper published in 2009, a bifunctional cotton fabric with both great UV-protective and water repellency was made.[27] HAB-treated fabric was made initually and silicon-compound methacryloxymethyltrimethylsilane

(MSi) was polymerized later using admicellar polymerization. Both process used DBSA as surfactant admicelle layer.

More examples of admicellar polymerization on textiles can be found in a recent review by Ulman and Shukla.[28]

1.1.1.5 Surface modification of other composite fillers

S. Das et. al. surface modified graphene with nylon 6-10 and nylon 6-6 polymer films and proved that the modification prevented aggregation and showed better dispersibility in a bulk nylon matrix.[29] Sodium dodecylbenzene sulfate (SDBS) was used to generate admicelle template and organic solvent carbon tetrachloride (CCl_4) was used to swell the admicelle surfactant to provide a better environment at the interface for polymerization. They showed nylon film can be non-covalently bonded onto a graphene surface and remained stable in low pH (1.7-2.5) conditions or after being freeze dried.

Y. Zhao et. al. successfully formed polymethyl methacrylate (PMMA) nanofilm on rice straw fiber (RSF) surface.[30] PMMA-modified rice straw showed good miscibility with polylactic acid (PLA). Modified RSF can be stably dispersed in PLA with less agglomeration. As the result, reinforcement of modified RSF into PLA composite showed improved tensile strength, increased elongation and increased thermal stability.

1.2 RAFT polymerization

Controlled/living radical polymerization (CLRP) establish the 'pseudo living' feature that minimize premature termination of chain propagation by reversible-deactivation of the primary radical, giving each chain to have the same chance to propagate throughout the polymerization process. As a result, a predetermined molecular weight polymer with low polydispersity (PDI)

close to 1 can be made. CLRP can be used to synthesize block copolymer customizing polymerization sequence with desired monomers in sequence. This is a breakthrough success which is not possible to achieve by the conventional free-radical polymerization. Three commonly utilized CRP techniques are atom transfer radical polymerization (ATRP), nitroxide-mediated polymerization (NMP), and reversible addition-fragmentation chain transfer (RAFT). Among them, RAFT polymerization was introduced more recent in the late-90s by Commonwealth Scientific and Industrial Research Organization (CSIRO) group[31,32] and a French group as Macromolecular Design via the interchange of Xanthates (MADIX).[33] Since then, RAFT polymerization has become a great focus due to its versatility and ability to control the molecular architecture with a wide variety of functional monomers. The mechanism of RAFT polymerization is illustrated in Scheme 1.1.

Scheme 1.1 RAFT mechanism

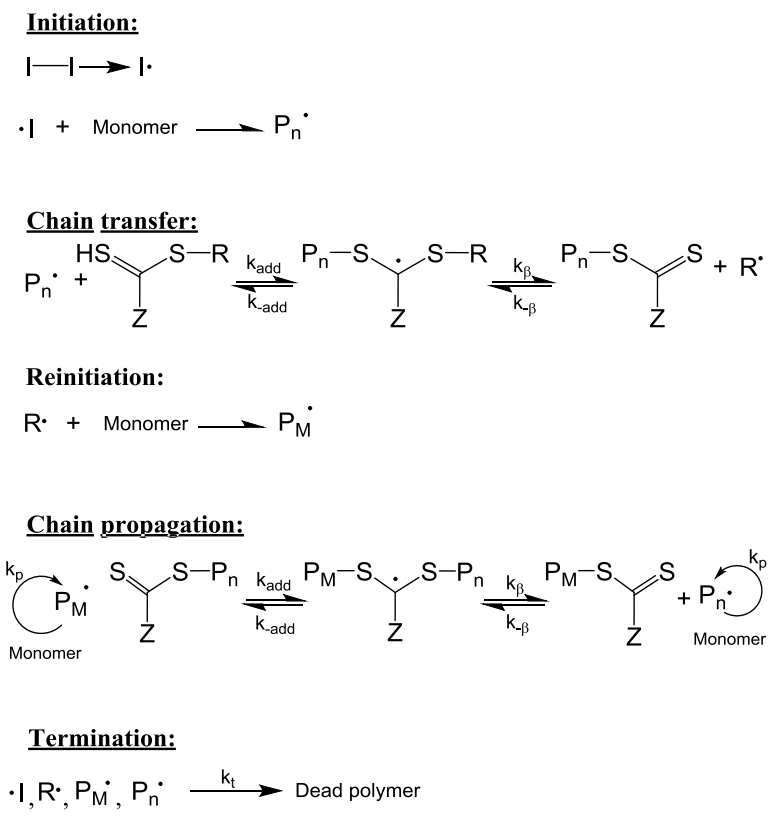

RAFT process is initiated by conventional free radical initiators to obtain the primary radical (I·) which reacts with the monomer to give a propagating oligomeric chain (P_n·). A chain transfer agent (CTA) reacts with P_n· to yield the intermediate radical. Typical CTAs consist of RSC(=S)Z in which Z group activates P_n· radical addition and avoid fast growing propagation. On the other hand, the R-group has to effectively fragment from the intermediate radical to reinitiate the polymerization process.

For RAFT in bulk/solution polymerization, theoretical $M_{n,th}$ and PDI can be estimated with the following equation.[34]

$$x_n = \frac{\gamma_o x}{1-(1-\alpha)(1-x)^{\beta}} \quad or \quad M_n = \frac{\gamma_o x}{1-(1-\alpha)(1-x)^{\beta}} M_o \qquad \text{(Equation 1.1)}$$

$$PDI = \frac{1}{\gamma_o} + \frac{1}{x}\left[2 + \frac{\beta-1}{\alpha-\beta}(2-x)\right] - \frac{2\alpha(1-\alpha)}{\beta-\alpha}\left[(1-(1-x)^{1+\frac{\beta}{\alpha}}\right] \qquad \text{(Equation 1.2)}$$

where M_o is the monomer molar mass, $\gamma_o=[M]_o/[CTA]_o$, x is fractional conversion, $\alpha =[P\cdot]/[CTA]$ (with P·, the concentration of propagating radicals) and $\beta =C_{tr,RAFT}$.

1.2.1 Chain transfer constant

The reactivity of chain transfer process is controlled by the chain transfer constant (C_{tr}), defined as the rate constant for chain transfer to propagation ($C_{tr} = k_{tr}/k_p$). As for reversible chain transfer process in RAFT mechanism, k_{tr} is expressed as a function of rate constant for the reversible addition (k_{add} and k_{-add}) and fragmentation (k_β) (Equation 1.3).[35]

$$k_{tr} = k_{add}\frac{k_\beta}{k_{-add}+k_\beta} \qquad \text{(Equation 1.3)}$$

Chiefari et. al. studied the effect of activating Z group of benzyl thiocarbonyl compounds Z-C(=S)SCH_2Ph in styrene polymerization by measuring the different chain transfer constant (C_{tr})

(Table 1.2).[36] Note that dithiocarbamates (Z = $N(alkyl)_2$) and xanthate (Z = O-alkyl) derivatives have relatively low reactivity resulting in broad PDI (>1.5) polymer. This is due to the ability of the O or N lone pairs to delocalize within the C=S double bond and reduces its reactivity. In other word, substituents with electron withdrawing will in turn enhance the activity and effectiveness of the CTA.[37] While R group has less effect in determining reactivity of radical addition to thiocarbonyl compunds, it has to be a good free radical leaving group (fragmentation from the intermediate radical) in order to be an effective CTA. Besides that, ·R radical has to be able to reinitiating the polymerization. Chong et. al. reported the effect of R group of dithiobenzoate in methyl methacrylate (MMA) polymerization (Table 1.3).[38] It showed that when the more steric the R group is, the better the leaving group. For instance, the stability of ·R radical is tertiary > secondary > primary. Oligomeric and polymeric R group is also a good leaving group. In the same study, all the dithiobenzoates tested in styrene polymerization gives very high C_{tr} (50-2000) with narrowed PDI and good molecular weight control. However, a highly significant retardation effect was observed when very high concentration of cumyl dithiobenzoates, R = $C(CH_3)_2Ph$ is used.[38,39]

Table 1.2 Apparent chain transfer (C_{tr}) for benzyl thiocarbonyl compounds Z-$C(=S)SCH_2Ph$ in styrene polymerization[36]

CTA	**C_{tr}**
Z = Ph	26
Z = SCH_2Ph	18
Z = CH_3	10
Z = pyrrole	9
Z = OC_6F_5	2.3
Z = lactam	1.6
Z = OPh	0.72
Z = NEt_2	0.01

Table 1.3 Apparent chain transfer (C_{tr}) for dithiobenzoate compounds PhC(=S)S-R in MMA polymerization[38]

CTA	C_{tr}
R = $C(CH_3)_2CN$	13
R = $C(CH_3)_2Ph$	10
R = $C(CH_3)_2CO_2Et$	1.7
R = $C(CH_3)_2CH_2C(CH_3)_3$	0.4
R = $CH(CH_3)Ph$	0.15
R = $C(CH_3)_3$	0.03
R = CH_2Ph	0.03

1.2.2 RAFT polymerization in dispersed system

Unlike bulk/solution polymerization, CRP in dispersed system depends on the compartmentalization featuring (i) segregation effect and (ii) confined space effect (Figure 1.2).[40] Segregation takes place when two species are distributed in different particles, unable to react with each other and slowing down the termination process. Meanwhile confined space features two species in the same particles have a higher probability to react with each other and increase the probability of deactivation process. Segregation effects takes place especially when the particles are small while confined space effect may not apply for RAFT in dispersed system due to the high concentration of the CTA. Based on the dominance of segregation effect, high rates and low termination can be achieved with emulsion and miniemulsion RAFT polymmerization.[41,42]

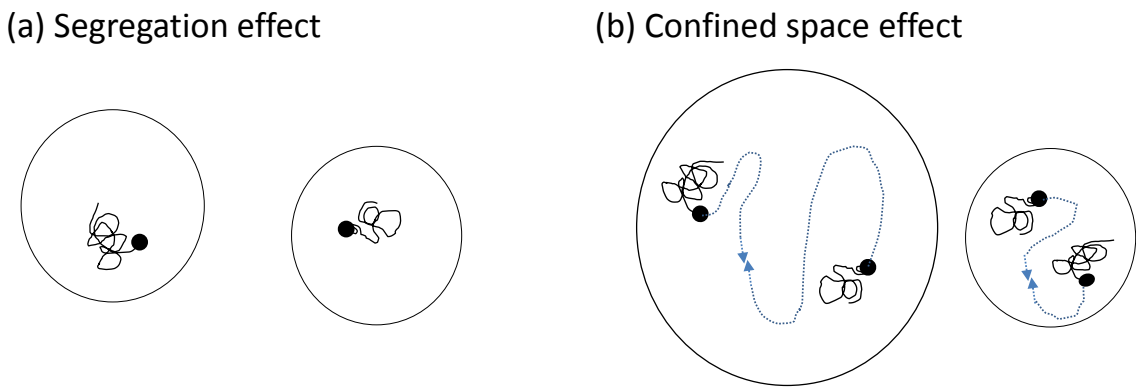

Figure 1.2 Compartmentalization of CRP in a dispersed system a) segregation effect and b) confined space effect.[40]

CRP in dispersed system is susceptible to colloidal stability problems concerning coalescence, Ostwald ripening or superswelling of RAFT oligomer.[43] Coalescence and Ostwald ripening cause the bigger particles/droplets to get bigger in size while smaller particles/droplets decrease in size. This resulted in a bimodal particles/droplets size distribution. Due to the "reversible-deactivation" mechanism of CRP, all chains are initiated and grow simultaneously but at lower rate. Consequently, high concentration of low molecular weight oligomers are present at low conversion, causing "superswelling" and phase separate eventually.[44] Besides that, slow mechanism of CRP causes low molecular weight oligomers to easily exit and swells. Luo and Cui theoretical simulated and experimental studied that colloidal instability caused poor control of the molecular weight and PDI.[45] Ab-initio emulsion RAFT polymerization of MMA were performed with 2-cyanoprop-2-yl dithiobenzoate (R = $C(CH_3)_2CN$, Z = Ph) as the CTA, KPS as the initiator and SDS as the surfactant. Colloidal stability can be enhanced with higher initiator and surfactant concentration and low CTA concentration (increasing theoretical $M_{n,th}$). However, broad PDI is observed when low CTA concentration is used to obtain high $M_{n,th}$.

CTA partitioning and diffusions in a dispersed RAFT polymerization becomes a major factor to determine the successfulness of the process. Due to the heterogeneous nature in a dispersed system, slow transport of CTA from droplets to particles in a RAFT emulsion polymerization will result in poor RAFT control. CTA with high water-solubility tends to partition in the aqueous phase causing retardation and poor RAFT control.[46–48] Meanwhile, CTA with high water-insolubility partitioned more in the monomer droplets rather than in the particles may resulted in bulk polymerization and flocculation of unreacted CTA with monomer could be observed.[46–51] 2-(ethoxycarbonyl) propyl-2yl dithiobenzoate (R= $C(CH_3)_2CO_2Et$, Z= Ph) CTA is reported to have a higher rate of retardation compared to cumyl dithiobenzoate (R = $C(CH_3)_2Ph$, Z =Ph) CTA in ab-initio/ seeded emulsion polymerization of styrene.[47,48] The study explained that the fragmentation of radical R= $C(CH_3)_2CO_2Et$ has a higher exit rate from the particles into the aqueous phase due to higher hydrophilicity. The exited radical may undergo cross-termination in the aqueous phase when the initiator concentration in the aqueous phase is high or reenter to the particle when the initiator concentration is low. Due to the different rates and fates of the exited radical, the ratio of CTA to initiator greatly influence the RAFT control. In the case for hydrophobic CTA, the lower the hydrophobicity, the higher the diffusion rate of the CTA from the aqueous phase into the polymer particles and the better the RAFT control in the order of: benzyl dithioacetate > benzyl dithiobenzoate > phenyl ethyl dithiobenzoate > cumyl dithiobenzoate.[50,51] However, the polymerization rate decreases with the increasing of RAFT control.[51] Hydrophobic CTA diffused better from more hydrophobic monomer phase (ie. styrene) into the polymer particles compared to a higher water solubility monomer (ie. methyl methacrylate).[50] When highly hydrophobic CTA is used (ie. cumyl dithiobenzoate), rate of polymerization increase with increasing initiator water solubility resulting in bad RAFT control. They explained that the PDI

obtained in their study of ab initio emulsion RAFT polymerization of styrene with SDS at 80°C are broad (>1.5), some were higher than bulk or solution RAFT polymerization was due to the polymerization at different reaction loci (continuous phase, particle, and interface) in a heterophase polymerization.[51]

Example of RAFT emulsion polymerization of styrene with different dithiobenzoates derivatives CTA was studied by Moad et. al. (Table 1.4).[39] All the polymerization observed high conversion and high polymerization rates except for cumyl dithiobenzoate (R = $C(CH_3)_2Ph$, Z = Ph) which showed a strong retardation effect at the early stage of polymerization. In addition, this compound did not uniformly dispersed in the system. As a result, the polymer formed has very broad PDI. While benzyl dithiobenzoate (R = CH_2Ph, Z = Ph) and benzyl dithioacetate (R = CH_2Ph, Z = CH_3) showed both good control of molecular weight and narrow PDI (< 1.4) and xanthates derivatives (R = CH_2Ph, Z = OC_2H_5 and R = $CH(CH_3)Ph$, Z = OEt) have relatively broad PDI (~ 2.0). This is because xanthates compounds have relatively low chain transfer constant in agreement with the findings in bulk polymerization.[36]

Table 1.4 Molecular weight, PDI and conversion results from emulsion RAFT polymerization of styrene at 80°C using different CTA, ZC(=S)S-R [39]

CTA	M_n (g/mol)	PDI	Conversion (%)
R = $C(CH_3)_2Ph$, Z = Ph	4.0 x 10^4	7.09	96
R = CH_2Ph, Z = Ph	5.3 x 10^4	1.37	>99
R = CH_2Ph, Z = CH_3	3.6 x 10^4	1.38	>99
R = CH_2Ph, Z = OC_2H_5	3.2 x 10^4	1.98	>99
R = $CH(CH_3)Ph$, Z = OEt	3.1 x 10^4	2.04	>99
-	1.3 x 10^5	2.71	>99

CHAPTER 2: OVERVIEW

The overall aim of this dissertation is to introduce reversible addition-fragmentation chain transfer (RAFT) polymerization technique in admicellar polymerization on silica particles.

Chapter 3 is a review on the works on adsolubilization over the years. This review elaborates the different components (substrate, surfactant, monomer, other solute) and parameters which impact the adsolubilization process. This review also summarizes the important observations and findings from previous studies and greatly enhanced the understandings the process.

Chapter 4 presents the study of initiator efficiency of free-radical admicellar polymerization of styrene on silica surfaces in the presence of oxygen versus oxygen-depleted environment. Experiment studies at different molar ratio of monomer: initiator (ie. 1000, 150, 15) was reported. Studies using different solubility nature of the initiator (water-soluble or water-insoluble) is compared. The effect of different monomer: initiator ratios to polymerization kinetics will also be examined.

Chapter 5 utilizes the reversible addition-fragmentation chain transfer (RAFT) polymerization, a form of controlled radical polymerization (CRP), in admicellar polymerization of silica. Two different chain transfer agent (CTA), two different radical initiator and different monomers (styrene, 4-methylstyrene and 4-methoxystyrene) were studied. The polymer formed via admicellar RAFT- polymerization was compared with those formed via conventional free-radical admicellar polymerization (deoxygenated). The results at different monomer/CTA value (ie. 1000, 150, 50) are presented and discussed.

Chapter 6 provides bibliography of this dissertation. Chapter 7, “Appendix”, presented with some supporting information/ work of this work.

CHAPTER 3: REVIEW ON ADSOLUBILIZATION

3.1 Introduction

Surfactant adsorption from a bulk phase onto a surface layer has been recognized for over 60 years.[52] The capability of micelle-like aggregates adsorbed on the solid/liquid interface to solubilize organic solutes is the surface analog of solubilization, termed 'adsolubilization'. Adsolubilization consists of the interaction of a solute with the admicelle (adsorbed surface micelles) enabling the partitioning of hydrophobic solutes at the interface which is not feasible in the absence of admicelles. The interactions between the four main components consists of the surface, surfactants, solutions and the solute compound are essential in an adsolubilization process.

Surfactant adsorption at solid-water interfaces has been widely studied in the literature over the years. In explaining the interactions between surfactant and solids, Somasundaran and Fuerstenau proposed a reverse orientation model which takes place after hemimicelle formation (4 distinct regions in the isotherm of ionic surfactants adsorption on hydrophilic surface)[53] while Harwell et. al. proposed an admicelle-bilayer model.[54] In our review, only those surfactant adsorption studies that were related to the adsolubilization process are addressed.

Mineral oxides are most widely used in adsolubilization studies due to their abundant industrial applications, the variety of their surface characteristics, and low cost. The amphiphilic behavior of admicelles interacting with organic solutes is typically studied via adsolubilization isotherms. The effect of changes in solute concentration, polarity and structure on the adsolubilization isotherms is examined. Additionally, we will examine the reported impact of cosurfactants and solution properties (such as pH, ionic strength and temperature) on

adsolubilization. We have reviewed the utilization of adsolubilization in various applications, including admicellar chromatography, admicellar catalysis, pharmaceuticals, wastewater treatment, surface modification etc. Finally, we examine the various analytical methods used to study adsolubilization.

3.2 Surfactant type, amount and structure

Partial or complete surfactant monolayer or bilayer coverage resulted in different solute-surfactant interactions, especially for ionic surfactants. Monolayer surfactant coverage usually has the tail out orientation and therefore hydrophobic interactions with organic solute species. Meanwhile, bilayer coverage with the head-out results in repulsion between ionized solute.[55] Nevertheless, surfactant bilayers are usually desired due to the higher capacity of admicelle volume to adsolubilize more solute. In addition, one may need to consider the hydrophobic coagulation and redispersion of particles due to the different orientation of adsorbed surfactant at the interface as reviewed by Esumi and Meguro.[56] In the study by Esumi et. al.,[57] the group reported SDS monolayers on alumina (10 mM NaCl, pH 3.5) has a higher 2-napthol adsolubilization efficiency than the SDS bilayers. The authors explained that the tail-out orientation of SDS monolayer on the alumina caused the flocculation of particles and enable the organic solutes to penetrate and adsolubilize via strong hydrophobic interaction. Further increases of surfactant concentration forms micelles and decreases solute adsolubilization due to solute partitioning in both micelles and admicelles.[58–66] However, a few studies found that no solute desorption occurred at surfactant concentrations above the CMC. Andrzejewska explained that the interaction between π-electron clouds of propyl gallate with cationic head groups of C_{16}TAB micelles is weaker than the hydrophobic interaction of solute with C_{16}TAB tail.[67] The same result

was observed for hydroxyethylcellulose (HEC) adsolubilization in SDS-alumina system in which no decreased of HEC adsolubilization in the presence of high concentration of SDS.[68]

Studies showed that the adsolubilized amount does not increase linearly with the increasing surfactant concentration in which the ratio of amount of solute adsolubilized over amount of surfactant adsorbed is different at different surfactant concentration (region 1, 2 or 3). At low surfactant coverage (region 1 or 2), adsolubilization depends on the arrangement of adsorbed surfactant while adsolubilization depends on the amount of adsorbed at high surfactant concentration (region 3).[69] The structure of surface aggregates /admicelle consists of the core (the hydrophobic tail-chain of the surfactants) and the palisade region (polar head group of the surfactants). The effectiveness of solute partitioning can be described by the admicellar partition coefficient K_{adm} which has been defined in different ways by different groups. Nevertheless, admicellar partition coefficient was found to be similar or higher than the micellar partition coefficient in most of the cases indicating the high potential and effectiveness of organic solute uptake by admicelle.[58,70–72] Table 3.1 showed the adsolubilization capacities (amount of solute adsolubilized over amount of surfactant adsorbed) that were reported in previous work.

Table 3.1: Solute adsolubilized: Surfactant adsorbed

Substrate	**Surfactant**	**Solute**	$\frac{\text{Solute adsolubilized}}{\text{Surfactant adsorbed}}$	**Reference**
Alumina	SDS	Styrene	1:2	Wu et. al.[2]
Glass fiber	C_{12}TAB	Styrene	1.2:1	Sakhalkar and Hirt[16]
Glass fiber	CPC	Styrene	1.4:1	Sakhalkar and Hirt[16]
Silica	C_{16}TAB	Styrene	1.7:1	Kitiyanan et.al.[73]
Silica	Triton X-100	Styrene	2.7:1	Tan et. al.[74]
Silica	C_{16}TAB	Propyl Gallate	1.2:1	Andrzejewska et. al.[67]
Clinoptilolite	BC	Sulfamethoxazole	1:5	Farias et. al.[75]

In general, the longer the carbon chain length, the more hydrophobic interaction between surfactant tails and the higher surface adsorption. This usually resulted in higher adsolubilization due to more admicelle volume.[59,65,76] However, in the study of naphthalene and α-napthol adsolubilization onto silica by homologue series of alkylammonium bromide cationic surfactant C_nTAB (n= 12, 14, 16), the authors found the intermediate carbon chain length, C_{14} has the most efficient packing (highest maximum amount of adsorption and smallest area per molecule) upon adsorbed on silica.[77] This phenomenon was explained by the fact that shorter carbon tail molecule was able to penetrate deeply into the pores of silica, however tail-tail interaction decreased when the carbon chain length gets too short resulting in more efficient packing in $C_{14}TAB$ than $C_{12}TAB$. Despite more $C_{14}TAB$ adsorbed on the silica, the solute adsolubilization capacity was lowest in $C_{14}TAB$ admicelle due to the tighter packing and thus less palisade region were available. As a result, surfactant carbon chain length becomes crucial in increasing adsolubilization of solute. The longer the carbon chain length, the more favorable the adsolubilization. In addition to their study, they also observed that C_nTAB-napthol and C_nTAB-napthalene saturated micelle equilibrated as unsaturated admicelle (higher adsolubilization capacities compared to micelle solubilization) except for $C_{14}TAB$-napthalene saturated micelles which equilibrated as the saturated admicelle (has equivalent ratio of mole solute to mole surfactant).

As we mentioned earlier that more hydrophobic tail-tail interaction in surfactant admicelle promotes the adsolubilization of organic solute, one can achieved the same effect using surfactant with a branched alkyl chain. Didodecyldimethylammonium bromide with two dodecyl chain was able to adsolubilize more 2-napthol compared to dodecyltrimethylammonium bromide with only one dodecyl chain per mole basis. The authors observed the increase of basal spacing in the

adsolubilization of 2-napthol into the branched chain cationic surfactant due to more steric hindrance but did not observe spacing difference in the single chain surfactant system.[65]

Due to the excellent surface active properties of fluorosurfactant, it emerges as unique class of surfactant for adsolubilization. K. Esumi studied adsolubilization of alcohols onto alumina with hydrocarbon or fluorocarbon surfactant bilayers as early as 1990.[78] Lithium dodecyl sulfate and lithium perfluorooctane sulfonate surfactant bilayers were used to adsolubilize hexanol and heptafluorobutanol on alumina. Adsolubilization using either pairing with the surfactant was able to achieve approximately same amounts of adsolubilization although the interaction between surfactant-solute combination pair may be different according to hydrocarbon-fluorocarbon theory discussed by Mukerjee in 1982.[79] Lai et. al.,[80] Hanumansetty and O'Rear[81] found fluorosurfactant adsolubilized fluorocarbon alcohols effectively on alumina and cotton fabric respectively. Both studies found the adsolubilization depends on the surfactant coverage on the surface as proposed in the two-site adsolubilization model. Partitioning at the admicelle hydrophobic perimeter is favored at low admicelles concentration while partitioning at the palisade core sites is dominant when surface is saturated with admicelles. The model was used to estimate the partition coefficient and aggregation number.

Extended surfactants having polypropylene oxide (PPO) internal linker has intermediate polarity and sits between the hydrophobic tail and hydrophilic head group of the molecules. Extended surfactants were often reported to have advantages over a system with the addition of lipophilic external linker (ie. long chain alcohols). Presence of long chain alcohols and the PO internal linker in the extended surfactants provide the same function in increasing the hydrophobicity of the admicelle and create tighter packing. In addition, extended surfactants usually have a lower CMC and therefore less surfactants were required to saturate of a surface

adsorption.[82,83] The interaction of PO internal linker varies with different solute depends on the solute's polarity. Presence of PO may enhanced the adsolubilization of rather polar solute (ie. phenylethanol) but decreased adsolubilization at high number PO group due to the surfactant tail coiling and "squeeze out" effect in the palisade. Meanwhile, increasing PO groups of extended surfactant showed enhancement in adsolubilization of less polar solute (ie. ethylcyclohexane) due to the increasing hydrophobic effect.[83] Arpornpong et. al. compared between ethoxy propoxylated carboxylate surfactant with propoxylate sulfate surfactant and observed the former has higher K_{adm} due to the larger palisade layer available to adsolubilize slight polar solute (ie. phenylethanol and styrene).[84] They reported K_{adm} were lower than K_{mic} for polar solutes but opposite for non-polar solutes (ie. phenanthrene).[84] It was believed that the micelle has a 3-D conformation and has more palisade layer than admicelle. In addition, the structure of extended surfactants with PO linker may pack more efficient in 3D micelle than 2D admicelle.[83] Therefore, admicelles were more effective in adsolubilizing non-polar solutes than micelles which can solubilize more polar solute. However, this is not always the case since a study showed that a rather less polar solute (ie. ethylcyclohexane) has a higher K_{mic} than K_{adm} in a single-head anionic/ twin-head cationic surfactant mixture system.[85] The authors explained that the mixed-surfactant micelle has larger and more hydrophobic core that favors the solubilization of non-polar solute.

In contrary to the PPO internal linker mentioned earlier, ethylene oxide functional group in a nonionic surfactant system acts as the surfactant head group. In general, the higher the number of surfactant head group (ie. ethylene oxide), the higher the CMC and the lesser the saturated adsorption of these surfactants due to the bulkiness and repulsion between the head group which causes looser packing density.[74,86,87] In a study by Y. Tan et. al. using non-ionic surfactant polyethoxylated octylphenol (PEO) of Triton series of C_8H_{17}-C_6H_4-$(OC_2H_4)_nOH$ with different

number of ethoxy group (n= 8.5-12.5) and reported a maximum of 67% styrene of the total styrene in the system was adsolubilized in the surfactant admicelle.[74] Results showed that increasing number of surfactant ethoxy group which is the hydrophilic (head group) part of the amphiphilic behavior in this nonionic surfactant system enhances the adsorption of Triton surfactant (steeper slope but lower plateau values) but did not enhance the total styrene adsolubilization. Meanwhile, Parida and Mishra concluded that the hydrophilic oxyethylene groups on the polyethylene glycol-treated silica were responsible to entrap and adsolubilize the chromophoric dyes.[88]

Mixture of anionic and cationic surfactant are believed to have synergistic behavior given that a well-mixed ratio of the two surfactant to avoid precipitation. Panswad et. al. used the mixture of cationic surfactant cetylpyridinium chloride (CPC) and extended anionic surfactant alkyl proxylated ethoxylated carboxylates (16-18 carbon tail, 4 mol PO groups, 2 or 5 mol EO group) to adsolubilize phenylethanol, styrene and ethylcyclohexane on silica.[89] The adsorption ability of CPC on silica was enhanced in the presence of extended anionic surfactant although the maximum amount of CPC adsorption was decreased. The overall K_{adm} were improved in mixed-surfactant system compare to single CPC surfactant. However, the desorption test showed that the mixed-surfactant has a limited stability because more CPC molecules were adsorbed initially. Fuangswadi et. al. studied the adsolubilization of styrene or ethylcyclohexane by mixture of single-head anionic surfactant (SDS) and twin-head cationic surfactant (PODD) admicelle on silica or twin-head anionic surfactants (SHDPDS) and single-head cationic surfactant (DPCl) admicelle on alumina with the highest K_{adm} obtained in 3:1 ratio of SHDPDS/DPCl mixed surfactant.[85,90] In the column studies, retardation factors in SDS/ PODD (1:3) columns was three times higher than the single surfactant PODD admicelle system. In addition to that, less desorption of mixed-surfactant admicelle upon water rinsing as compared to single surfactant system. In order to prevent

surfactant desorption, Thakulsukanant et.al. introduced the chemically-modified mineral surface, octadecyltrichlorosilane (ODS)-bonded silica for adsolubilization of organic solute.[91] The authors found that the substrate was stable under agitation up to 310 rpm and temperature below 40^{o}C and only slightly affected by pH changes.

Aside from studying the effect of mixing oppositely charged surfactant on adsolubilization, Esumi et. al. focused on using ionic and non-ionic surfactants to adsolubilize 2-napthol onto alumina and silica.[92–94] Interaction parameters of the mixed surfactant pair were calculated by regular solution theory. Higher magnitudes of the interaction parameter β indicated a higher hydrophobic interaction among the surfactant pair and reduced the head-head repulsion. The authors found that single-head ionic surfactant either SDS or HTAB mixed with non-ionic surfactant hexaoxyethylene decyl ether ($C_{10}E_6$) gives a higher interaction (ie. $\beta = -3.4$) as compared to twin-head ionic surfactant 1,2-bis(dodecyldimethylammonio) ethane dibromide (2RenQ) with $C_{10}E_6$ (ie. $\beta = -1.5$). The study further proved that the adsolubilization results are in agreement with the interaction parameter data that the mixed surfactant of single-head ionic and non-ionic surfactant admicelle has higher adsolubilization efficiency than single surfactant system while the pairing of twin-head cationic and non-ionic surfactant system was not. They concluded that the adsolubilization of 2-napthol by these mixed surfactant systems depends on the mixed-surfactant adsorbed layer structure and the alkyl chain length.

Nayyar et al. studied the behavior of sodium dodecylsulfate (SDS) "modified admicelle" on alumina surface at the temperature below the Kraff temperature (T_k for SDS is 16^{o}C).[70] The study found no significant changes on surfactant adsorption at 4 to 21^{o}C and its adsolubilization properties of the "modified admicellar" were retained. This finding showed that the potential of performing adsolubilization at below T_k with no surfactant bleeding in the process and no

surfactant replenishment would be necessary to maintain the admicellar layer on the packed column.

Sakai et. al. studied the adsolubilization of 2-napthol using photosensitive cationic surfactant adsorbed silica surfaces.[95] This spiropyran-modified quaternary ammonium cationic surfactant isomerized between merocyanine (MC) in the dark and spiro (SP) upon light exposure. Adsolubilization was found higher in MC form due to the planar structure and zwitterionic properties. Conformation of adsorbed hydration layer was estimated by quartz crystal microbalance with dissipation measurements (QCM-D). MC form has a higher 2-napthol adsolubilization efficiency because of the swelling and greater dissipation (more viscoelastic) of the adsorbed layer.

Polymerizable gemini surfactant has receiving great attention in adsolubilization applications due to the better performance such as lower surface tension, lower CMC and less surfactant desorption from the surface with polymerized gemini surfactant.[86,96,97] These surfactant have a higher effective area per head group molecule due to the coiling of long hydrophobic tail and the repulsion between the head group. In general, the higher the number of surfactant head group (e.g. ethylene oxide),[86] the higher the area per molecule and therefore the maximum amount of adsorption is lesser due to the bulky or repulsion between head group. As a result, the looser packing orientation of the gemini surfactant on a surface has a more expanded admicelle layer and often gives a higher adsolubilization efficiency compared to monomeric surfactant.[98]

An interesting type of surfactant emerged in the field of adsolubilization called amphiphilic invertible polymers (AIP) which is a polyester that can be synthesized from polyethylene glycol (PEG) and dicarboxylic acid.[99] Acid fragment in these polyester surfactant provides hydrogen bonding and hydrophobic interaction with the surface and therefore able to adsorb on both polar

and non-polar surface. Longer hydrophobic chains (C_{10} better than C_8) in acid fragment proved to have better AIP adsorption and 2-napthol adsolubilization. Adsolubilization of 2-napthol was found to be independent of adsorbent polarity, but exhibits different adsorption mechanism when observed from the adsorption isotherm. Results indicated rather slow but more AIP saturated adsorption on polar silica whereas faster but lesser AIP saturated adsorption on non-polar silica. On the other hand, it was found that higher surfactant desorption occurred from silica due to the weaker hydrogen bonding after solute adsolubilization. Another type of polymeric surfactant established the similar behavior mentioned above was the triblock copolymer which consists of PEO-PPO-PEO (Pluronics) in which PEO plays the hydrophilic part in the surfactant role. Esumi's group adsolulized 2-napthol with the Pluronics admicelle and measured it on both hydrophobic or hydrophilic silica.[100,101] Adsolubilization of 2-napthol did not decreased after rinsing the silica particles with surfactant-free solution despite few Pluronics surfactant desorbed from the surface. Due to the advantage over the conventional monomeric surfactant, the group suggested the sequential addition of preadsorption and equilibrium of Pluronics surfactant, then adsolubilization of 2-napthol in surfactant-free solution could solve the issue of polymolecular micelles formation in the solution phase that reduced the adsolubilization efficiency.

3.3 Substrate composition and structure

Most adsolubilization studies had been focusing on inorganic oxides such as, silica, alumina, zirconia etc. The popularity of using these materials are attributed to their enormous surface area as well as the high porosity surface. B. Kitiyanan et.al. found that the surface area of cetyltrimethylammonium bromide (C_{16}TAB) head group per molecule from the surfactant adsorption isotherm on silica Hil-Sil 255 (BET: 170 m^2/g) to be 51 $Å^2$/molecule, on silica Hil-Sil 233 (BET: 145 m^2/g) to be 89 $Å^2$/molecule and compared to the surface area at the water-air

interface (C_{16}TAB adsorption density: 30 $Å^2$/molecule).[73] Despite the formation of local bilayers, the calculated surface area adsorbed per C_{16}TAB molecule were higher than 30 $Å^2$/molecule because not all the BET measured surface area were accessible by the C_{16}TAB surfactant compared to N_2 molecules due to the highly porous silica surface. Surface charge densities at the interface corresponding to the solution pH also plays an important role in the adsorption/ adsolubilization (Refer to Section 3.6: Solution properties). On the other hand, Adak et. al. did the extended adsolubilization studies on surfactant-modified alumina (Refer to Section 3.7: Applications).[102–107]

Esumi et. al. presented adsolubilization studies on chemically modified titanium dioxide.[108–113] Titanium dioxide was treated with siloxane compound via chemical vapor deposition and subsequently undergoes hydrosilylation to obtain different anchor chain. They found that the pairing of titanium dioxide with the dodecyl chain or the quaternary ammonium group with cationic or anionic surfactant gives a different adsolubilization efficiency depends on the electrostatic or hydrophobic interaction of the anchored group and surfactant structure.

The Salgaonkar group utilized adsolubilized aniline to successfully make a polyaniline film-coated zirconia surface to be used in conducting materials.[20,21] They had used both C_{16}TAB and SDS in the system with their corresponding pH adjustment and electrolytes concentration (ie. NaCl) to achieve the optimum results. The point of zero charge (pzc) of zirconia is reported to be 5.5 and therefore pH 2.1 gives the maximum SDS adsorption[20] while pH 9 was conditioned for C_{16}TAB adsorption[21] onto zirconia. Addition of salt (eg. NaCl) reduces the competitive effect of adsorption/ adsolubilization between SDS/C_{16}TAB and aniline by reducing the electrostatic repulsion between surfactant head group which enhances more surfactant adsorption and more aniline adsolubilization.

Besides these, mineral clays such as kaolinite, montmorillonite and zeolite are commonly used due to their high surface adsorptive, availability for ion-exchange, catalytic nature and natural abundance. Mineral clays enable ion-exchange between surfactant counter ions to form clay-surfactant bilayered intercalations and provide a unique systems for organic adsolubilization. Clinoptilolite, montmorillonite and zeolite exhibit physiochemical stability in biological environments and have been used to adsolubilize drugs (Refer to Section 3.7: Applications).[98,114,115] Hayakawa et. al. examined the zeolite-cationic surfactant complexes in adsolubilization and release of chloroquin.[115] P-type zeolite (with sodium as the counterion) with tetratrimethylammonium bromide complexes had the highest chloroquin adsolubilization as well as the most solute released using NaCl solution. In another study, the group also found P-type zeolite more efficient in adsolubilizing the cationic dye Rhodamine compared to high silica mordinite.[116] Backhaus et.al. studied the sorption mechanism of the pollutants 2,4-dichlorophenol on montmorillonite in the presence of the non-ionic Triton-X series surfactants.[87] These non-ionic surfactant exhibit higher affinity to the Ca montmorillonite surfaces compared to silica gel due to the ring complexation between the interlayer cations of the mineral and polyether chain of surfactant. However, Ca montmorillonite has lower adsolubilization efficiency for 2,4-dichlorophenol compared to silica gel at the same surfactant load. The study explained that only co-adsorption of surfactant and solute in Ca montmorillonite at the particular surfactant coverage. Meanwhile, surfactant admicelle were formed on silica gel surfaces provide higher effectiveness of adsolubilization. Kaolinite-SDS[117] and kaolinite-CPC[63] were used in removing nitrophenol pollutants in wastewater or for soil remediation purposes. The presence of both permanent basal negative charges in its crystal structure and pH-dependent positive charges on the edges enable kaolinite to work with both anionic and cationic surfactant. Wang et. al. further used mixtures of

cationic surfactant C_{14}TAB and hydrophobically modified polyacrylamide (HMPAM) polymer to study the adsolubilization of 2-napthol on kaolinite. They found that the presence of HMPAM increased the adsolubilization efficiency at low surfactant concentration but lowered the stability of clay dispersion.[118] Venkataraman et. al. studied both solubilization and adsolubilization method to functionalize layered cadmium thiophosphate interlayer with C_{16}TAB and uncharged organic species.[119] They found that intercalation of long chain aliphatic alcohols have similar lattice spacing regardless of the method they were prepared but diffraction pattern showed that adsolubilization preserved better crystallinity. The interlayer spacing may increase (larger molecules), decrease (smaller molecules) or remain the same upon intercalation of the organic species. Esumi et. al. showed that copper ions readily adsorbed on laponite in the absence of surfactant via cation exchange but not for 2-napthol. However, modification of laponite with cationic surfactant adsorption were able to remove both ionic copper ions and organic contaminants 2-napthol simultaneously.[120] Klumpp et. al. studied the adsolubilization of 2-napthol using cationic surfactants on two types of clay mineral with different cation exchange capacities (CEC): 90meq/100g bentonite and 27meq/100g illite and found that illite had a efficiency in the adsolubilization of 2-napthol with the same amount of adsorbed surfactants.[65] When the surfactant concentration achieved 100% CEC, 2-napthol works as cosurfactant and enhanced both surfactant adsorption and its adsolubilization simultaneously.

Layered double hydroxides (LDHs) specifically hydrotalcite minerals consist of a positively-charged brucite-like $Mg(OH)_2$ layer of mixed metal hydroxides with exchangeable anions at the interlayer spaces. The general formula for LDHs can be expressed as $[M^{2+}_{1-x}M^{3+}_{x}(OH)_2]^{x+}$-$(A^{n-})_{x/n}.yH_2O$; M^{2+} = divalent cation, M^{3+} = trivalent ion, A= interlayer anion, n= charge on interlayer anion, and x,y are fraction constants. Due to the unique features of LDHs for

ion exchange and its relative high surface area of interlayer (50-80 m^2/g), it has emerged as advanced material for application in various field. Various groups found interest in using LDH (eg. MgAl-LDH, MgFe-LDH, NiTi-LDH and ZnAl-LDH) as an effective adsorbent for adsolubilization by initially exchanging interlayer anion with anionic surfactant (eg. SDS, SDBS or AOT), and admicelle phase provides the "adsolubilization sites" for solute partitioning.[121–130] Ion exchange between anionic surfactant head groups and anions at the LDH-interlayer through electrostatic and hydrogen bonding cause further occupation of the interlayer regions with hydrophobic alkyl-chains. A 3-D hydrophobic phase will be formed at the interlayer region which is capable of adsolubilizing organic compounds via hydrophobic interaction. Research showed adsolubilization is primarily enhanced by the surfactant saturation. Adsolubilization study of hydrophobic and hydrophilic organic contaminants adsolubilization onto SDS-modified MgFe-LDH by Ruan et. al reported that higher hydrophobicity and polarity favored the adsolubilization.[129] P. Zhao et. al. studied the adsolubilization of 2,4,6 trichlorophenol into SDS or SDBS-intercalated ZnAl-LDH in which the latter has higher adsolubilization efficiency due to the π-π interaction between the benzene rings.[130] The authors proposed 4 types of interactions in the process: (a) π-π interactions, (b) non-polar interactions, (c) hydrogen bonding, and (d) electrostatic interactions. In the study of Cu^{2+} and p-cresol adsolubilization on SDS-EDTA-modified MgAl-LDH, p-cresol was found to compete with Cu^{2+} adsolubilization.[128] However, the presence of Cu^{2+} were in fact enhanced the adsolubilization p-cresol. Other examples of organic contaminant adsolubilization studies includes Carbetamide and Metamitron pesticide on modified MgAl-LDH with dodecyl sulfate.[124] Adsolubilization of these pesticides increased with increasing dodecyl sulfate saturation in the LDH. Lowest adsorption were observed when the pesticides were ionized (Carbetamide is negatively charged at pH 11; Metamitron protonated at pH 3), showed

that hydrophobic interaction between pesticides and surfactant chain is dominant factors for the adsolubilization mechanism in this case. Adsolubilization of 2-napthol was studied on SDS-modified MgAl-LDH by Esumi et. al.[127] The authors explained that adsolubilization of 2-napthol increased and gradually decreased with increasing concentration of SDS is due to the electrostatic repulsive interaction between SDS and ionized 2-napthol. In the later study, the same phenomena was observed in adsolubilization of 2-napthol on SDS-modified alumina.[57] It was explained that monolayer of SDS has the tail-out orientation results in strong hydrophobic interaction while bilayers SDS results in repulsion of head group with the ionized solute. Klumpp et. al. studied the adsolubilization of 2,4-dichlorophenol on SDS or AOT-modified MgAl-LDH and found the latter has two times higher adsolubilization efficiency than the former.[126] Higher hydrophobic interaction resulted in higher adsolubilization efficiency showed that hydrophobic sorption is the dominant. Zhao et. al. studied the adsorption behavior of thiophene on carbonate (CO_3^-) or DDS-intercalated ZnAl-LDH and found that thiophene adsorption on CO_3-LDH was pH dependent while thiophene adsorption on SDS-LDH was pH independent.[122] The efficiency for thiophene sorption was maximum at zero zeta potential of CO_3-LDH and the S-type curve of thiophene sorption on CO_3-LDH with increasing concentration of thiophene suggests that the sorption mechanism is the result from hydrophobic interaction between thiophene-thiophene molecules. Meanwhile, thiophene sorption on DDS-LDH increased linearly with increasing thiophene concentration indicates the partitioning of thiophene at the hydrophobic DDS interlayer regions rather than the external surfaces of the DDS-LDH. In the study of pentachlorophenol adsorption on hydrophobilized NiTi-LDH by Gao et. al., dodecylbenzenesulfonate-modified Ni_5Ti has the highest interlayer spacing with looser DBS stacking mode and gives the highest pentachlorophenol sorption compared to cyanate- or dodecyl sulfate-intercalated NiTi-LDH.[123] All the sample has a

linear sorption mechanism showed that pentachlorophenol partitioning at the three-dimensional interlayer regions and was independent of surface area. Maximum adsolubilization occurred at pH 8 when DBS-Ni_5Ti is uncharged (pzc of 8) and pentachlorophenol is negatively charged (pKa of 4.75), implied that hydrophobic interaction is predominant over hydrogen bonding and electrostatic attraction. Other than the common remediation purpose, SDBS-Co-Al hydrotalcite thin layer on the glass electrode can be used for electrochemical determination of phenol.[125] SDBS-Co-Al has the highest effectiveness in adsolubilizing phenol, has higher stability and resistance to surface fouling caused by phenol oxidation. Cursino et. al. also presented on synthesis of SDS intercalated ZnAl-LDH to adsolubilize up to 9% (w/w) of benzophenone, a UV absorbers and found a good adsorption and stability to UV radiation.[121]

A few research groups have used a novel type of adsorbent which combined conventional adsorbent with superparamagnetic nanoparticles to demonstrate a new type of mixed hemimicelles solid-phase extraction (MHSPE) column. Zhao et. al. first coated pure Fe_3O_4 nanoparticles with cationic surfactants CPC or C_{16}TAB for adsolubilization of phenolic compounds that are usually found in wastewater.[131] The group further improved this MHSPE adsorbent by coating Fe_3O_4 nanoparticles with silica to minimize the loss of Fe_3O_4 magnetism after oxidation in acidic environment.[132] Sun et. al synthesized the Fe_3O_4 nanoparticles which coated with alumina and further modified by anionic surfactant SDS were used to extract and preconcentrate trimethoprim (TMP).[133]

Admicellar polymerization has been done on cellulose/ cotton fibers with the potential of making functionalized textile fabric having ultra-violet protective agent, water repellency,[27] whitening agents[134] etc. The abundance of these natural cellulose fibers which are low cost and biorenewable make them advantageous for industrial applications.[59,76] Pal et. al. also introduced

a new emerging biomaterial, the chitosan hydrogel beads as an effective adsorbent for removal of both SDS and crystal violet dye synergistically.[135]

More examples of adsorbent that generated from waste material were useful for adsolubilization of organic pollutants and often applicable for soil remediation or wastewater treatment can be found in Section 3.7: Applications.

3.4 Effect of solute

Solute adsolubilization is expected to increase with increasing concentration in the bulk. A two-site adsolubilization model was used to express the partitioning of solute at different surfactant coverage as discussed earlier, the model was used to explain the interaction between admicelles and solutes with different polarity.[136] Partitioning of alcohols (polar solute) and alkanes (non-polar solute) into SDS admicelle on alumina was examined. The model showed that polar solute partitioned at the core and the edges of the admicelle while non-polar solute partitioned at the core. Polar solute competes with surfactant for adsorbed sites at low surfactant coverage but "edge" effects decreased and "core" volume increased when surfactant coverage increased. This phenomenon was explained by the decreased ratio of circumferences to covered area at increasing surfactant coverage. As a result, partition coefficient K of polar solute decreased while K of non-polar solute increased at high surfactant coverage. Research studies over the years provide many discussions involving the effect of solute polarity in adsolubilization process. In general, it is believed that polar solutes partition primarily in the admicelle palisade while non-polar solutes partition to the admicelle core. While studying the effect of the admicellar partition coefficient K_{adm} on the fraction of solute in the bulk, X_{aq}, one can postulate the partitioning locations of organic solutes in the admicelle.[70,77,89,137] When log K_{adm} increases with increasing X_{aq}, the organic solute is non-polar, eg. diphenylmethane,[137] 4-bromotoluene,[137] diphenylether (more polar due to

cation-pi bonding with CPC)[137] which partitioned into the core. Meanwhile when log K_{adm} decreases with increasing X_{aq}, this showed that the organic solute is polar, eg. phenylethanol,[89] α-napthol,[70,77] p-tolunitrile,[137] isoprene[73] which partitioned into the palisade. Nayyar et. al. used dodecane to study the admicellar core simulation studies (dodecane were used to simulate the same carbon chain length of SDS) and found the partition coefficient of organic solutes into the dodecane, K_{C12} measured for naphthalene (less polar) have a value closed to K_{adm} and K_{mic} compared to K_{C12} measured for napthol (more polar) was slightly off from K_{adm} and K_{mic}.[70] This observation agrees with the hypothesis that the less polar solute is more favorable to partition into the core ($K_{adm} \approx K_{C12}$). Meanwhile, when log K_{adm} slightly increases/ decreases or constant with increasing X_{aq}, the organic solute is intermediate polar (relative to the environment), eg. styrene,[89,73] ethylcyclohexane,[89] napthalene[70,77]) was most possible to be partitioned at both palisade and core. In the study of Y. Tan et. al., the authors found two adsolubilization stages in which styrene adsolubilized in both palisade and core of PEO admicelle at low styrene concentration and into the admicelle core at higher styrene concentration.[74] This observation indicated that the location for adsolubilization was determined by the nature of the solute and the amount of the solute loading. In the case of adsolubilization of ionizable organic solutes that were readily adsorbed on an oppositely charged surface, ie. 4-amino-1-napthalenesulfonic acid (ANSA), surfactant admicelles did not facilitated adsolubilization but rather displaced the adsorbed solute.[70]

Besides K_{adm}, solute partition coefficient P_{ads} were also used to quantify the adsolubilization efficiency where P_{ads} is defined as $P_{ads} = \frac{\Gamma_{max}^{solute}}{\Gamma_{max}^{surfactant} \Gamma_{bulk}^{solute} \tilde{V}}$. The Treiner group studied the adsolubilization of different types of solute with C_{16}TAB on silica, alumina, titanium dioxide system and mixed two non-ionic surfactant (Triton X-100 and Poloxamer 188) on polystyrene latex particles.[138–140] The authors found that the solute partition coefficient P_{ads} are

independent of pH, salt concentration and solid substrate, in spite of the different absolute value of the total amount of adsolubilized solute. In explanation, the solute partition coefficient depends on the total amount of surfactant adsorbed on the surface. In fact, Funkhouser et. al. reported that increase of surfactant coverage with increasing salt concentration were indeed caused by a decreased K_{ads}.[141] The study showed that high packing of surfactants reduced the adsolubilization at the perimeter of admicelle and the negative radii of admicelle curvature on porous substrate had caused the drop in K_{ads}. The group also found P_{ads} to be equal to the micellar partition coefficient P_{mic} for neutral solute (ie. aromatic alcohol) while higher for weak acids/bases (ie. aromatic amine) and steroids molecules. They were able to develop a simple thermodynamic model that correlates to P_{ads}, binding constant and pK value which fits well in weak acids and bases solute adsolubilization.[142]

In the study of mixed solute adsolubilization, the positive synergism in polar solute adsolubilization with the addition of non-polar solute was attributed to the swelling of the admicelle core by non-polar solute and thus increase the admicelle palisade volume for more polar solute adsolubilization acetophenone in the presence of toluene,[69,143] and isoprene in the presence of styrene.[73] On the other hand, negative or no synergism in adsolubilization of less polar solute in the addition of polar solute due to the competitive partitioning at the palisade (naphthalene with naphthol).[77] Okamoto observed the different behaviors of binary solute of 2-napthol and naphthalene adsolubilization on monolayer or bilayer of C_{16}TAB surfactant in a range of pH.[60] Interestingly, despite more C_{16}TAB adsorption on the surface with increasing pH, competitive adsolubilization of both solutes (pH> 4) was observed on monolayer of C_{16}TAB due to tail-out orientation which tends to flocculate and only hydrophobic adsolubilization sites were available. Meanwhile, synergistic adsolubilization of both solutes with C_{16}TAB surfactant template were

observed where 2-napthol (more polar) partitioned into the palisade and biphenyl (less polar) partitioned into the core of admicelle bilayer. In addition, increasing pH in the system increased the C_{16}TAB adsorption and also deprotonated 2-napthol at high pH region improved the C_{16}TAB-napthol interaction. The authors observed the adsolubilization of less polar biphenyl was enhanced by polar 2-napthol which is contrary to previous studies.[77]

Generally, solute with lower water solubility or higher K_{ow} has a higher K_{adm}.[59,70,84,86,89,137] Adsolubilization of different haloacetonitriles in homologue series showed that the higher the degree of halogen substitution, the higher the hydrophobic interaction resulting higher adsolubilization.[97] Aliphatic alcohols, hexanol with high and comparable K_{ow} competed with adsolubilization of 1-hepthanol while alcohols with low K_{ow} showed no competition effect but rather co-solvent effect.[144] Nevertheless, in the study of steroids molecules adsolubilization onto nonionic surfactant-polystyrene latex system, P_{ads} did not seems to follow the K_{ow} trend.[140]

Adsolubilization of polymer-type solutes such as hydrophobic modified hydroxyethyl cellulose (HMHEC) was higher compared to hydroxyethyl cellulose (HEC) as a function of the hydrophobic grafted alkyl chain length.[68] In addition to that, presence of these polymer on the alumina interface were able to gives a stable particle dispersion via steric repulsion compared to the electrostatic repulsion when only SDS admicelles adsorbed at the interface.

The effect of substituent position of nitro-phenolic compound was studied by Pura et. al. using phenol, ortho-nitrophenol (ONP), meta-nitrophenol (MNP) and para-nitrophenol (PNP) on SDS-adsorbed kaolinite.[117] Phenol did not adsolubilize in the presence of SDS due to the electrostatic repulsion resulted from the negatively charge nature of both species. Meanwhile, aromatic nitrophenol compound can be adsolubilize with SDS with the order of adsolubilization efficiency followed by ONP, MNP and PNP. It was believed that intermolecular bond was reduced

while intramolecular bond between hydroxyl group and nitro group increased when these polar substituent groups are closer to each other.

Some of the adsolubilization isotherm becomes vertical when solute concentration in excess.[74] Possible explanation by Y. Tan et. al. stated that the phenomenon was caused by the phase separation of the solute in the admicelle or a formation of "two dimensional" microemulsions in which each of the droplets formed in the admicelle core served as large adsolubilization reservoirs.[74]

Solute diffusion coefficients were measured by a voltammetry method using an ultramicroelectrode (UME). Diffusion coefficients were calculated based on the diffusion equation and the effect of the solution viscosity were negligible in most cases. It was proposed that the interaction between dihydroxybenzenes (ie. Catechol and hydroquinone) with free surfactant was electrostatic interaction while interaction with the micelle was the π-electron cloud of the aromatic ring and surfactant hydrophobic tail. As a result, catechol-C_{16}TAB admicelle showed two times the adsolubilization efficiency compared to hydroquinone-C_{16}TAB admicelle on silica because of the adjacent dihydroxyl group did not shield the hydrophobic attraction.[66]

3.5 Impact of cosurfactants

The addition of lipophilic linkers (long linear chain alcohols with number of carbon above 8) was proved to slightly increase total surfactant adsorption especially for those surfactant that loosely packed on the surface. For example, dodecanol was found to have the best impact to increase saturation adsorption of POE non-ionic surfactant with more EO group on silica[74] and has a synergistic effect in SDS adsorption on alumina.[82] Hydrophobic tail-tail interaction was increased in the presence of long chain alcohol and created a closer packing in the adsorbed layer because it has the same number of carbon tail as the surfactant carbon tail, and able to partition at

the hydrophobic core which enhanced the tail-tail interaction. However, alcohols with long carbon chain tends to coil and fold causing steric hindrance and poor packing of surfactant adsorbed layer. In the POE-lipophilic linker study, POE-adsorbed silica showed 25% enhancement of styrene adsolubilization in the presence of octanol lipophilic linker.[74] The study reported the maximum ratio of styrene adsolubilized to surfactant adsorbed to be 2.7:1 while interaction between surfactant adsorbed to lipophilic linker was 12:1 and therefore interactions between styrene adsolubilized to lipophilic linker was calculated as ≈ 32:1. These ratio indicated the interaction between styrene to lipophilic linker was less significant compared to the higher affinity between PEO and aromatics solute in this case. Increasing number of carbon chain length of lipophilc linker from C_8 to C_{12} showed 30% enhancement in styrene adsolubilization. The authors claimed that, instead of increasing its concentration, a greater impact in adsolubilization is achieved by increasing the hydrophobic chain of the lipophilic linker. The maximum effect of effective hydrophobic chain in lipophilic linker versus surfactant was calculated to be 2:1. While lipophilic linker with the same number of hydrocarbon chain length has the best performance in adsolubilization, an average between the surfactant and the oil-phase hydrophobic tail length has the best performance in solubilization by microemulsion.[145] Synergistic effect were also observed in adsolubilization of fluorocarbon alcohols using fluorocarbon surfactants on alumina in which the higher the alcohols chain length, the more effective the surfactants adsorption and adsolubilization efficiency (solute partition coefficients were increased).[80] Despite the advantage of lipophilic linker in improving the surfactant adsorption, surfactant with internal linker and commonly called extended surfactants showed more beneficial properties in terms of surfactant concentration required and also the adsolubilization capacities (Refer to Section 3.2: Surfactant type, amount and structure).

3.6 Solution properties

Changes of the surface charge with varied pH environment was found to give a significant effect on the amount of adsorption of the oppositely charged surfactant and thus influencing the amount of solute adsolubilized. Silica (pzc 2-3) showed enhancement of cationic surfactant adsorption at higher pH due to the increase of negative charge density on silica surface. On the other hand, alumina (pzc 9.1) is readily use for anionic surfactant adsorption in which the adsorption increases with the increasing of positive surface charge density at low pH. As a result, adsolubilization was enhanced due to the availability of more admicelle volume.[67,69 138,143,146] The same case in cellulose matrix that swell and increase the surface area with increasing pH due to carboxylic group ionization at pH 5.[59] However, increasing surface charge of a substrate is not always beneficial. Behrends et. al. reported that even though there was higher amount of C_{16}TAB surfactants adsorbed on the silica at higher pH (ie. pH 8 compared to pH 5) resulted in non-isolated, hydrophobic patches of adsorbed surfactant layers which were not favorable for anthracene adsolubilization.[55,147]

Adsolubilization of ionizable solute very well depends on the changes of pH. Das et. al. showed that maximum adsolubilization of a cationic dye Malachite Green (MG, pK_a = 6.9) on SDS-modified alumina at pH = 4.75 due to the attractions of negative charged SDS head group and ionized form of MG solute.[148] Adsolubilization of phenol by SDS-admicelle alumina decreased when pH increased from 2 to 11 due to the transition of non-ionized form phenol into phenolate ion (phenol pK_a = 9). SDS anionic head group tends to repel negative charged phenolate ion and SDS desorbed from alumina (pzc = 9.15) at high pH. The same observation in deprotonation of 2,4-dichlorophenol (pK_a = 7.8) at high pH decreased adsolubilization on nonionic surfactant-modified montmorillonite[87] and 2,4,6-trichlorophenol (pK_a = 6.23) adsolubilization

onto SDS or SDBS-modified ZnAl-LDH.[130] In the case for kaolinite with CPC studied by Talbot et. al.,[63] adsolubilization of 4-nitrophenol decreased with increasing pH before the pK_a= 7.15 at low CPC coverage due to the repulsion between phenolic ion and negative-charged kaolinite. Meanwhile, adsolubilization of 4-nitrophenol increased with increasing pH at high CPC coverage due to the attraction between phenolic ion and positive-charged CPC admicelle layer. The study compared between kaolinite and silica system and showed both has the same adsolubilization pattern but kaolinite has rather smaller pH effect due to the constant basal charged in the crystal structure. Monticone et. al. observed a maximum adsolubilization at the pH close to the pK for a series of weak acids and weak bases.[142] The authors deduced that adsolubilization increases by the solute-surfactant interaction, while adsolubilization decreases due to solute-substrate repulsion upon changing the pH. The same observation was obtained in adsolubilization steroid molecules in cationic surfactant-silica system.[58]

In general, most admicellar polymerization systems incorporate with the addition of salt (eg. NaCl, KCl etc.) in order to increase the ionic strength of the aqueous system. This is beneficial in achieving a lower CMC with tighter packing due to shielding effect of the same charge surfactant head groups. This phenomena has been proved to be effective in admicelle formation as well and often assists in increasing adsolubilization efficiency.[20,21,59,138,141,146,147]. On the other hand, the effect of common interfering substances such as anions, cations and pesticides have to be considered in order to establish a wastewater treatment model utilizing the adsolubilization technique. Presence of interfering substance may react with surface (adsorbent), ionic surfactant or solute and altered the behavior of the species in the system by charge shielding or competitive adsolubilization. Das et. al. showed the presence of Fe^{2+}, $H_2PO_4^{2-}$, endosulfan or humic acid have significant effect in decreasing the adsolubilization efficiency of Malachite Green solute in SDS

admicelle on alumina system.[148] Adak et. al. found the presence of anions (ie. Cl^-, NO_3^-, SO_4^{2-} and HPO_4^{2-}) worked as the "salting-out" agent which increased the adsolubilization efficiency while the presence of cation Mg^{2+} slightly decreased adsolubilization efficiency by competitively adsorbed onto SDS-admicelle.[105] In Li's work, both Cu^{2+} and p-cresol adsolubilized onto the SDS-EDTA-modified MgAl-LDH. While p-cresol competes with Cu^{2+} adsolubilization, the presence of Cu^{2+} enhanced p-cresol adsolubilization.[128]

W. Saphanuchart et. al. studied adsolubilization of aromatic solutes on silica using cetylpyridinium chloride (CPC) at different temperature (20, 35, 50, 65ºC).[137] CPC maximum adsorption on silica showed 20% reduction with temperature increased from 20 to 65ºC. Admicellar partition coefficient of solute with varies polarity was expected to decrease with increasing temperature due to the increase in solubility. Assume admicellar phase is an ideal solution: $Ln\ Kp \approx \frac{-\mu 0_{aq\rightarrow adm}}{kT} \approx \frac{-\mu 0_{pure\rightarrow adm}}{kT} - \ln X_{aw}^{sat}$ where k is the Boltzmanm's constant, T is the temperature, X^{sat}_{aw} is the aqueous solubility of solutes, μ is the standard chemical potential for transferring a solute molecule (aq→adm refers aqueous to admicellar, pure→adm refers pure solute to admicellar). Referring to the surfactant self-assembly theory for solubilization proposed by Nagarajan and Ruckenstein,[149] this equation addressed the four main factors that affect the partition coefficient:

i. Aqueous solubility of solute
ii. Surfactant tail deformation energy in admicelle core
iii. Admicelle core/water interfacial energy
iv. Surfactant tail-solute mixing energy

However it was found that no significant effect at moderate temperature because increasing temperature created a looser molecular packing at the palisade that can adsolubilized more solute.

Other than that, the strong attractive forces of cation-pi bonding between CPC-diphenylether did not change adsolubilization in the range of studied temperature.

Desorption of species from admicelles or adsorbent for recycle use is necessary to be cost-effective. This process can be achieved by treating with solvent at the right condition (Table 3.2).

Table 3.2 Desorption of species from admicelle or adsorbent

Desorption species	**System**	**Agent/ condition**	**Reference**
PFCs	C_{16}TAB on silica	Methanol/ pH 6	X. Zhao et. al.[150]
PFCs	SDS on alumina	Acetonitrile/ pH 9	X. Zhao et. al.[150]
Malachite Green (MG)	SDS on alumina	Acetone/ -	Das et. al.[148]
MG and SDS	Alumina	0.25M NaOH/ high pH	Das et. al.[148]
C_{16}TAB and Orange II/ Methyl Blue/ 2,4-D Herbicide	Silica gel	18% HCl/ low pH	Koner et. al.[151]
Phenol/ Crystal Violet (CV)	SDS on alumina	Rectified spirit or acetone/-	Adak et. al.[102]
Phenol/ CV and SDS	Alumina	0.25M NaOH/ high pH	Adak et. al.[102]
SDS	Alumina	0.1M NaOH or methanol	Merino et. al.[152]
Carbetamide	DDS-LDH	Ethanol	Bruna et. al.[124]
2,4,6 trichlorophenol	DBS/ DDS-LDH	Acetone	P. Zhao et. al.[130]

3.7 Applications

J. Wu et. al. published the first admicellar polymerization paper on formation of polystyrene ultrathin film on alumina using sodium dodecylsulfate (SDS) surfactant bilayers.[1] Packing densities of sulfate head groups on alumina surface (4.8 molecule/ nm^2) was twice as much as the monolayer adsorption densities calculated from other measurement method (~2.5 molecule/ nm^2), which proved the formation of surfactant bilayer. Addition of ethanol and styrene have positive synergistic effect to slightly increase SDS total adsorption on alumina surface. This is the result of increasing hydrophobic interaction when more and more styrene adsolubilized into the admicelle interior and thus lowered the free energy in the system. Ratio of styrene adsolubilized

to adsorbed SDS was approximately 1: 2 and a sandwich-type structure were proposed. Film thickness formed on the oxide surface, measured with ellipsometry showed increasing film thickness with time, initiator and styrene concentration (up to 13 nm thick in 60 min). Deposit of spherical polymer particles on alumina surfaces were observed when emulsion polymerization took place in the presence of large excess of styrene concentration. Results from the UV spectrum on extracted polystyrene and FTIR on modified surface showed initial delay and oxygen inhibition during polymer conversion with time (< 2% conversion and no polystyrene at 5 min after reaction). This polymerization kinetics followed the classical Smith-Ewart emulsion polymerization theory. Other admicellar polymerization work on modifying the surface characteristics of solid substrates were extensively studied for applications such as rubber reinforcement,[6,17,18] corrosion control,[8,19] formation of conducting films, [21–23,153,154] surface modification of glass fibers,[155,16] and cotton.[14,25,156,157]

Adsolubilization technique has been used in wastewater treatment using low cost adsorbent or recycled waste material such as surfactant-modified alumina (SMA),[148,158–160] silica gel waste,[151] leather shavings,[161] kaolinite,[117,118] fly ash,[62] etc. Among these wastewater treatment studies, kinetic and adsorption models are essential. The kinetics study usually meet the second order or pseudo-second model while adsolubilization isotherm follows the Langmurian or Freundlich model. SDS-adsorbed alumina was used to adsolubilize a toxic cationic coloring dye, ie. Malachite green (MG) which is usually found in water environment. Anionic head group of the SDS admicelle enhanced the adsolubilization of cationic solute MG.[148] 99% of MG removal (concentration of 10 mg/L) can be achieved in an hour using 5g/L of SMA. Langmuirian model of adsolubilization indicated monolayer formation of MG on SDS admicelle. Regeneration of SMA using acetone was possible in which the performance of reused SMA achieved 80% efficiency.

Adak et. al. demonstrated the adsolubilization efficiency of phenol[104–106] and cationic dye crystal violet (CV)[102,103,107] in batch SMA or fixed SMA column along with the detail study in the mechanism and its kinetic model. The study for both solute adsolubilization followed a second order kinetics with Langmuirian isotherm and were able to achieve 90% and >99% removal efficiency for phenol (with 12g/l of SMA) and CV (with 6g/L of SMA) respectively. Kinetics study on CV removal showed it was not limited by film diffusion nor pore diffusion during the sorption process. In the column study for phenol removal, Bohart and Adams model (simplified using Bed Depth Service Time (BDST) approach by Hutchins) was used to evaluate the different parameters for the column. In the study of 10, 20, 30cm bed depth, height of exchange zone was found to be 3.83cm, adsorption rate constant K was 0.2584 L/mg-h and adsorption capacity N_o of 2880mg/L. Proposed model can be used to design the column at different influent concentration and flow rates. While experimental and theoretical breakthrough curve was proved to be comparable, testing with real wastewater proved to be more efficient. On the other hand, the removal of phenanthrene in batch and column SMA was studied by Smith and Valsaraj.[158–160] The group developed the mathematical model by generating the concentration profiles and breakthrough curve obtained from the experiment. The model successfully predicts the adsorption and adsolubilization pattern but not for the desorption pattern. Nevertheless column regeneration was done by introducing eluent with high pH (~10) and the column performance remained effective after three cycles of regeneration.

Other adsolubilization examples of removing organic pollutants commonly found in wastewater such as anionic dye (methyl orange, MO), cationic dye (methyl blue, MB) and 2,4-D herbicide include studies using cationic surfactant-modified silica gel (SG) with the optimum dosage of 3.5, 8, 12 g/L with the removal efficiency of 97, 92 and 94% respectively.[146] Further

column design study of MO removal (50mm bed depth, 25mm diameter)using BDST approach (Bohart-Adams equation) found that the column design parameters such as the height of exchange zone of 3.38cm, adsorption rate constant K of 0.00149L/mg-h and adsorption capacity N_o of 88849mg/L. Second-cycle regenerated SG remained to have the efficiency of up to 88%.[151] They also did the column study (20, 30, 40 cm bed depth with 2.5 cm diameter) for removal of 2,4-D herbicide using the same system. They determined the column design parameters of exchange zone height to be 12.7cm with adsorption rate constant K of 0.0094L/mg-h and adsorption capacity N_o of 6100mg/L.[162] Shavings waste from leather producing industry were used to adsolubilize 2-napthol pollutants. Operating conditions such as pH, surfactant concentration, and equilibrium time as well as the adsolubilization isotherm were studied.[161] Collagen fibres modified with anionic surfactant were also used to adsolubilize 2-napthol with the optimum pH at 2-3 after two hours of treatment.[163] Kinetic study showed that the adsolubilization process follows a pseudo-second order model and the thermodynamic study showed it is exothermic and spontaneous. Fly ash was used to adsolubilize the cationic dye, toluidine blue in the presence of surfactant. As expected, anionic surfactant SDS is a better agent for adsolubilization of cationic dye due to the oppositely charged attraction.[62] Danzer et. al. studied the transport of phenanthrene and ethoxylated nonionic surfactant on the aquifier for the purpose of subsurface remediation.[72] The transport of the hydrocarbon solute in aquifier or retardation factor in the presence of surfactant can be well predicted with the known constant of the porous medium properties such as bulk density and effective porosity, solute partition coefficient in admicelles and micelles, apparent distribution coefficient (without surfactant), adsorbed surfactant concentration and the micelles concentration. Ko et. al. addressed that the immobilization of hydrophobic organic compounds using adsolubilization technique is very effective but not for mobilization purpose such as in the

surfactant-enhanced remediation (SER) application.[71] The same case for polycyclic aromatic hydrocarbons remediation study by X. Zhao et. al. in a dispersant (surfactant)-sediment-seawater system.[164]

Several researchers have established the use of adsolubilization in using mixed hemimicelle solid phase extraction (MHSPE) as a pre-concentration of contaminants in environment samples prior analytical testing. This coupled method of SPE-chromatography/ spectroscopy has the function to preconcentrate and follow by high sensitivity determination of trace amount of target analyte. High preconcentration factor and low detection limit (few ng/L) have been reported by researchers. Generation of MHSPE required surfactant concentration below the CMC when hemimicelle or admicelle were present. Generally hemimicelles or admicelles consist of oppositely charged ionic surfactants adsorbed on the adsorbent. For instance, anionic surfactants on alumina and cationic surfactants on silica. Due to the ionic interaction of oppositely charged surfactants-adsorbent, pH adjustment is essential to ensure sufficient surface charge density in constructing hemimicelle/ admicelle. Merino et. al. generated MHSPE with SDS-coated alumina to retain benzalkonium chloride surfactants found in sewage and river water before LC-ESI-MS analysis run.[152] Optimum condition reported was at the acidic environment and optimum dosage was 25mg SDS per gram of alumina. Preconcentration factor of 500 (1 L sample volume, 2ml methanol elution) was able to be achieved. Moral et. al. too performed study on SDS-coated alumina for the extraction of benzimidazolic fungicides from river or underground water prior further analysis by LC/fluorimetry.[165] Column was conditioned at the optimum pH 2 and the recommended dosage was 100mg SDS per gram of alumina. Preconcentration factor of 400-1000 (400 or 1000 ml sample volume, 1 ml methanol elution). The group found the presence of calcium ion in the sample decreased the efficiency of adsolubilization and proposed a solution to pretreat

the sample with SDS in order to precipitate out calcium ion before passing through the column. In the study by Prieto et. al. to extract estrogens (common steroid hormones excreted by human or animals), SDS-coated alumina was found to be more effective than C_{16}TAB-coated silica in achieving preconcentration prior to LC-diode array/ fluorescence analysis.[166] X. Zhao et. al. on the other hand showed that C_{16}TAB-coated silica was better MHSPE in order to pre-concentrate perfluorinated compounds (PFCs) (common contaminants found in river and wastewater sample) prior testing the target compounds using liquid chromatography-electrospray tandem mass spectrometry (LC/ESI-MS/MS).[150] PFCs interact with C_{16}TAB adsorbed silica via hydrophobic and electrostatic interactions. Maximum adsolubilization of 40-300mg PCFs per gram of C_{16}TAB-coated silica with more than 80% extraction efficiency and a preconcentration factor up to 500 (500 mL sample volume) were reported. The study showed no effect when changing sample flow rate from 3-20 ml/min. Further analysis in LC/ESI-MS/MS proved the proposed method has good precision with a detection limits of 0.05-0.28 ng/l and relative standard deviation (RSD) of 2-8%. A nanosized MHSPE adsorbent with magnetic novel properties were demonstrated by group of researcher in water treatment application.[131,133] They were able to achieve preconcentration factors of 800-1000 in their study.

Adsolubilization has been examined for use in drug delivery by some research groups. Sulfamethoxazole and metronidazole were successfully incorporated into cationic benzalkonium chloride surfactants-adsorbed zeolite.[114] Detailed study on sulfamethoxazole drugs adsolubilization showed that the mol ratio of drug adsolubilized to surfactant adsorbed to be 1:5 and 90% equilibrium was achieved at the first 5 min before reaching total equilibrium in 5 hours.[75] Sakai et. al. showed more effective adsolubilization of Vitamin E (α-tocopherol) into cationic gemini surfactant admicelle rather than cationic monomeric surfactant admicelle on the same

substrate, ie. montmorillonite.[98] Andrzejewska et. al. showed the adsolubilization of antioxidant, propyl gallate on silica particle depends on the amount of C_{16}TAB adsolubilization.[67] Meanwhile author Cherkaoui was able to adsolubilize neutral and also ionic steroid molecules onto silica surface by using cationic surfactant cetyltrimethylammonium bromide.[58,64] Another drug adsolubilization example was incorporation of chloroquin into zeolite-C_{12}/C_{14}TAB surfactant complexes.[115] Maximum chloroquin adsolubilization (adsolubilized chloroquin to adsorbed surfactant mole ratio of 1:20) can be obtained with Z-type zeolite and C_{14}TAB concentration at ~10μmol/g. The study also reported that desorption of chloroquin along with surfactant increases with increasing NaCl concentration of the eluent. Jansen et. al. also reported the adsolubilization study of three steroids, hydrocortisone, testosterone, and progesterone on nonionic surfactant, Triton X-100 or Poloxamer 188-adsorbed polystyrene latex particles.[140] Surfactant adsorption facilitated the steroids adsolubilization up to 50 wt% of total solute concentration added compared to no adsolubilization in the absence of surfactant.

In 2007 K. Yamada presented a new photoelectrochemical method to oxidize organic compound, 2-napthol via visible light. Decomposition of 2-napthol was achieved on the surfactant-adsorbed α-Fe_2O_3/SnO_2 film coated on glass substrate.[167] The system exhibited high photoreactivity with high photocurrent stability and may be worked as nanoreactor for water purification or organic synthesis.

Other adsolubilization application including the admicellar catalysis of trimethylorthobenzoate (TMOB) via acid hydrolysis to methyl benzoate (MB) by SDS on porous alumina.[168,169] Adsolubilization of TMOB reported to increase with increasing SDS adsorption but decreases at very high SDS adsorption (> 300 μmoles/g). Despite having lower adsolubilization at very high SDS adsorption, higher packing density of the admicelle layer with high charge density

can attracts more hydrogen ions which in turn enhanced the rate of hydrolysis. Admicellar catalysis can also use to synthesize polysubstituted 3-hydroxy-2-pyrrolidinone by using TiO_2 nanoparticles and C_{16}TAB admicelle template.[170] Reaction with 4-methyl benzaldehyde, 4-chloro aniline and diethyl acetylenedicarboxylate ester at the optimum condition of 10 mol% TiO_2 nanoparticles as the catalysts in 0.8mM C_{16}TAB solution reported in 82% yield. Positive-charged C_{16}TAB adsorbs readily on negative-charged TiO_2 and further formed a bilayer. Hydrophobic tail of the admicelle facilitated the adsolubilization of organic reactants at the interface of TiO_2 nanoparticles while Ti^{4+} catalyzed the overall reaction. Synthesis of various polysubstitued pyrrolidones by reacting different aryl amines, aromatic aldehydes and carboxylate ester reported to have high yield > 70%.

3.8 Analytical analysis

Besides the changes of the surface charge at different pH medium depends on the pzc, surface charge is expected to change when ionic surfactant adsorbed on an oppositely charged surface which may result in flocculation or redispersion of particles. By using the zeta potential measurement, Apornpong et. al. observed the adsorption/ desorption of ethoxy propoxylated carboxylate surfactant and propoxylated sulfate surfactant on alumina surface.[84] Positive surface charge of a bare alumina (+57 mV) reversed to negative surface charge and plateau well at saturation adsorption (≈ -90 mV) upon anionic surfactant adsorption. This has well described the formation of complete anionic surfactant bilayers with the head group heading towards the solution. Zeta potential of surfactant-modified alumina increased but remained strongly electronegative charged (≈ -50 mV) even after washing in deionized water for 48 hours indicated only partial desorption takes place. Other research utilizing the same techniques for adsorption/ desorption studies can be found in Esumi et. al.,[61,171] Salgaonkar et. al.,[21] Zhao et. al.,[132,150] Attaphong et. al.,[86] Arpornpong et. al.,[172] Panswad et. al.[89]

Esumi et. al. started to perform measurements of steady-state emission of I_1/I_3 pyrene on pretreated surface in order to study the changes in the physical environment of surfactant bilayers polarity after alcohol adsolubilization.[78] The ratio of I_1/I_3 enable the observation of polarity change in a system in which lower value for less polar environment, ie. 1.8 for water to 0.6 in hydrocarbon media. The group further incorporated Electron Spin Resonance (ESR) testing in studying the microviscosity upon adsolubilization.[171] The ESR spectrum consists of 3-line pattern where the relative anisotropic measured is directly correlated to the microviscosity in the adsorbed layer. The study showed that surfactant adsorption on a surface decreases the micropolarity (surfactant with longer alkyl chain length has lower micropolarity) and is lower than in the micelles. Further with solute adsolubilization may or may not increase the micropolarity, but increases the microviscosity (surfactant with longer alkyl chain length were able to adsolubilize more solute resulting in higher microviscosity) and is higher than in the micelles. Since then, the group studied the microenvironment properties at the adsolubilization site extensively using either fluorescence, ESR or both in their other works[68,108,110,111,113,127,173–177].

See and O'Haver observed the phase transition of styrene adsolubilization on C_{16}TAB-mica interface using the Tapping-mode and Contact-mode of Atomic Force Microscopy (AFM).[178] Adsorbed layers may transformed from hemi-cylindrical structures to large globular structures with increasing concentration of styrene into the admicelle. This is because styrene mostly adsolubilized at the admicelle-water interface when the concentration is low. Styrene starts to partition at the core region and swells the admicelle at high styrene concentration. It may eventually formed the phase-separated styrene droplets within the admicelle at much higher styrene concentration as observed in the very high molar ratio of adsolubilized solute/ adsorbed surfactant. The strong short-range repulsive force observed from the force curve explained by

Hertz model and JKR model under the proper assumption suggests that the adsorbed layer exhibits a viscoelastic behavior.

Asnachinda et. al. has also used the AFM to study the adsolubilization of styrene onto polymerized gemini surfactant-modified mica surfaces.[179] The authors observed the increasing of surface roughness when styrene adsolubilization transition from initial to equilibrium state. This is in agreement with the previous finding by See in which the flat layer of styrene droplets at the initial state eventually equilibrated as the connected emulsion-like droplets.[178] Meanwhile, force-separation curve measurements showed a stronger adhesives forces between the tip and the surface when there is higher loading of styrene. This was explained by the increase of microviscosity and strong capillary forces at the admicelle layer in the presence of large amount of adsolubilized styrene.

Saphanuchart et. al. studied the effect of solute with different polarity and different dipole moment adsolubilized into the cationic surfactant CPC admicelles adsorbed on the mica via AFM.[180] They observed the higher potential of admicelles layers transformations (from full-cylindrical aggregates to featureless bilayer) with the addition of higher hydrophobicity or higher dipole moment solute and found the latter has more dominant factor.

Benalla and Zajac used the titration calorimetry to study the adsolubilization of alcohols into benzyldimethyldodecylammonium bromide (BDDAB)-silica system.[181] Adsolubilization of alcohols into admicelles showed to be more exothermic and has greater enthalpy of displacement compared to solubilization into the micelles. They explained that alcohols may incorporated into two adsolubilization sites, one which is like the micelles or at the surfactant tail-water solution perimeter area in the admicelle layer.

Holzheu et. al. studied the process of adsolubilization of 26 aromatic compounds (different polarity) using chromatographic method (C_{16}TAB-silica system).[182] From the study of surfactant concentration and pH against the retention time, they were able to see the effect of surfactant orientation at the interface on the solute partitioning. The authors deduced that surfactant layers with the head-on orientation favors the non-polar solute, while the head-out orientation favors the polar solute.

Tan and O'Haver were able to develop a modified BET adsorption isotherm equation $\frac{\Gamma_{ad}}{\Gamma_s} = \frac{k_1 S}{(1-k_2 S)[1+S(k_1-k_2)]}$ where S is the solute in bulk, Γ_{ad} is the amount of adsolubilized solute, Γ_s is the amount of adsorbed surfactant and k_1, k_2 are the constants, to explain and predict the adsolubilization of styrene onto silica adsorbed with non-ionic POE surfactant.[183] This model has accounted for the surfactant-solute interaction (k_1) and solute-solute interaction (k_2) where k_1 decreased 50% with increasing number of EO from 8.5 to 12.5 of the non-ionic surfactant, k_1 also increased with the increasing concentration of lipophilic linker or hexane in which hexane has a lesser impact due to the different adsolubilization site. Meanwhile k_2 is constant when the same solute was used in their adsolubilization studies.

3.9 Summary

This review elaborates the different components (substrate, surfactant, monomer, other solute) and parameters which impact the adsolubilization process. Adsorption mechanism of surfactant onto the substrate depends on the interaction of different surfactant type, structure and amount adsorbed on different type of substrate. This review also summarizes the important observations and findings from previous studies and greatly enhanced the knowledge of the adsolubilization process. Better understandings of these mechanism should enable researchers to explore and design new applications utilizing adsolubilization.

CHAPTER 4: EFFECT OF OXYGEN ON ADMICELLAR POLYMERIZATION OF STYRENE ON SILICA SURFACES

Poh Lee Cheah, John H. O'Haver, **Adam E. Smith**
Department of Chemical Engineering, University of Mississippi, University, MS 38677, US
Correspondence to: A. E. Smith (E-mail: *aes@olemiss.edu*)
Additional Supporting Information can be found in the Appendix.

ABSTRACT

Although admicellar polymerization has been termed the surface analog of emulsion polymerization, previous reports utilizing free radical-initiated admicellar polymerization for the synthesis of ultrathin polymer films on surfaces relied on high levels of the free radical initiator (as high as one initiator per monomer) when compared to emulsion polymerization (typically one initiator per 1000 or more monomer molecules). We hypothesize that this higher initiator requirement is due in part to the presence of oxygen in the reported systems. The effect of oxygen on the requisite amount of initiator and the polymer formed through the admicellar polymerization of styrene on silica particles was studied using cetyltrimethylammonium bromide (CTAB) as the adsorbed surfactant bilayer template, 2,2′-azobisisobutyronitrile (AIBN) as a water-insoluble initiator or 4, 4'-azobis (4-cyanovaleric acid) (V-501) as a water-soluble initiator. The solutions were deoxygenated by purging the headspace with nitrogen prior to the initiation of polymerization. The formed polymer film was extracted from the silica surface, characterized using Fourier transform infrared (FTIR) spectroscopy, thermogravimetric analysis (TGA), and gel permeation chromatography (GPC), and the results compared to polymer extracted from control samples performed without deoxygenation. The results demonstrate that removal of oxygen leads

to the formation of higher weight-averaged molecular weight (M_w) polymer films. While insufficient polymer was obtained for analysis of the control polymerization samples at the lowest initiator loading studied, the deoxygenated admicellar polymerizations exhibited both the formation of high M_w polystyrene and high apparent conversion of the monomer. From the results, we believed that oxygen consume the initiator in the system and caused early termination resulting in lower M_w polymer formed in control samples at moderate initiator loadings. Admicellar polymerizations using the water-soluble initiator (V-501) also exhibited higher M_w polymer compared to the systems using the water-insoluble initiator (AIBN) due to less degree of partitioning of water-soluble initiator in the admicelle compared to water-insoluble initiator, resulting in fewer polymerization sites and higher molecular weight polymer.

KEYWORDS: admicellar polymerization, deoxygenated polymerization, radical polymerization, surface modification

4.1 INTRODUCTION

Since the initial report in the mid-1980s,[1,2] the admicellar polymerization technique has proven to be an effective way to modify the surface characteristics of solid substrates for applications such as rubber reinforcement,[6,17,18] corrosion control,[8,19] formation of conducting films,[21–23,153,154] surface modification of cotton fibers,[12,14,24–28] and composite fillers.[29,30] Admicellar polymerization has been summarized as a four-step process: formation of adsorbed surfactant aggregates (admicelles), monomer solubilization into the admicelle (adsolubilization), polymerization, and removal of accessible surfactant. Though this technique has been called the surface analog of emulsion polymerization,[1,2] there are major differences. Admicellar polymerization systems typically utilize surfactant concentrations just below the critical micelle concentration (CMC). Sparingly soluble monomers preferentially partition from the bulk into the interior of the admicelle prior to and during polymerization. Following polymerization, the

adsorbed surfactant can be partially removed by repeated washings with negligible loss of the formed polymer.[7]

A significant difference between emulsion and admicellar polymerization can be seen in the molar ratios of monomer to initiator (M/I) that are typically used. In an emulsion polymerization system, this ratio is typically greater than 500 and may exceed 1000. Previous admicellar polymerization studies demonstrated that low M/I values (below 15) were needed in order to achieve significant conversion of monomer to polymer.[5,6,9–15] Pongprayoon et al. studied the effect of M/I values ranging from 1 to 5 for the synthesis of a polystyrene-coated cotton fabric via admicellar polymerization.[156,184] Cotton fibers with the highest surface hydrophobicity were formed at M/I values of 1. The authors hypothesized that polymerization at higher initiator concentrations formed more polystyrene, resulting in increased hydrophobicity despite the low molecular weight of the polymer thin films (M_w of 6 x 10^3 g/mol). This study also demonstrated that emulsion and admicellar polymerization performed under similar conditions were able to achieve polymer molecular weights of approximately 2 x 10^5 g/mol, however polymer obtained via admicellar polymerization often contained a substantial fraction of lower molecular weight polymer.[184]

Admicellar polymerization has usually been carried out in the presence of oxygen in the headspace and thus dissolved in the solution. Oxygen is a well-known radical inhibitor, forming peroxide radicals that competes with the normal propagation reaction.[185–187] However, sparging admicellar polymerization systems with an inert gas would cause foaming of the surfactant solution and significant loss of monomer, only limited reports have employed an inert environment in admicellar polymerization.[86,153,188–190] Lai et al. performed admicellar polymerization of tetrafluoroethylene in a perfluorocarbon surface admicelles on alumina in a nitrogen-purged reactor.[188] The authors reported a five-fold increase in monomer conversion (from 7% to 35%)

when the initiator concentration increased by a factor of 1000. However, the authors pointed out the possibility of solution-phase polymerization at the highest initiator concentration (2.5 wt% initiator) despite having the system below the CMC. A second study, by Seul et al., reported the polymerization of methyl methacrylate on calcium carbonate in a nitrogen-purged reactor, finding an optimal M/I value of 250 to achieve 100% monomer conversion in five hours.[189] Despite these examples, the impact of removing oxygen from the system on the properties of the polymer formed by admicellar polymerization has not been systematically studied. The study on the effect of oxygen in free radical admicellar polymerization may open a way to implement oxygen-sensitive mechanism such as reversible addition-fragmentation chain transfer (RAFT) polymerization.

Herein, we report the admicellar polymerization of styrene in the presence and in the absence of oxygen using cetyltrimethylammomnium bromide (CTAB) to form admicelles on the surface of porous silica particles. We examine M/I values varying from 15 (typical for admicellar polymerization) to 1000 (typical of emulsion polymerizations). As part of the study, we also investigate the effect of utilizing a water-insoluble initiator, 2,2'-azobisisobutyronitrile (AIBN) versus a water-soluble initiator, 4,4'-azobis(4-cyanovaleric acid) (V-501) on the molecular weight of the formed polymer.

4.2 EXPERIMENTAL

4.2.1 Materials

Precipitated silica Hi-Sil^{TM} 233 (N_2 BET surface area of 135 m^2/g) was obtained from PPG Industries (Pittsburgh, PA). CTAB, AIBN and V-501 were purchased from Sigma Aldrich (St Loius, MO). Styrene was obtained from Acros Organics (New Jersey) and was purified by passing it through a bed of aluminium oxide to remove inhibitor. Ultrapure water was dispensed from a

Direct-Q 3UV dispenser system, resistivity 18.2 MΩ-cm, 25 ^{o}C. All other chemicals were purchased from Fisher Scientific (New Jersey) and used as received.

4.2.2 Methods

Silica, CTAB, initiator, and distilled water in appropriate ratios determined from adsorption and adsolubilization studies (See Supporting Info: Figure A1, A2, and A3) were added to a 250 mL flask. In a typical experiment, silica (10 g) and CTAB (0.99 g, 2.7 mmol) were added to water (150 mL) to form admicelles on the silica surface and equilibrate at a bulk concentration of CTAB of ~90% of the CMC (CMC ~950 µM).[191] Subsequently, the initiator (V-501 or AIBN) was added to give M/I values of 1000, 150 or 15. The deoxygenated samples were purged with nitrogen for 30 minutes. Styrene (0.54 g, 5.2 mmol) was then added before removing the nitrogen purge, yielding a styrene to adsorbed CTAB molar ratio of 2:1. After the addition of the styrene, samples were mixed for 3 hours prior to immersion in a preheated water bath at 70^{o}C. Polymerization was terminated after the desired reaction time by immersion in a cold-water bath and by introduction of air into the samples. Subsequently, the supernatant of the sample was decanted and the surface-modified silica sample was washed with 1 L of 1:1 (v/v) methanol and water mixture followed by 3 L of water. Control samples were prepared in the same manner without nitrogen purging. Samples were collected and dried at ~100^{o}C for at least 6 hours before analysis with an Agilent Technologies Cary 630 FTIR ATR (4000-650 cm^{-1}). Samples were also analyzed with a TA Instruments Q500 thermogravimetric analyzer (TGA), heating from room temperature to 650 ^{o}C at 20 ^{o}C/min, nitrogen flowrate of 60 ml/min. Polymer was recovered from the modified silica via Soxhlet extraction with refluxing THF for 48 hours followed by precipitation in water. The polymer was rinsed with water and dried prior to analysis via a guard column (Styragel, 20 µm, 4.6 mm x 30 mm, 100-10K, THF) and two GPC column (Styragel, HR 5E, 7.8 mm x 300 mm, 2K-

4M, THF) with Wyatt Technology miniDawn TREOS and a Wyatt Technology Optilab T-rEX to absolute determine M_W and polydispersity index (PDI). THF was used as the mobile phase at a flowrate of 1 mL/min, regulating with Thermo Scientific™ Dionex™ UltiMate 3000 pump and WPS-3000 autosampler.

4.3 RESULTS AND DISCUSSION

TGA profile of modified silica samples (M/I of 1000) upon heating from room temperature to 650^{o}C are presented in Figure 4.1. Weight loss below ~150^{o}C was attributed to water loss from the samples. Weight lost between 200 and 300^{o}C is attributed to residual CTAB decomposition (decomposition temperature of CTAB is 230^{o}C). Meanwhile, weight lost above 300^{o}C is due to the decomposition of polystyrene and is representative of the amount of polymer formed on the silica surface. Interestingly, all modified silica samples showed significant polystyrene decomposition above 300^{o}C (only deoxygenated samples at M/I 1000 shown in Figure 4.1) while control samples at M/I 1000 has a minimal weight loss. After a polymerization time of six hours at an M/I value of 1000, a distinctive difference is observed between the deoxygenated sample (4% weight loss; Figure 4.1 curve b) and the control sample (~0.5% weight loss; Figure 4.1 curve c). FTIR further confirmed the formation of polystyrene on the surface of the silica substrate. FTIR spectra for a polystyrene standard, extracted polystyrene, untreated silica, silica modified by AIBN-initiated deoxygenated admicellar polymerization (M/I of 1000, polymerization time of 6 hours) and silica modified by the control admicellar polymerization (M/I of 1000, polymerization time of 6 hours) are presented in Figure 4.2. The qualitative analysis of the extracted polystyrene and modified silica under an inert atmosphere (Figure 4.2, curve b & d) exhibits the characteristic phenyl group absorbance at ~700 cm^{-1}, demonstrating the presence of a polystyrene thin film on the surface. All modified samples showed the presence of polystyrene on the surface except for

the control samples at M/I 1000, where minimal polystyrene is detectable (Figure 4.2, curve e), consistent with the observation in TGA analysis.

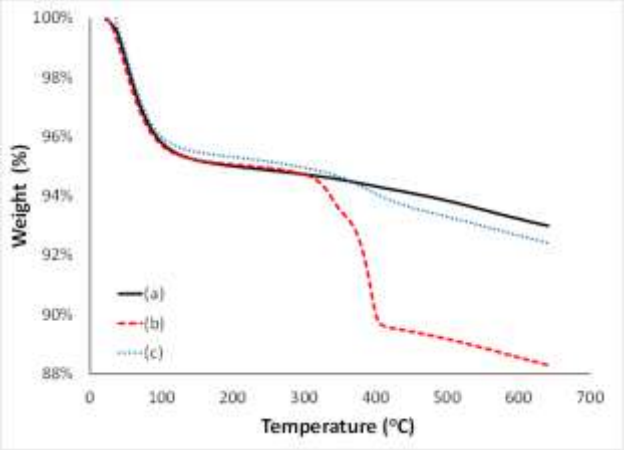

Figure 4.1 TGA profile for (a) Untreated silica, (b) Deoxygenated admicellar polymerization silica (M/I of 1000, 6 hours of polymerization), (c) Control admicellar polymerization silica (M/I of 1000, 6 hours of polymerization).

Based on a material balance, 100% conversion of the styrene into polymer would result in a 5.1% weight loss above 300°C for the modified silica. Therefore, the apparent conversion for each sample can be calculated by polymer weight loss (%)/5.1%. The effect of varying the M/I value on the kinetics of admicellar polymerization was examined by determining the apparent conversion at varying polymerization times (0 to 24 hours) as shown in Figure 4.3. Results show that increasing the M/I value reduced the admicellar polymerization rate. The polymerization at an M/I value of 15 achieved ~97% conversion in two hours. In contrast, the samples with an M/I value of 1000 achieved 60% monomer conversion at two hours and achieved a maximum conversion of ~84% at six hours. These results are consistent with the mechanism of emulsion polymerization where the rate of polymerization (R_p) is proportional to the concentration of active propagating chains with more active chains generated by higher initiator concentrations.

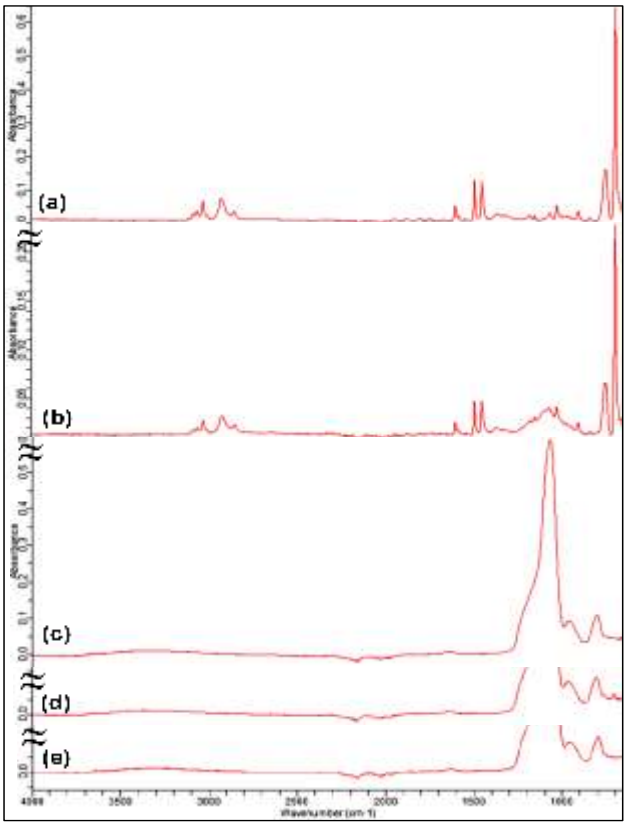

Figure 4.2 FTIR spectra for (a) Polystyrene standard (M_w 6 x 10^5 g/mol), (b) Extracted polystyrene (M/I of 1000, polymerization time of 6 hours), (c) Untreated silica, (d) Deoxygenated admicellar polymerization silica (M/I of 1000, polymerization time of 6 hours), (e) Control admicellar polymerization silica (M/I of 1000, polymerization time of 6 hours).

In order to investigate the effect of deoxygenation on the polymer yield and molecular weight, we examined M/I values of 15, 150, and 1000 for six hour polymerizations initiated by either AIBN or V-501 (Table 4.1). The weight-averaged molecular weight (M_w) of the polymers extracted from the polystyrene-modified silica samples are presented in Figure 4.4. The polymer with the highest M_w (~1.9 x 10^6) was formed on the silica sample at M/I of 1000 in a deoxygenated V-501 system. Measurements of the polydispersity index (PDI) of the polymer samples ranged from ~1.2 to ~2.5 with PDI decreasing with increasing M/I. The observation that the M_w increases with increasing

M/I agrees with the mechanism of free radical polymerization where the degree of polymerization (neglecting the effects of chain transfer) can be expressed as a function of $M/I^{0.5}$ (Equation 4.1).[192]

$$x_n \propto \frac{[M]}{[I]^{0.5}} \qquad \text{(Equation 4.1)}$$

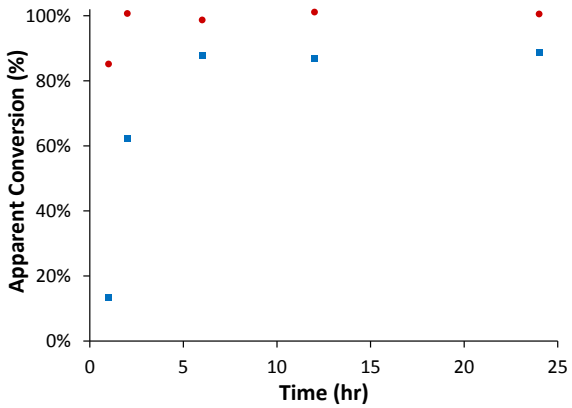

Figure 4.3 Apparent conversion versus polymerization time in AIBN-initiated, deoxygenated admicellar polymerization. (● M/I of 15, ◆ M/I of 1000).

In general, deoxygenated samples have slightly higher apparent monomer conversion and higher M_w than the control samples. This effect can best be observed in the samples at an M/I value of 1000. At an M/I of 1000, the deoxygenated admicellar polymerization initiated by AIBN achieved an apparent conversion of 80% and an M_w of 1.8×10^6 while the control sample had an apparent conversion of 11% and resulted in insufficient polymer recovery for GPC analysis. Oxygen appears to be suppressing the yield and molecular weight of the polymer formed. The presence of oxygen has less effect on the yield of the polystyrene formed at an M/I value of 15 (Table 4.1), likely due to excess initiator available to compensate for the loss of active radicals to oxygen. Previous studies on the emulsion polymerization of styrene suggested that oxygen is present in both the bulk aqueous phase as well as the monomer-rich phase.[193,194] Cunningham et. al.

Table 4.1 Polymer weight loss of modified silica (in terms of apparent monomer conversion %) and weight-averaged molecular weight (M_w) of extracted polymer for deoxygenated and control admicellar polymerizations initiated by AIBN and V-501

M/I molar ratios	AIBN system				V-501 system			
	Deoxygenated		Control		Deoxygenated		Control	
	Apparent conversion (%)	M_w (g/mol)	Apparent conversion (%)	M_w (g/mol)	Apparent conversion (%)	M_w (g/mol)	Apparent conversion (%)	M_w (g/mol)
15	91 ± 4.9	$3.7x10^5$	94 ± 3.9	$1.7x10^5$	92 ± 6.8	$8.0x10^5$	92 ± 6.5	$5.5 x10^5$
150	88 ± 5.1	$8.5x10^5$	57 ± 5.9	$7.1x10^5$	86 ± 5.1	$1.2x10^6$	62 ± 1.4	$1.2x10^6$
1000	82 ± 9.3	$1.8 x10^6$	11 ± 2.7	NA	82 ± 7.6	$1.9x10^6$	15 ± 4.0	NA

demonstrated that the molecular weight of polymer was low at early polymerization times due to inhibition effects from the oxygen but eventually increased after consumption of the oxygen.[193] Nevertheless, they were able to achieve a final M_w similar to the oxygen-free system at the end of the reaction. In our case, the molecular weights are lower in the presence of oxygen (Figure 4.4). Styryl radicals preferentially react with oxygen to form peroxide radicals that are less active and the addition of styrene monomer to the chains are slow and leads to an increased likelihood of termination. This resulted in lower conversion and lower molecular weight of polymer formed in the control system. Similar observations were also reported in previous studies.[195,196] Lavrov and Nikolaev studied the effect of atmospheric oxygen on polymerization of 2-hydroxyethyl methacrylate in water initiated by redox system of ammonium persulfate-ascorbic acid and found that the presence of oxygen greatly decreased the effectiveness of initiator and lowered the molecular weight of final polymer.[195] Emulsion polymerization of n-butyl methacrylate in the absence of oxygen by Krishnan et. al. resulted in higher the particle concentration (no induction period, higher reaction rate, more propagating chains) and higher molecular weight.[196] Lower molecular weight was obtained in the system with oxygen because oxygen increases the rate of

dead chain formation by early termination. This effect is more profound than the lower rate of radical entry into the particles due to oxygen induction that would result in the increase of the molecular weight which was not observed in this case.

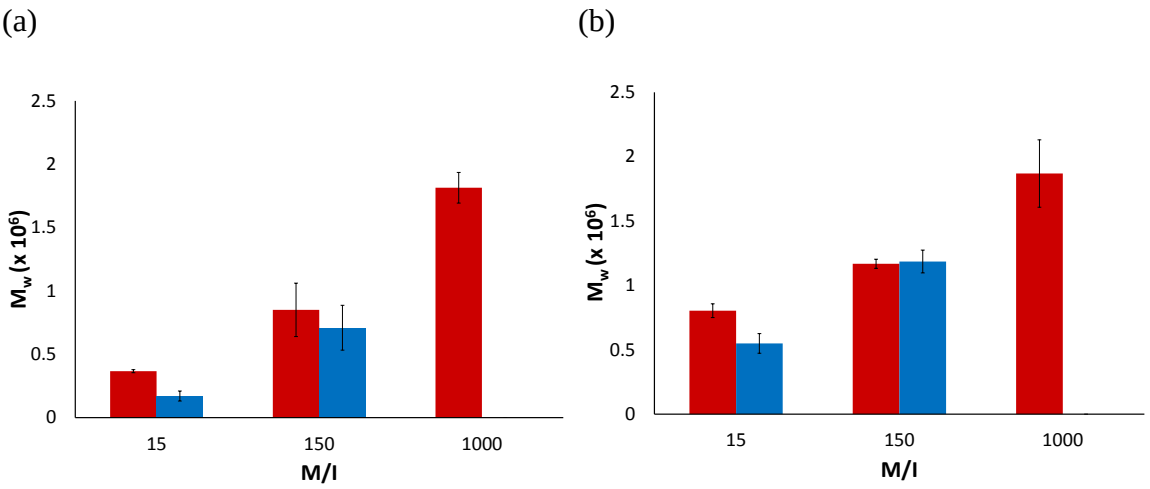

Figure 4.4 Weight-averaged molecular weight (M_w) of extracted polymer from modified silica in (a) AIBN- and (b) V-501-iniitiated deoxygenated and control admicellar polymerization at M//I values of 15, 150, and 1000 (■ Deoxygenated ■ Control).

We also investigated the effect of using a water-soluble and a water-insoluble initiator on the yield and molecular weight of polymer formed via admicellar polymerization. The apparent conversion was similar for comparable M/I values regardless of the initiator solubility (Table 4.1). However, higher M_w polymer was formed in admicellar polymerization with the water-soluble initiator (V-501) especially at an M/I value of 15 (Figure 4.5). Water-soluble initiators partition into the admicelle to a lower degree than the more insoluble initiators, resulting in fewer polymerization sites and higher molecular weight polymer in agreement with Equation 4.1. The molecular weights for both initiators showed no significant difference at M/I value at 1000 indicated that at very low initiator concentration, polymerization sites are limiited by initiator concentration rather than the

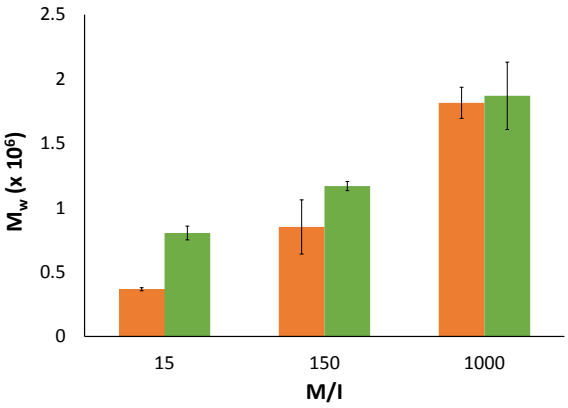

Figure 4.5 Weight-averaged molecular weight of extracted polymer from modified silica in AIBN and V-501-initiated deoxygenated admicellar polymerization at M/I of 15, 150, and 1000. (■ AIBN ■ V-501).

effect of diffusion/ partitioning of initiator with different water solubility. The importance of initiator solubility on polymer yield on admicellar polymerization of methyl methacrylate on aluminium pigment was previously studied by Karlsson et al.[190] In contrary to our result, the report demonstrated that the utilization of a hydrophobic initiator resulted in polymer with higher yield due to higher concentration of initiator partitioned at hydrophobic domain of surfactant bilayer adsolubilized with monomer. Nevertheless, they observed the formation of lower molecular weight oligomers that decomposed at moderate temperature from the TGA weight loss analysis, hinting at the formation of lower molecular weight polymer. This observation was attributed to a greater fraction of hydrophobic initiator partitioning to the admicelle core thereby increasing the number of polymerization sites in the admicelle and lowering molecular weight of polymer in agreement to Equation 4.1. These findings by Karlsson et. al. however were solely based on weight loss data and did not include absolute determination of the polymer molecular weight.

4.4 CONCLUSIONS

Previous reports utilizing free radical-initiated admicellar polymerization relied on M/I values between 1 and 15 for the modification of substrates with polymer. This study examined the effect of oxygen on the requisite amount of initiator and the polymer formed through the admicellar polymerization of styrene on silica particles in CTAB admicelles. Oxygen in the polymerization system consumed active radicals and formed the peroxide radicals, resulting in decreased molecular weight and apparent monomer conversion. Meanwhile, deoxygenated admicellar polymerizations featured the typical mechanism of free radical polymerization and enabled the formation of high molecular weight polystyrene and high apparent conversions of monomer. Additionally, admicellar polymerizations using a water-soluble initiator increased molecular weight compared to polymerizations utilizing a water-insoluble initiator. This study demonstrated deoxygenated free radical admicellar polymerization which could be used to implement other oxygen-sensitive technique in the future.

ACKNOWLEDGEMENTS

Acknowledgment is made to the Donors of the American Chemical Society Petroleum Research Fund for support of this research.

CHAPTER 5: FORMATION OF POLYSTYRENE FILMS BY ADMICELLAR RAFT POLYMERIZATION

Poh Lee Cheah, John H. O'Haver, Adam E. Smith
Correspondence to: A. E. Smith (E-mail: *aes@olemiss.edu*)
Department of Chemical Engineering, University of Mississippi, University, MS 38677
Additional Supporting Information are included in the Appendix.

ABSTRACT

Since the initial reports in the 1980's, admicellar polymerization, the surface analog of emulsion polymerization, has been utilized for many applications including filler/matrix compatibility, corrosion control, electrically conductive films, and fabric coatings. Admicellar polymerization produces a polymer film on the order of few nanometer, significantly thinner than other surface coating techniques. Our earlier study on deoxygenated admicellar polymerization by purging the headspace with nitrogen prior to the initiation of the admicellar polymerization of styrene demonstrated that the presence of oxygen drastically lowers the molecular weight and mass of the polymer film formed on the surface of porous silica substrates. These results open the way for the formation of more advanced thin films via a controlled radical polymerization technique, reversible addition-fragmentation chain transfer (RAFT) polymerization. This technique is noted as a highly controlled synthetic method and is compatible with a wide variety of functional monomers under similar conditions to those utilized in admicellar polymerization. Our initial investigation focuses on admicellar RAFT polymerization of styrene, 4-methylstyrene, and 4-methoxystyrene inside cetyltrimethylammonium bromide (CTAB) admicelles on the surface of silica particles using AIBN and 2,2'-Azobis(2-methylpropionamidine) dihydrochloride (V-50) as

the free radical initiator and 4-cyano-(dodecylsulfanylthiocarbonyl)sulfanyl pentanoic acid (CDP) and 2-phenyl-2-propyl benzothioate (CDB) as the chain transfer agent. The preliminary results demonstrate the ability to reduce the molecular weight of the formed polymer films and suggest the living characteristics of RAFT polymerization inside admicelles compared to the traditional admicellar polymerization technique though there were poor control on the molecular weight distribution.

5.1 INTRODUCTION

Surface modification via admicellar polymerization, the surface analog of emulsion polymerization, was first published in the literature in the mid-1980s by Wu et. al.[1] This seminal work demonstrated the formation of ultrathin polymer films in adsorbed surfactant bilayers via admicellar polymerization. Since then, the admicellar polymerization technique has proven to be an effective method to modify the surface characteristics of substrates for applications such as rubber reinforcement,[6,17,18] corrosion control,[8,19] formation of conducting films,[21–23,153,154] surface modification of cotton fibers,[12,14,24–28] and composite fillers.[29,30] Admicellar polymerization consists of a 4 step process: admicelle formation on the surface; monomer adsolubilization; polymerization in the admicelle; and finally the removal of accessible surfactant. In spite of the similarities between emulsion and admicellar polymerization, the polymer formed under the same polymerization conditions were different in molecular weight and polydispersity.[184] In our previous study, we investigated the effect of oxygen on the molecular weight, polydispersity and the surface coverage of polymer formed via admicellar polymerization (Chapter 4). We were able to utilize an oxygen-depleted environment in order to achieve high conversion and high molecular weight at high M/I values. These findings offer the potential to utilize oxygen-sensitive controlled

radical polymerization RAFT technique in admicellar polymerization in order to make advanced film.

Reversible addition-fragmentation chain transfer (RAFT) polymerization was introduced more recent in the late-90s.[31–33] Unlike the conventional free-radical polymerization, RAFT polymerization has the 'pseudo living' nature to minimize premature termination of chain propagation, giving each chain the same chance to propagate throughout the polymerization process. As a result, one can achieve a desired molecular weight polymer with low polydispersity (PDI) close to 1. RAFT polymerization has become a great focus due to its versatility and ability to control the molecular architecture with a wide variety of functional monomers. The mechanism of RAFT polymerization is illustrated in (Chapter 1, Scheme 1.1). RAFT process is initiated by conventional free radical initiators to obtain the primary radical (I·) which reacts with the monomer to give a propagating oligomeric chain (P_n·). A chain transfer agent (CTA) reacts with P_n· to yield the intermediate radical. Typical CTAs consist of RSC(=S)Z in which Z group activates P_n· radical addition and avoid fast growing propagation. On the other hand, the R-group has to effectively fragment from the intermediate radical to reinitiate the polymerization process. Based on the controlled nature of the RAFT mechanism, one can predict the theoretical $M_{n,th}$ of the final polymer by Equation 5.1 where $[M_n]_o/[CTA]_o$ is the ratio of initial monomer to CTA concentration, x is the apparent conversion, $MW_{r.u.}$ is the molecular weight of repeating unit.

$$M_{n,th} = \frac{[M]_o}{[CTA]_o} \times x \times MW_{r.u.} \qquad \text{(Equation 5.1)}$$

While RAFT polymerization proved to be highly effective in bulk and solution polymerization, previous research showed the early development of RAFT in emulsion polymerization has been a challenge as reviewed by the Gilbert group.[197] Problems encountered including poor colloidal

stability (phase separation or coagulation), poor control of M_n, or poor control of polydispersity. The review addressed the problems of emulsion RAFT polymerization in the mechanistic approach: inhibition and retardation of the polymerization rate, and entry and exit of the radical into/from the micelle.

Surface modification technique using RAFT polymerization mainly focused in making polymer chains covalently bonded to the surface using a grafting method.[198–201] Instead of the chemisorption mechanism done in the past, we demonstrated a surface modification technique, the admicellar RAFT polymerization which is facile and versatile yet highly compatible with various type of surfaces. Promising and successful deoxygenation admicellar polymerization in our earlier study (Chapter 4) leads us to implement this oxygen-sensitive technique. The choice of initiators and RAFT agent is particularly critical considering the partition and diffusion of these chemicals in the monomer saturated admicelle and affecting the addition and fragmentation mechanism of RAFT. In our study, we used a amphiphilic CTA, CDP (Figure 5.1a) and hydrophobic CTA, CDB (Figure 5.1b) paired with either a water-soluble initiator, V-50 (Figure 5.2a) or a water-insoluble initiator, AIBN (Figure 5.2b) in the admicellar polymerization of styrene, 4-methylstyrene, and 4-methoxystyrene on silica particles.

a)

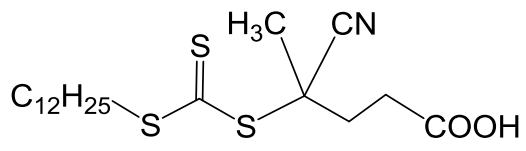

b)

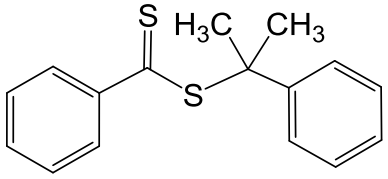

Figure 5.1 Structure for amphiphilic CTA, a) 4-cyano-(dodecylsulfanylthiocarbonyl) sulfanyl pentanoic acid (CDP) and hydrophobic CTA, b) 2-phenyl-2-propyl benzothioate (CDB).

a) b)

Figure 5.2 Structure for water-soluble initiator, a) 2,2'-Azobis(2-methylpropionamidine) dihydrochloride (V-50) and water-insoluble initiator, b) Azobisisobutyronitrile (AIBN).

5.2 EXPERIMENTAL

5.2.1 Materials

Precipitated silica Hi-Sil^{TM} 233 (N_2 BET surface area of 135 m^2/g) was obtained from PPG Industries (Pittsburgh, PA). CTAB, AIBN, V-50, CDP, CDB, styrene, 4-methylstyrene and 4-methoxystyrene were purchased from Sigma Aldrich (St Loius, MO). All the monomers were purified by passing through a bed of aluminium oxide to remove inhibitor. Ultrapure water was dispensed from a Direct-Q 3UV dispenser system, resistivity 18.2 MΩ-cm, 25 ^oC. All other chemicals were purchased from Fisher Scientific (New Jersey) and used as received.

5.2.2 Methods

Silica, CTAB, initiator, and distilled water in appropriate ratios determined from adsorption and adsolubilization studies (See Supporting Info: Figure A1, A2, A3) were added to a 250 mL flask. Silica (10 g) and CTAB (0.99 g, 2.7 mmol) were mixed with water (150 mL) to form admicelles on the silica surface and equilibrate at a bulk concentration of ~90% of the CMC. V-50 or AIBN was added to give a CTA/I ratio of 10 or 2. The deoxygenated samples were purged with nitrogen for an hour. Styrene (0.54 g, 5.2 mmol), 4-methylstyrene (0.7 g, 5.2 mmol), or 4-methoxystyrene (0.6 g, 5.2 mmol) was mixed with either CDP or CDB yielding a monomer to adsorbed CTAB molar ratio of 2:1, monomer to CTA ratio of 50, 150, 1000. After the addition of the monomer and

CTA, samples were mixed for 3 hours prior to immersion in a preheated bath at 56°C (initiated by V-50) or 70°C (initiated by AIBN). Polymerization was terminated after the 48 hours of reaction time by immersion in a cold-water bath and by introduction of air into the samples. Subsequently, the supernatant of the sample was decanted and the surface modified silica sample was washed with 1 L of 1:1 (v/v) methanol and water mixture followed by 3 L of water. Modified silica samples were collected and dried at ~60°C for at least 6 hours before TGA analysis with a TA Instruments Q500 thermogravimetric analyzer (TGA), heating from room temperature to 650°C at 20°C/min, nitrogen flowrate of 60 ml/min. Polymer was recovered from the modified silica via Soxhlet extraction with refluxing THF for 48 hours and precipitated in water. The polymer was rinsed with water and dried prior to GPC analysis. GPC consists of a guard column (Styragel, 20µm, 4.6mm x 30mm, 100-10K, THF) and two GPC column (Styragel, HR 5E, 7.8mm x 300 mm, 2K-4M, THF) with Wyatt Technology miniDawn TREOS and a Wyatt Technology Optilab T-rEX to absolute determine M_n and polydispersity index (PDI). THF was used as the mobile phase at flow rate of 1mL/min with Thermo Scientific™ Dionex™ UltiMate 3000 pump and WPS-3000 autosampler.

5.3 RESULTS and DISCUSSIONS

Degree of polymerization by RAFT mechanism with a highly efficient CTA is governed by the ratio of M/CTA while degree of polymerization in conventional free radical polymerization is a function of $M/I^{0.5}$ (Equation 4.1). For comparison, the M_n's of the extracted polymer formed by admicellar free radical system at M/I 15, 150, and 1000 are compared to admicellar RAFT polymerization at M/CTA 15, 150, and 1000. The difference between admicellar RAFT polymerization and conventional admicellar free radical (deoxygenated) polymerization is shown in Figure 5.3. The M_n's in the RAFT systems are significantly reduced compared to the free radical systems, hinting at the control of RAFT mechanism.

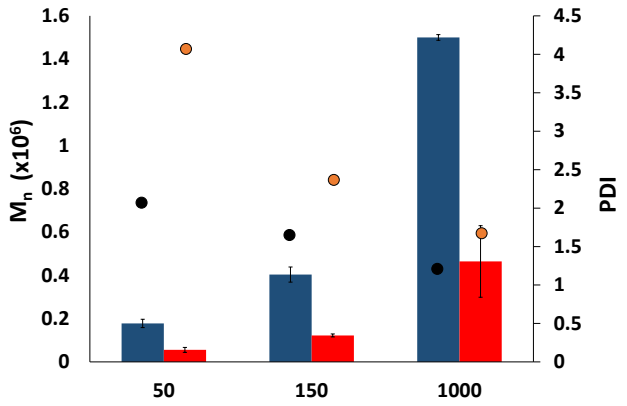

Figure 5.3 Number-averaged molecular weight M_n (left-axis, column) and PDI (right-axis, circle) of extracted polymer from modified silica by admicellar free-radical M/I of 15, 150, 1000 (Chapter 4) and RAFT polymerization at M/CTA of 15, 150, and 1000 (CDP as CTA, AIBN as the initiator with CTA:I of 2). (M_n of Free-radical PDI of Free radical M_n of RAFT PDI of RAFT).

In order to further investigate admicellar RAFT polymerization on silica, different pairings of CTA and initiator were used to optimize the polymerizations. The apparent conversions and the corresponding M_n of extracted polystyrene from different admicellar RAFT samples are summarized in Table 5.1. Results showed that admicellar RAFT polymerization using CDB as the CTA has very low conversion and produced insufficient polymer especially at high concentration of CDB. Conversion can be improved with decreasing CDB concentration (ie. high M/CTA) or increasing the initiator concentration (CTA/I from 10 to 2). This observation of the retardation effect from CDB is in agreement with previous studies on bulk/solution polymerization of styrene,[39] methyl acrylate,[202] methyl methacrylate[38] which demonstrated a strong inhibition and retardation effect at high concentration of CDB. Moad et. al. found that the expelled cumyl radical does not readily reinitiate in chain propagation process despite being a good leaving group.[39] The cumyl radical prefers to add to CTA rather than react with the monomer resulting in strong

retardation effect. Nevertheless, they were able to solve this retardation issue by switching to a cyanoisopropyl radical.

Table 5.1 Polymer weight loss of modified silica (in terms of apparent monomer conversion %) and number-averaged molecular weight M_n of extracted polymer for admicellar RAFT polymerization of styrene initiated by AIBN-CDB and V50-CDB system at M: CTA 50, 150, 1000; CTA/I molar ratio of 10 and 2, polymerization time of 48 hours

CTA/I molar ratio	M/CTA molar ratio	AIBN-CDB				V50-CDB			
		Apparent conversion (%)	M_n (g/mol)	PDI	$M_{n,th}$ (g/mol)	Apparent conversion (%)	M_n (g/mol)	PDI	$M_{n,th}$* (g/mol)
10	50	24 ± 7.8	NA	NA	$1.2x10^3$	17 ± 1.3	NA	NA	$9.0x10^2$
	150	26 ± 4.8	NA	NA	$4.0x10^3$	18 ± 2.1	NA	NA	$2.8x10^3$
	1000	77 ± 5.2	$5.5x10^5$	1.4	$8.0x10^4$	40 ± 8.1	$4.5x10^5$	1.9	$4.2x10^4$
2	50	51 ± 6.7	NA	NA	$2.7x10^3$	30 ± 5.1	NA	NA	$1.5x10^3$
	150	82 ± 1.5	$2.4x10^4$	2.5	$1.3x10^4$	31 ± 4.3	NA	NA	$4.8x10^3$
	1000	66 ± 2.8	$6.2x10^5$	1.8	$6.9x10^4$	69 ± 11	$2.0x10^5$	2.2	$7.2x10^4$

* $M_{n,th}$ calculated at the corresponding conversion

On the other hand, RAFT emulsion polymerization in an AIBN/CDP system observed no retardation (Table 5.2). Previous studies showed that the cyanoalkyl radical is a good leaving group and can effectively reinitiate the polymerization.[39,38] In our case, CDP consists of a cyanoalkyl leaving group with an ionizable carboxylic end group. At high CTA and low initiator concentration (M/CTA 50 and CTA/I 10), the extracted polymer has M_n higher than $M_{n,th}$ indicating lack of control in the molecular weight (Table 5.2, Figure 5.4). Polymerization in the admicelles consists mainly AIBN initiator-derived chain growing rather than the RAFT control mechanism because of water-soluble radical ·R prefers to partition and cross-terminate in the water phase. Monteiro et. al. reported that ·R radical with higher exit rate from the particles into the aqueous phase will cause a strong retardation in seeded emulsion polymerization of styrene.[47,48] They explained in their work that these exited ·R radical may undergo cross-termination in the water phase at high radical

concentration in the aqueous phase or termination between growing chain by reentry to the particles at low radical concentration. Nevertheless, at lower CTA concentration M/CTA 150 and 1000, M_n increases with increasing M/CTA which agrees the trend in Equation 5.1 but doesn't follow the $M_{n,th}$ because of higher experimental M_n. M_n is observed to increase with increasing initiator concentration (from CTA/I 10 to 2), the behavior is different than the typical mechanism of free radical polymerization in which degree of polymerization decreased with increasing initiator concentration. This shows that control of M_n in admicellar RAFT polymerization mainly depends on the CTA concentration. Any ·R radical that left the admicelle was able to re-enter and reinitiate the polymerization in the admicelle. The ratio of CTA to initiator is usually kept high to prevent initiator-derived chains, ensuring the livingness of control polymerization (CTA/I of 10 is suggested).[203]

Table 5.2 Polymer weight loss of modified silica (in terms of apparent monomer conversion %) and number-averaged molecular weight (M_n) of extracted polymer for admicellar RAFT polymerization of styrene initiated by AIBN-CDP system at M/CTA 50, 150, 1000; CTA/I molar ratio of 10 and 2, polymerization time of 48 hours

CTA/I molar ratio	M/CTA molar ratio	AIBN-CDP			
		Apparent conversion (%)	M_n (g/mol)	PDI	$M_{n,th}$* (g/mol)
10	50	93 ± 1.2	$4.8x10^5$	1.7	$4.8x10^3$
	150	81 ± 3.4	$9.8x10^4$	2.4	$1.3x10^4$
	1000	39 ± 2.4	$2.5\ x10^5$	2.0	$4.1x10^4$
2	50	85 ± 11	$5.6x10^4$	4.1	$4.4x10^3$
	150	84 ± 7.0	$1.2x10^5$	2.4	$1.3x10^4$
	1000	75 ± 1.0	$4.6x10^5$	1.7	$7.8x10^4$

* $M_{n,th}$ calculated at the corresponding conversion

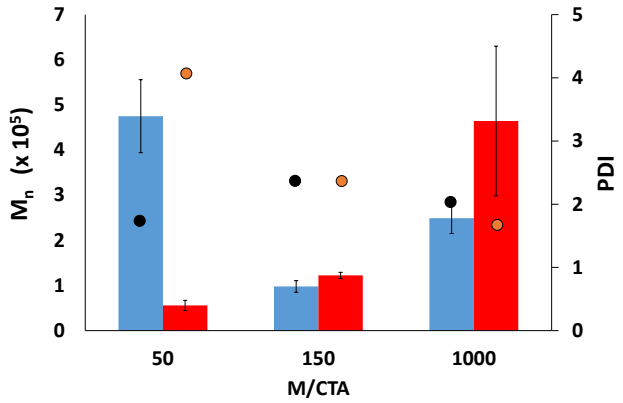

Figure 5.4 Number-averaged molecular weight M_n (left-axis, ■ CTA/I=10, ■ CTA/I=2) and PDI (right-axis, ● CTA/I=10, ● CTA/I=2) of extracted polymer from admicellar RAFT polymerizations initiated by AIBN-CDP system at M/CTA 50, 150, 1000.

Based on the polarity of different species, we further investigate the admicellar RAFT polymerization of a less polar monomer, 4-methylstyrene and polar monomer, 4-methoxystyrene. The apparent conversion and the M_n and PDI of extracted polymer are summarized in Table 5.3. M_n and PDI were plotted for a better illustration and comparison (Figure 5.5). Interestingly, results showed that admicellar RAFT polymerization of poly(4-methylstyrene) in AIBN-CDB system has a promising conversion with no retardation and M_n is closer to $M_{n,th}$ in contrast to the observation for styrene-AIBN-CDB system. 4-methylstyrene is noted to have a lower water solubility (753 µM) compared to styrene with higher water-solubility (~2870 µM).[204] We expect 4-methylstyrene to partition more in the admicelle due to a lower water solubility, in agreement with our review in Chapter 3. This result also indicated that the behavior of CDB cannot be generalized and each CTA/monomer system has to be investigated individually as reviewed by Barner-Kowollik et. al.[205]

Meanwhile, the 4-methoxystyrene-AIBN-CDP system showed decreasing conversion with increasing M/CTA (Table 5.3). At M/CTA 50 and 150, a similar trend to the styrene-AIBN-CDP

system was observed where M_n increases with increasing M/CTA. However, at low CTA concentration (M/CTA 1000), results showed that low conversion and insufficient polymer was formed. This may be due to a higher propensity of the polymethoxystyryl radical to undergo primary radical termination. This is in good agreement with the previous findings in bulk polymerization of substituted styrenes with AIBN.[206] This study reported the primary radical termination in increasing order of 4-methylstyrene< styrene< 4-methoxystyrene.

Table 5.3 Polymer weight loss of modified silica (in terms of apparent monomer conversion %) and number-averaged molecular weight M_n of extracted polymer for admicellar RAFT polymerizations of 4-methylstyrene and 4-methoxystyrene initiated by AIBN-CDP and AIBN-CDB system respectively at M/ CTA 50, 150, 1000; CTA/I molar ratio of 2, polymerization time of 48 hours

CTA/I molar ratio	M/CTA molar ratio	methylstyrene-AIBN-CDB				methoxystyrene-AIBN-CDP			
		Apparent conversion (%)	M_n (g/mol)	PDI	$M_{n,th}$ (g/mol)	Apparent conversion (%)	M_n (g/mol)	PDI	$M_{n,th}$* (g/mol)
2	50	89 ± 1.1	$8.7x10^3$	2.5	$5.3x10^3$	76 ± 2.7	$1.4x10^4$	5.7	$5.1x10^3$
	150	97 ± 6.2	$3.3x10^4$	2.6	$1.7x10^4$	61 ± 4.7	$3.8x10^4$	3.6	$1.2x10^4$
	1000	76 ± 2.5	$2.6x10^5$	1.7	$9.0x10^4$	17 ± 1.2	NA	NA	$2.3x10^4$

* $M_{n,th}$ calculated at the corresponding conversion

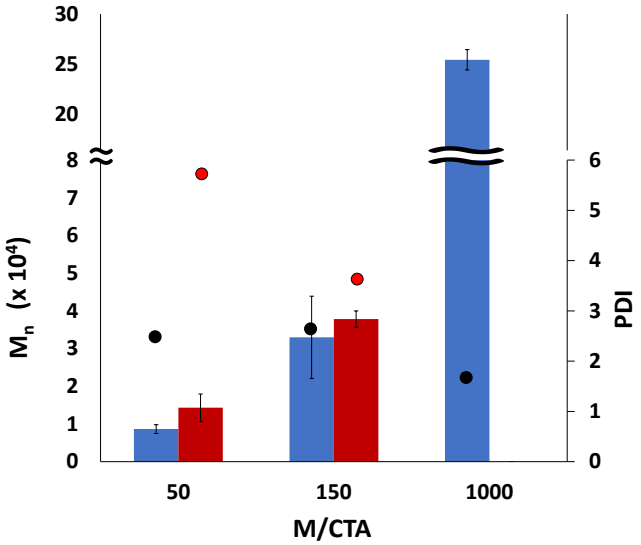

Figure 5.5 Number-averaged molecular weight M_n (left axis, ■ poly (4-methyl)styrene with AIBN-CDB, ■ poly(4-methoxy)styrene with AIBN-CDP) and PDI (right axis, ● poly (4-methyl)styrene with AIBN-CDB, ● poly(4-methoxy)styrene with AIBN-CDP) of extracted polymer from admicellar RAFT polymerizations with CTA:I=2 and M: CTA 50, 150, 1000.

5.4 CONCLUSIONS

RAFT polymerization was attempted in the admicellar polymerization process in our study. Admicellar RAFT polymerization provide better molecular weight control (reduced molecular weight) compared to conventional admicellar free radical polymerization. However, due to the complexity of the admicellar RAFT system, theoretical $M_{n,th}$ and low PDI's were not achieved. M_n is always higher than $M_{n,th}$ and a broad PDI were obtained. Selection of CTA, initiator, and the monomer in dispersed media like admicellar RAFT polymerization are essential to achieve good control of M_n. CTA's with high transfer constants are essential to obtain effective control in RAFT. Besides being a good leaving group, the ·R radical has to be able to reinitiate the polymerization. In addition, an ·R radical with a higher exit rate to the water phase greatly affect the effectiveness of the CTA. Cross termination of water-soluble ·R radical in the water phase may occurred when

radical concentration in the water phase is high or reentry of these ·R radical leads to termination with a growing chain within the admicelle, explained by Monteiro et. al.[47,48] We found that the mechanism of each monomer/initiator/CTA system cannot be generalized. Admicellar RAFT polymerization of 4-methylstyrene-AIBN-CDB system gives the most promising RAFT control among our studies compared to the high retardation effect observed in styrene-AIBN-CDB system may be explained by higher adsolubilization efficiency of 4-methylstyrene. The fact that our observed M_n was always higher than $M_{n,th}$ with broad PDI demonstrates that further studies are required to obtain the optimized result.

6. LIST OF REFERENCES

(1) Wu, J.; Harwell, J. H.; O'Rear, E. A. *Langmuir* **1987**, *3*, 531–537.
(2) Wu, J.; Harwell, J. H.; O'Rear, E. A. *J. Phys. Chem.* **1987**, *111*, 623–634.
(3) Odian G. *Principles of Polymerization, Chapter 4: Emulsion Polymerization*; John Wiley & Sons, Inc., 2004; Vol. 4th Ed.
(4) Smith, W. V.; Ewart, R. H. *J. Chem. Phys.* **1948**, *16*, 592.
(5) Yooprasert, N.; Pongprayoon, T.; Suwanmala, P.; Hemvichian, K.; Tumcharern, G. *Chem. Eng. J.* **2010**, *156*, 193–199.
(6) Pongprayoon, T.; Yooprasert, N.; Suwanmala, P.; Hemvichian, K. *Radiat. Phys. Chem.* **2012**, *81*, 541–546.
(7) O'Haver, J. H.; Hamell, J. H.; O'Rear, E. A.; Snodgrass, L. J.; Waddell, W. H. *Langmuir* **1994**, *10*, 2588–2593.
(8) Matarredona, O. .; Mach, K.; Rieger, M. .; O'Rear, E. A. *Corros. Sci.* **2003**, *45*, 2541–2562.
(9) Wattanakul, K.; Manuspiya, H.; Yanumet, N. *J. Appl. Polym. Sci.* **2011**, *119*, 3234–3243.
(10) Siriviriyanun, A.; O'Rear, E. A.; Yanumet, N. *J. Appl. Polym. Sci.* **2007**, *103*, 4059–4064.
(11) Siriviriyanun, A.; O'Rear, E. A.; Yanumet, N. *J. Appl. Polym. Sci.* **2008**, *109*, 3859–3866.
(12) Tragoonwichian, S.; Kothary, P.; Siriviriyanun, A.; O'Rear, E. A.; Yanumet, N. *Colloids Surfaces A Physicochem. Eng. Asp.* **2011**, *384*, 381–387.
(13) Tragoonwichian, S.; O'Rear, E. a.; Yanumet, N. *J. Appl. Polym. Sci.* **2008**, *108*, 4004–4013.
(14) Tragoonwichian, S.; O'Rear, E. A.; Yanumet, N. *Colloids Surfaces A Physicochem. Eng. Asp.* **2008**, *329*, 87–94.
(15) Pongprayoon, T.; Yanumet, N.; O'Rear, E. A.; Alvarez, W. E.; Resasco, D. E. *J. Colloid Interface Sci.* **2005**, *281*, 307–315.
(16) Sakhalkar, S. S.; Hirt, D. E. *Langmuir* **1995**, 3369–3373.
(17) Nontasorn, P.; Chavadej, S.; Rangsunvigit, P.; O'Haver, J. H.; Chaisirimahamorakot, S.; Na-Ranong, N. *Chem. Eng. J.* **2005**, *108*, 213–218.
(18) Thammathadanukul, V.; O'Haver, J. H.; Harwell, J. H.; Osuwan, S.; Na-Ranong, N.; Waddell, W. H. *J. Appl. Polym. Sci.* **1996**, *59*, 1741–1750.
(19) Le, D. V; Kendrick, M. M.; O'Rear, E. A. *Langmuir* **2004**, *20*, 7802–7810.
(20) Salgaonkar, L. P.; Jayaram, R. V. *J. Polym. Mater.* **2004**, *21*, 335–341.
(21) Salgaonkar, L. P.; Jayaram, R. V. *J. Colloid Interface Sci.* **2005**, *291*, 92–97.
(22) Pojanavaraphan, T.; Chirasakulkarun, A.; Muksing, N.; Magaraphan, R. *J. Appl. Polym. Sci.* **2009**, *112*, 1552–1564.
(23) Pojanavaraphan, T.; Magaraphan, R. *Polymer (Guildf).* **2010**, *51*, 1111–1123.
(24) Ren, X.; Kou, L.; Kocer, H. B.; Zhu, C.; Worley, S. D.; Broughton, R. M.; Huang, T. S. *Colloids Surfaces A Physicochem. Eng. Asp.* **2008**, *317*, 711–716.
(25) Siriviriyanun, A.; O'Rear, E. A.; Yanumet, N. *Polym. Degrad. Stab.* **2009**, *94*, 558–565.
(26) Maity, J.; Kothary, P.; O'Rear, E. A.; Jacob, C. *Ind. Eng. Chem. Res.* **2010**, *49*, 6075–6079.
(27) Tragoonwichian, S.; O'Rear, E. A.; Yanumet, N. *Colloids Surfaces A Physicochem. Eng. Asp.* **2009**, *349*, 170–175.
(28) Ulman, K. N.; Shukla, S. R. *Adv. Polym. Technol.* **2015**, 21556.
(29) Das, S.; Wajid, A. S.; Shelburne, J. L.; Liao, Y.-C.; Green, M. J. *ACS Appl. Mater. Interfaces* **2011**, *3*, 1844–1851.
(30) Zhao, Y.; Qiu, J.; Feng, H.; Zhang, M.; Lei, L.; Wu, X. *Chem. Eng. J.* **2011**, *173*, 659–

666.
(31) Le, T. P.; Moad, G.; Rizzardo, E.; Thang, S. H. Polymerization with living characteristics. WO 1998001478 A1, 1998.
(32) Chiefari, J.; Chong, Y. K. B.; Ercole, F.; Krstina, J.; Jeffery, J.; Le, T. P. T.; Mayadunne, R. T. A.; Meijs, G. F.; Moad, C. L.; Moad, G.; Rizzardo, E.; Thang, S. H.; South, C. *Macromolecules* **1998**, *31*, 5559–5562.
(33) Corpart, P.; Charmot, D.; Zard, S.; Franck, X.; Bouhadir, G. Method for block polymer synthesis by controlled radical polymerisation from dithiocarbamate compounds. WO 1999035177 A1, 1999.
(34) Muller, A. H. E.; Zhuang, R. G.; Yan, D. Y.; Litvinenko, G. *Macromolecules* **1995**, *28*, 4326–4333.
(35) Moad, C. L.; Moad, G.; Rizzardo, E.; Thang, S. H. *Macromolecules* **1996**, *29*, 7717–7726.
(36) Chiefari, J.; Mayadunne, R. T. A.; Moad, C. L.; Moad, G.; Rizzardo, E.; Postma, A.; Skidmore, M. A.; Thang, S. H. *Macromolecules* **2003**, *36*, 2273–2283.
(37) Mayadunne, R. T. a; Rizzardo, E.; Chiefari, J.; Chong, Y. K.; Moad, G.; Thang, S. H. *Macromolecules* **1999**, *32*, 6977–6980.
(38) Chong, B. Y. K.; Krstina, J.; Le, T. P. T.; Moad, G.; Postma, A.; Rizzardo, E.; Thang, S. H. *Macromolecules* **2003**, *36*, 2256–2272.
(39) Moad, G.; Chiefari, J.; Chong, Y. K.; Krstina, J.; Mayadunne, R. T. a; Postma, a; Rizzardo, E.; Thang, S. H. *Polym. Int.* **2000**, *49*, 993–1001.
(40) Zetterlund, P. B.; Okubo, M. *Macromolecules* **2006**, *39*, 8959–8967.
(41) de Brouwer, H.; Tsavalas, J. G.; Schork, F. J. *Macromolecules* **2000**, *33*, 9239–9246.
(42) Butte, A.; Storti, G.; Morbidelli, M. *Macromolecules* **2000**, *33*, 3485–3487.
(43) Zetterlund, P. B.; Kagawa, Y.; Okubo, M. *Chem. Rev.* **2008**, *108*, 3747–3794.
(44) Luo, Y.; Tsavalas, J.; Schork, F. J. *Macromolecules* **2001**, *34*, 5501–5507.
(45) Luo, Y.; Cui, X. *J. Polym. Sci. Part A Polym. Chem.* **2006**, *44*, 2837–2847.
(46) Uzulina, I.; Kanagasabapathy, S.; J., C. *Macromol. Symp.* **2000**, *150*, 33–38.
(47) Monteiro, M. J.; Hodgson, M.; De Brouwer, H. *J. Polym. Sci. Part A Polym. Chem.* **2000**, *38*, 3864–3874.
(48) Monteiro, M. J.; De Barbeyrac, J. *Macromolecules* **2001**, *34*, 4416–4423.
(49) Prescott, S. W.; Ballard, M. J.; Rizzardo, E.; Gilbert, R. G. *Macromolecules* **2002**, *35*, 5417.
(50) Nozari, S.; Tauer, K.; Ali, A. M. I. *Macromolecules* **2005**, *38*, 10449–10454.
(51) Nozari, S.; Tauer, K. *Polymer (Guildf).* **2005**, *46*, 1033–1043.
(52) Iler, R. K. *The Colloid Chemistry of Silica and Silicates*; Cornell University Press, 1955.
(53) Somasundaran, P. Furstenau, D. W. *J. Phys. Chem.* **1966**, *70*, 90–96.
(54) Harwell, J. H.; Hoskins, J. C.; Schechter, R. S.; Wade, W. H. *Langmuir* **1985**, 251–262.
(55) Behrends, T.; Herrmann, R. *Colloids Surfaces A Physicochem. Eng. Asp.* **2000**, *162*, 15–23.
(56) Meguro, K.; Esumi, K. *J. Coatings Technol.* **1990**, *62*, 69.
(57) Esumi, K.; Sakai, K.; Torigoe, K. *J. Colloid Interface Sci.* **2000**, *224*, 198–201.
(58) Cherkaoui, I.; Monticone, V.; Vaution, C.; Treiner, C. *Int. J. Pharm.* **2000**, *201*, 71–77.
(59) Aloulou, F.; Boufi, S.; Belgacem, N.; Gandini, A. *Colloid Polym. Sci* **2004**, *283*, 344–350.
(60) Okamoto, N.; Yoshimura, T.; Esumi, K. *J. Colloid Interface Sci.* **2004**, *275*, 612–617.
(61) Esumi, K. *J. Colloid Interface Sci.* **2001**, *241*, 1–17.
(62) Talman, R. Y.; Atun, G. *Colloids Surfaces A Physicochem. Eng. Asp.* **2006**, *281*, 15–22.

(63) Talbot, D.; Bee, a; Treiner, C. *J. Colloid Interface Sci.* **2003**, *258*, 20–26.
(64) Cherkaoui, I.; Monticone, V.; Vaution, C.; Treiner, C. *Int. J. Pharm.* **1998**, *176*, 111–120.
(65) Klumpp, E.; Schwuger, M. J. *Colloids and Surfaces* **1993**, *78*, 93–98.
(66) Li, L.; Wang, L.; Du, X.; Lu, Y.; Yang, Z. *J. Colloid Interface Sci.* **2007**, *315*, 671–677.
(67) Andrzejewska, A.; Narkiewicz- Michalek, J.; Szymula, M. *J. Dispers. Sci. Technol.* **2007**, *28*, 239–245.
(68) Yamanaka, Y.; Esumi, K. *Colloids Surfaces A Physicochem. Eng. Asp.* **1997**, *122*, 121–133.
(69) Asvapathanagul, P.; Malakul, P.; O'Haver, J. *J. Colloid Interface Sci.* **2005**, *292*, 305–311.
(70) Nayyar, S. P.; Sabatini, D. a; Harwell, J. H. *Environ. Sci. Technol.* **1994**, *28*, 1874–1881.
(71) Ko, S.-O.; Schlautman, M. a.; Carraway, E. R. *Environ. Sci. Technol.* **1998**, *32*, 2769–2775.
(72) Danzer, J.; Grathwohl, P. *Phys. Chem. Earth* **1998**, *23*, 237–243.
(73) Kitiyanan, B.; Haver, J. H. O.; Harwell, J. H. **1996**, *7463*, 2162–2168.
(74) Tan, Y.; O'Haver, J. H. *Colloids Surfaces A Physicochem. Eng. Asp.* **2004**, *232*, 101–111.
(75) Farías, T.; de Ménorval, L. C.; Zajac, J.; Rivera, A. *J. Colloid Interface Sci.* **2011**, *363*, 465–475.
(76) Aloulou, F.; Boufi, S.; M., C. *Colloid Polym. Sci* **2004**, *282*, 699–707.
(77) Dickson, J.; Haver, J. O. **2002**, 9171–9176.
(78) Esumi, K.; Shibayama, M.; Meguro, K. *Langmuir* **1990**, *6*, 826–829.
(79) Mukerjee, P. *JAOCS* **1982**, *59*, 573–578.
(80) Lai, C.; O'Rear, E. A.; Harwell, J. H.; Hwa, M. J. **1997**, *95*, 4267–4272.
(81) Hanumansetty, S.; O'Rear, E. *Langmuir* **2014**.
(82) Charoensaeng, A.; Sabatini, D. a.; Khaodhiar, S. *J. Surfactants Deterg.* **2008**, *11*, 61–71.
(83) Charoensaeng, A.; Sabatini, D. a.; Khaodhiar, S. *J. Surfactants Deterg.* **2009**, *12*, 209–217.
(84) Arpornpong, N.; Lewlomphaisan, J.; Charoensaeng, A.; Sabatini, D. a.; Khaodhiar, S. *J. Surfactants Deterg.* **2013**, *16*, 291–298.
(85) Fuangswasdi, a.; Charoensaeng, a.; Sabatini, D. a.; Scamehorn, J. F.; Acosta, E. J.; Osathaphan, K.; Khaodhiar, S. *J. Surfactants Deterg.* **2006**, *9*, 29–37.
(86) Attaphong, C.; Asnachinda, E.; Charoensaeng, A.; Sabatini, D. a; Khaodhiar, S. *J. Colloid Interface Sci.* **2010**, *344*, 126–131.
(87) Backhaus, W. K.; Klumpp, E.; Narres, H.-D.; Schwuger, M. J. *J. Colloid Interface Sci.* **2001**, *242*, 6–13.
(88) Parida, S. K.; Mishra, B. K. *Colloids Surfaces A Physicochem. Eng. Asp.* **1998**, *134*, 249–255.
(89) Panswad, D.; Sabatini, D. a.; Khaodhiar, S. *J. Surfactants Deterg.* **2012**, *15*, 787–795.
(90) Fuangswasdi, a; Krajangpan, S.; Sabatini, D. a; Acosta, E. J.; Osathaphan, K.; Tongcumpou, C. *Water Res.* **2007**, *41*, 1343–1349.
(91) Thakulsukanant, C.; Lobban, L. L.; Osuwan, S. **1997**, *7463*, 4595–4599.
(92) Esumi, K.; Maedomari, N.; Torigoe, K. **2000**, 9217–9220.
(93) Esumi, K.; Maedomari, N.; Torigoe, K. **2001**, 7350–7354.
(94) Esumi, K. *Prog. Colloid Polym. Sci.* **2004**, *123*, 44–47.
(95) Sakai, K.; Yamazaki, R.; Imaizumi, Y.; Endo, T.; Sakai, H.; Abe, M. *Colloids Surfaces A Physicochem. Eng. Asp.* **2012**, *410*, 119–124.

(96) 2010, E. Asnachinda Styrene and Phenylethanol Adsolubilization of a Polymerizable Gemini Surfactant.pdf, 2010.
(97) Prarat, P.; Ngamcharussrivichai, C.; Khaodhiar, S.; Punyapalakul, P. *J. Hazard. Mater.* **2013**, *244-245*, 151–159.
(98) Sakai, K. Adsorption of cationic monomeric and gemini surfactants on montmorillonite and adsolubilization of vitamin E, 2008.
(99) Sieburg, L.; Kohut, a; Kislenko, V.; Voronov, a. *J. Colloid Interface Sci.* **2010**, *351*, 116–121.
(100) Tsurumi, D.; Sakai, K.; Yoshimura, T.; Esumi, K. *J. Colloid Interface Sci.* **2006**, *302*, 82–86.
(101) Tsurumi, D.; Yoshimura, T.; Esumi, K. *J. Colloid Interface Sci.* **2006**, *297*, 465–469.
(102) Adak, A.; Bandyopadhyay, M.; Pal, A. *J. Surf. Sci. Technol.* **2005**, *21*, 97–112.
(103) Adak, A.; Bandyopadhyay, M.; Pal, A. *J. Environ. Sci. Heal. Part A* **2005**, *40*, 167–170.
(104) Adak, A.; Pal, A.; Bandyopadhyay, M. *Colloids Surfaces A Physicochem. Eng. Asp.* **2006**, *277*, 63–68.
(105) Adak, A.; Pal, A. *Sep. Purif. Technol.* **2006**, *50*, 256–262.
(106) Adak, A.; Pal, A. *Desalin. Water Treat.* **2009**, *6*, 269–275.
(107) Adak, A.; Pal, A. *J. Environ. Sci. Heal. Part A* **2006**, *41*, 2283–2297.
(108) Esumi, K.; Uda, S.; Goino, M.; Ishiduki, K.; Suhara, T.; Fukui, H.; Koide, Y. *Langmuir* **1997**, *13*, 2803–2807.
(109) Esumi, K.; Uda, S.; Suhara, T.; Fukui, H.; Koide, Y. **1997**, *318*, 315–318.
(110) Esumi, K.; Toyoda, H.; Goino, M.; Suhara, T.; Fukui, H. *Langmuir* **1998**, *14*, 199–203.
(111) Esumi, K.; Toyoda, A.; Goino, M.; Suhara, T.; Fukui, H.; Koide, Y. *J. Colloid Interface Sci.* **1998**, *202*, 377–384.
(112) Esumi, K.; Hayashi, H.; Koide, Y.; Suhara, T.; Fukui, H. *Colloids Surfaces A Physicochem. Eng. Asp.* **1998**, *144*, 201–206.
(113) Esumi, K. *Colloids Surfaces A Physicochem. Eng. Asp.* **2001**, *176*, 25–34.
(114) Farías, T.; de Ménorval, L. C.; Zajac, J.; Rivera, A. *Colloids Surf. B. Biointerfaces* **2010**, *76*, 421–426.
(115) Hayakawa, K.; Mouri, Y.; Maeda, T.; Satake, I.; Sato, M. *Colloid Polym. Sci* **2000**, *278*, 553–558.
(116) Hayakawa, K.; Dobashi, A.; Miyamoto, Y.; Satake, I. *Adsolubilization equilibrium of rhodamine B by zeolite/surfactant complexes*; 1997.
(117) Pura, S.; Atun, G. *Colloids Surfaces A Physicochem. Eng. Asp.* **2005**, *253*, 137–144.
(118) Wang, J.; Han, B.; Yan, H.; Li, Z.; Thomas, R. K.; Road, S. P.; Ox, O. **1999**, 8207–8211.
(119) Venkataraman, N. V.; Mohanambe, L.; Vasudevan, S. *J. Mater. Chem.* **2003**, *13*, 170–171.
(120) Esumi, K.; Yoshida, K.; Torigoe, K.; Koide, Y. *Colloids Surfaces A Physicochem. Eng. Asp.* **1999**, *160*, 247–250.
(121) Cursino, A. C. T.; Lisboa, F. D. S.; Pyrrho, A. D. S.; de Sousa, V. P.; Wypych, F. *J. Colloid Interface Sci.* **2013**, *397*, 88–95.
(122) Zhao, Q.; Chang, Z.; Lei, X.; Sun, X. *Ind. Eng. Chem. Res.* **2011**, *50*, 10253–10258.
(123) Gao, Z.; Du, B.; Zhang, G.; Gao, Y.; Li, Z.; Zhang, H.; Duan, X. **2011**, 5334–5345.
(124) Bruna, F.; Pavlovic, I.; Barriga, C.; Cornejo, J.; Ulibarri, M. *Appl. Clay Sci.* **2006**, *33*, 116–124.
(125) Fernández, L.; Borrás, C.; Carrero, H. *Electrochim. Acta* **2006**, *52*, 872–884.

(126) Klumpp, E.; Contreras-Ortega, C.; Klahre, P.; Tino, F. J.; Yapar, S.; Portillo, C.; Stegen, S.; Queirolo, F.; Schwuger, M. J. *Colloids Surfaces A Physicochem. Eng. Asp.* **2004**, *230*, 111–116.
(127) Esumi, K.; Yamamoto, S. *Colloids Surfaces A Physicochem. Eng. Asp.* **1998**, *137*, 385–388.
(128) Li, Y.; Bi, H.-Y.; Zang, Y.-B. *Sep. Purif. Technol.* **2013**, *116*, 448–453.
(129) Ruan, X.; Huang, S.; Chen, H.; Qian, G. *Appl. Clay Sci.* **2013**, *72*, 96–103.
(130) Zhao, P.; Liu, X.; Tian, W.; Yan, D.; Sun, X.; Lei, X. *Chem. Eng. J.* **2015**, *279*, 597–604.
(131) Zhao, X.; Shi, Y.; Cai, Y.; Mou, S. *Environ. Sci. Technol.* **2008**, *42*, 1201–1206.
(132) Zhao, X.; Shi, Y.; Wang, T.; Cai, Y.; Jiang, G. *J. Chromatogr. A* **2008**, *1188*, 140–147.
(133) Sun, L.; Zhang, C.; Chen, L.; Liu, J.; Jin, H.; Xu, H.; Ding, L. *Anal. Chim. Acta* **2009**, *638*, 162–168.
(134) Iamazaki, E. T.; Pereira-da-silva, M. A.; Carvalho, A. J. F.; Romero, R. B.; Gonc, M. C.; Atvars, T. D. Z. **2009**.
(135) Pal, A.; Pan, S.; Saha, S. *Chem. Eng. J.* **2013**, *217*, 426–434.
(136) Lee, C.; Yeskie, M. A.; Harwell, J. H. *Langmuir* **1990**, 1758–1762.
(137) Saphanuchart, W.; Saiwan, C.; O'Haver, J. H. *Colloids Surfaces A Physicochem. Eng. Asp.* **2008**, *317*, 303–308.
(138) Monticone, V.; Treiner, C. *Colloids Surfaces A Physicochem. Eng. Asp.* **1995**, *104*, 285–293.
(139) Favoriti, P.; Monticone, V.; Treiner, C. *J. Colloid Interface Sci.* **1996**, *179*, 173–180.
(140) Jansen, J.; Treiner, C.; Vaution, C. *J. Colloid Interface Sci.* **1996**, *179*, 578–586.
(141) Funkhouser, G. P.; Arvalo, M. P.; Glatzhofer, D. T.; O'Rear, E. A. **1995**, 1443–1447.
(142) Monticone, V.; Favoriti, P.; Lemordant, D.; Treiner, C. **2000**, *55*, 258–264.
(143) Pradubmook, T.; O'Haver, J. H.; Malakul, P.; Harwell, J. H. *Colloids Surfaces A Physicochem. Eng. Asp.* **2003**, *224*, 93–98.
(144) Lee, C.-L.; Lee, J.-C. *Chemosphere* **2002**, *47*, 277–282.
(145) Salager, J.-L.; Graciaa, A.; Lachaise, J. *J. Surfactants Deterg.* **1998**, *1*, 403–406.
(146) Koner, S.; Pal, A.; Adak, A. *Desalin. Water Treat.* **2010**, *22*, 1–8.
(147) Behrends, T.; Herrmann, R. *Phys. Chem. Earth* **1998**, *23*, 229–235.
(148) Das, A. K.; Saha, S.; Pal, A.; Maji, S. K. Surfactant-modified alumina: An efficient adsorbent for malachite green removal from water environment, 2009, 896–905.
(149) Nagarajan, R. *Langmuir* **1991**, *7*, 2934–2969.
(150) Zhao, X.; Li, J.; Shi, Y.; Cai, Y.; Mou, S.; Jiang, G. *J. Chromatogr. A* **2007**, *1154*, 52–59.
(151) Koner, S.; Pal, A.; Adak, A. *Desalination* **2011**, *276*, 142–147.
(152) Merino, F.; Rubio, S.; Pérez-Bendito, D. *Anal. Chem.* **2003**, *75*, 6799–6806.
(153) Lei, L.; Qiu, J.; Sakai, E. *Chem. Eng. J.* **2012**, *209*, 20–27.
(154) Yuan, W.-L.; O'Rear, E. a.; Grady, B. P.; Glatzhofer, D. T. *Langmuir* **2002**, *18*, 3343–3351.
(155) Somnuk, U.; Yanumet, N.; Ellis, J. W.; Grady, B. P.; Orear, E. **2003**, *24*, 171–180.
(156) Pongprayoon, T.; Yanumet, N.; Yuan, W. *Langmuir* **2003**, *19*, 3770–3778.
(157) Kothary, P.; Yanumet, N.; O'Rear, E. A. *Fibers Polym.* **2013**, *14*, 710–717.
(158) T. Valsaraj, K.; Jain, P. M.; Kommalapati, R. R.; Smith, J. S. *Sep. Purif. Technol.* **1998**, *13*, 137–145.
(159) Smith, J. S.; Valsaraj, K. T. *Sep. Purif. Technol.* **1998**, *13*, 147–159.
(160) Jain, P. M.; Smith, J. S.; Valsaraj, K. T. **1999**, *17*, 21–30.

(161) Marsal, A.; Elena Bautista, M.; Manich, A. M.; Cuadros, S.; Maldonado, F. *Chem. Eng. J.* **2013**, *222*, 77–84.
(162) Koner, S.; Adak, a. *J. Inst. Eng. Ser. A* **2013**, *93*, 187–191.
(163) Maldonado, F.; Manich, A. M.; Marsal, A. *J. Soc. Leather Technol. Chem.* **2012**.
(164) Zhao, X.; Gong, Y.; O'Reilly, S. E.; Zhao, D. *Mar. Pollut. Bull.* **2015**, *92*, 160–169.
(165) Moral, A.; Sicilia, M. D.; Rubio, S.; Pérez-Bendito, D. *Anal. Chim. Acta* **2006**, *569*, 132–138.
(166) Garcia-Preto, A. Hemimicelle-based solid-phase extraction of estrogens from environmental water samples, 2006.
(167) Yamada, K.; Mukaihata, N.; Kawahara, T.; Tada, H. *Langmuir* **2007**, *23*, 8593–8596.
(168) Yu, C. C.; Wong, D. W.; Lobban, L. L. *Langmuir* **1992**, *8*, 2582–2584.
(169) C, Y.; Lobban, L. L. In *Surfactant Adsorption and Surface Solubilization*; 1995; pp. 67–76.
(170) Sarkar, R.; Mukhopadhyay, C. *Tetrahedron Lett.* **2013**, *54*, 3706–3711.
(171) Esumi, K.; Nagahama, T.; Meguro, K. *Colloids and Surfaces* **1991**, *57*, 149–160.
(172) Arpornpong, N.; Charoensaeng, A.; Sabatini, D. a.; Khaodhiar, S. *J. Surfactants Deterg.* **2010**, *13*, 305–311.
(173) Esumi, K.; Yamanaka, Y. *J. Colloid Interface Sci.* **1995**, *172*, 116–120.
(174) Esumi, K.; Mizuno, K.; Yamanaka, Y. *Langmuir* **1995**, *11*, 1571–1575.
(175) Esumi, K.; Goino, M.; Koide, Y. *Colloids Surfaces A Physicochem. Eng. Asp.* **1996**, *118*, 161–166.
(176) Esumi, K.; Goino, M.; Koide, Y. *J. Colloid Interface Sci.* **1996**, *183*, 539–545.
(177) Esumi, K.; Matoba, M.; Yamanaka, Y. *Langmuir* **1996**, *12*, 2130–2135.
(178) See, C. H.; O'Haver, J. H. *Colloids Surfaces A Physicochem. Eng. Asp.* **2004**, *243*, 169–183.
(179) Asnachinda, E.; O'Haver, J. H.; Sabatini, D. A.; Khaodhiar, S. *J. Appl. Polym. Sci.* **2010**, *115*, 1145–1152.
(180) Saphanuchart, W.; Saiwan, C.; O'Haver, J. H. *Colloids Surfaces A Physicochem. Eng. Asp.* **2007**, *307*, 71–76.
(181) Benalla, H.; Zajac, J. *J. Colloid Interface Sci.* **2004**, *272*, 253–261.
(182) Holzheu, S.; Behrends, T.; Herrmann, R. In *Surfactant-Based Separations*; 1999; pp. 314–328.
(183) Tan, Y.; O'Haver, J. H. *J. Colloid Interface Sci.* **2004**, *279*, 289–295.
(184) Pongprayoon, T.; Yanumet, N.; O'Rear, E. A. *J. Colloid Interface Sci.* **2002**, *249*, 227–234.
(185) Mayo, F. R. *J. Am. Chem. Soc.* **1958**, *80*, 2465.
(186) Flory, P. J. *Principles of Polymer Chemistry, Chapter IV: Polymerization of unsaturated monomers by free radical mechanisms*; Cornell University Press, 1953.
(187) Bhanu, V. A.; Kishore, K. *Am. Chem. Soc. Chem. Rev.* **1991**, *91*, 99.
(188) Lai, C.; Harwell, J. H.; O'Rear, E. A.; Komatsuzaki, S.; Arai, J.; Nakakawaji, T.; Ito, Y. *Langmuir* **1995**, *11*, 905–911.
(189) Seul, S. D.; Lee, S. R.; Kim, Y. H. *J. Polym. Sci. Part A Polym. Chem.* **2004**, *42*, 4063–4073.
(190) Karlsson, P. M.; Esbjörnsson, N. B.; Holmberg, K. *J. Colloid Interface Sci.* **2009**, *337*, 364–368.
(191) Okuda, H.; Imae, T.; Ikeda, S. *Colloids and Surfaces* **1987**, *27*, 187–200.

(192) Young, R. J.; Lovell, P. A. *Introduction to polymers*; Third Ed.; CRC Press Taylor & Francis Group, 2011.
(193) Cunningham, M. F.; Geramita, K.; Ma, J. W. *Polymer (Guildf).* **2000**, *41*, 5385–5392.
(194) López de Arbina, L.; Gugliotta, L. M.; Barandiaran, M. J.; Asua, J. *Polymer (Guildf).* **1998**, *39*, 4047–4055.
(195) Lavrov, N. A.; Nikolaev, A. F. *J. Appl. Chem. USSR* **1986**, *59*, 2396.
(196) Krishnan, S.; Klein, A.; El-Aasser, M. S.; Sudol, E. D. *Ind. Eng. Chem. Res.* **2004**, *43*, 6331–6342.
(197) Prescott, S. W.; Ballard, M. J.; Rizzardo, E.; Gilbert, R. G. *Aust. J. Chem.* **2002**, *55*, 415.
(198) Ding, P.; Zhang, J.; Song, N.; Tang, S.; Liu, Y.; Shi, L. *Compos. Part a* **2015**, *69*, 186–194.
(199) Liu, C. H.; Pan, C. Y. *Polymer (Guildf).* **2007**, *48*, 3679–3685.
(200) Yuan, K.; Li, Z. F.; Lü, L. L.; Shi, X. N. *Mater. Lett.* **2007**, *61*, 2033–2036.
(201) Prucker, O.; Rühe, J. *Macromolecules* **1998**, *31*, 592–601.
(202) Drache, M.; Schmidt-Naake, G.; Buback, M.; Vana, P. *Polymer (Guildf).* **2005**, *46*, 8483–8493.
(203) Monteiro, M. J. *J. Polym. Sci. Part A Polym. Chem.* **2005**, *43*, 3189–3204.
(204) Mackay, D.; Shiu, W. Y.; Ma, K. C. *Illustrated Handbook of Physical-Chemical Properties and Environmental Fate for Organic Chemicals*; 1993; Vol. 3.
(205) Barner-Kowollik, C.; Coote, M. L.; Davis, T. P.; Radom, L.; Vana, P. *J. Polym. Sci. Part A Polym. Chem.* **2003**, *41*, 2828–2832.
(206) Berry, R. W. H.; Ludlow, A. J.; Mazza, R. J. *Macromol. Chem. Phys.* **1997**, *198*, 1579–1595.

7. LIST OF APPENDICES

APPENDIX A: SUPPORTING INFO

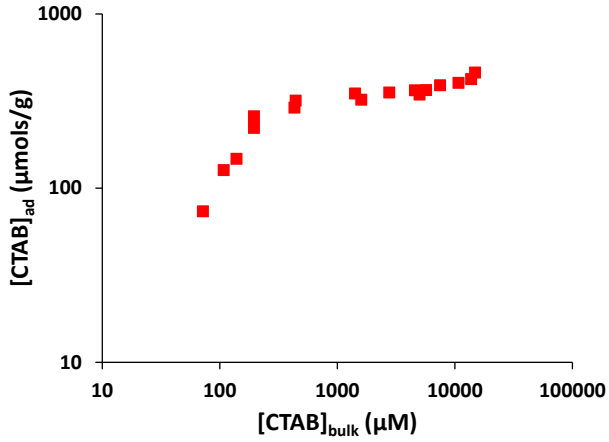

Figure A.1 Adsorption isotherm of CTAB adsorbed on Hi-Sil 233 at maximum of 300 µmols of CTAB adsorbed per gram of Hi-Sil 233.

a)

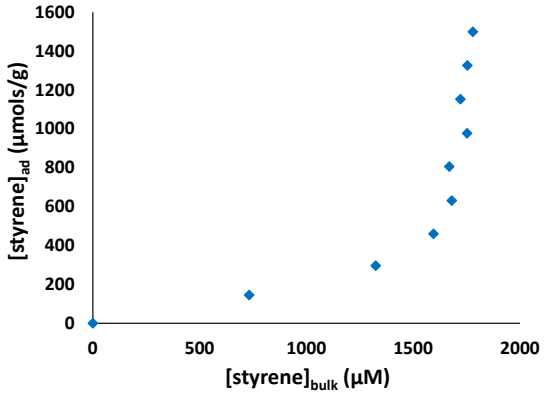

b)

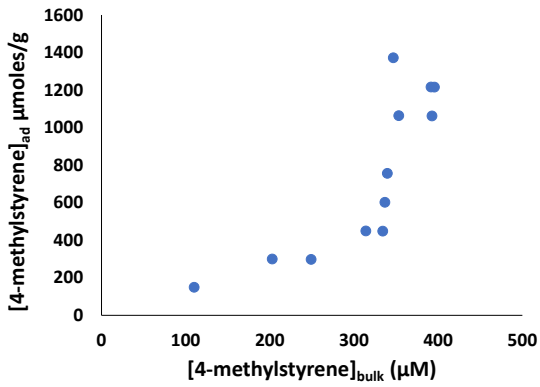

Figure A.2 Adsolubilization of a) styrene and b) 4-methylstyrene on Hi-Sil 233 at 260 µmols of CTAB adsorbed per gram of Hi-Sil 233.

a)

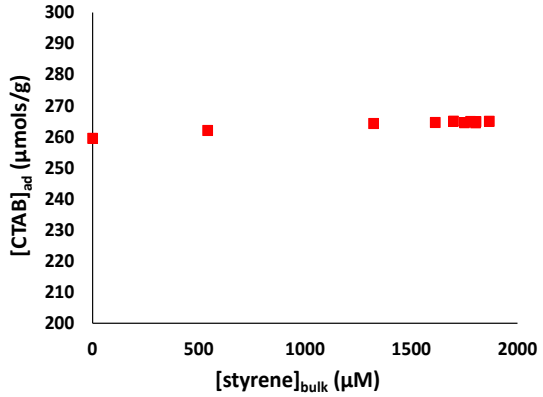

b)

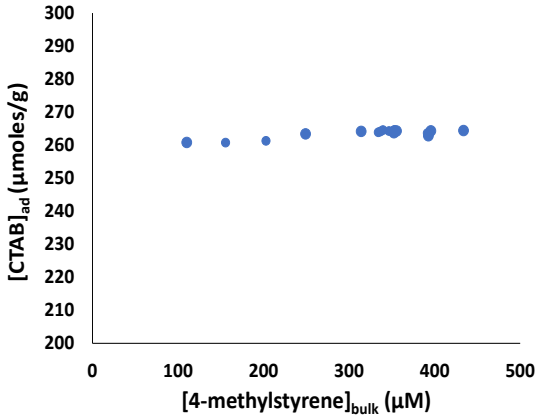

Figure A.3 Constant CTAB adsorption (260 umols of CTAB adsorbed per gram of Hi-Sil 233) with increasing amount of a) styrene and b) 4-methylstyrene.

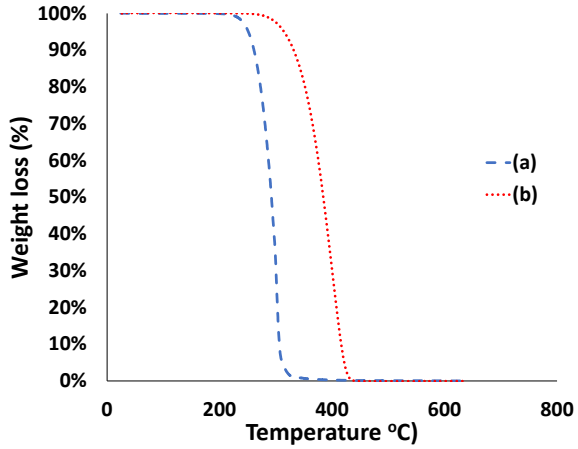

Figure A.4 TGA profile for (a) C_{16}TAB and (b) polystyrene standard (M_w 6 x 10^5 g/mol).

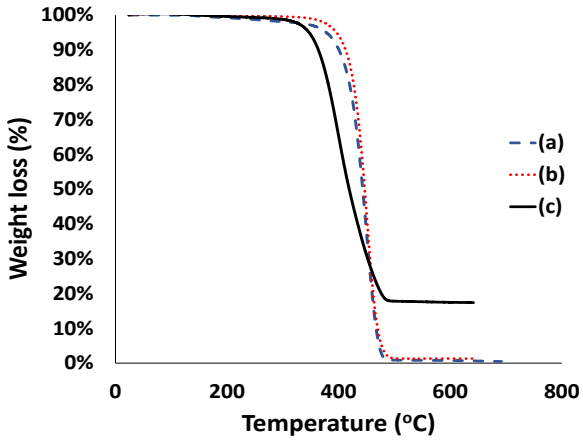

Figure A.5 TGA profile for extracted polymer (a) poly (4-methoxystyrene), (b) poly (4-methylstyrene) and (c) polystyrene.

Table A.1 Poly-4-methylstyrene weight loss of modified silica (in terms of apparent monomer conversion %) and weight-averaged molecular weight (M_w) of extracted polymer for deoxygenated and control admicellar polymerizations initiated by AIBN and V-501

M/I molar ratios	AIBN system				V-501 system			
	Deoxygenated		Control		Deoxygenated		Control	
	Apparent conversion (%)	M_w (g/mol)	Apparent conversion (%)	M_w (g/mol)	Apparent conversion (%)	M_w (g/mol)	Apparent conversion (%)	M_w (g/mol)
15	92 ± 9.5	$8.3x10^5$	90 ± 14	$8.7x10^5$	82 ± 18	$9.9x10^5$	97 ± 9.0	$7.9x10^5$
150	99 ± 1.9	$1.6x10^6$	64 ± 12	$1.4x10^6$	88 ± 11	$1.8x10^6$	58 ± 13	$1.6x10^6$
1000	84 ± 10	$2.0x10^6$	32 ± 4.1	$1.7x10^6$	68 ± 15	$1.8x10^6$	11 ± 1.4	NA

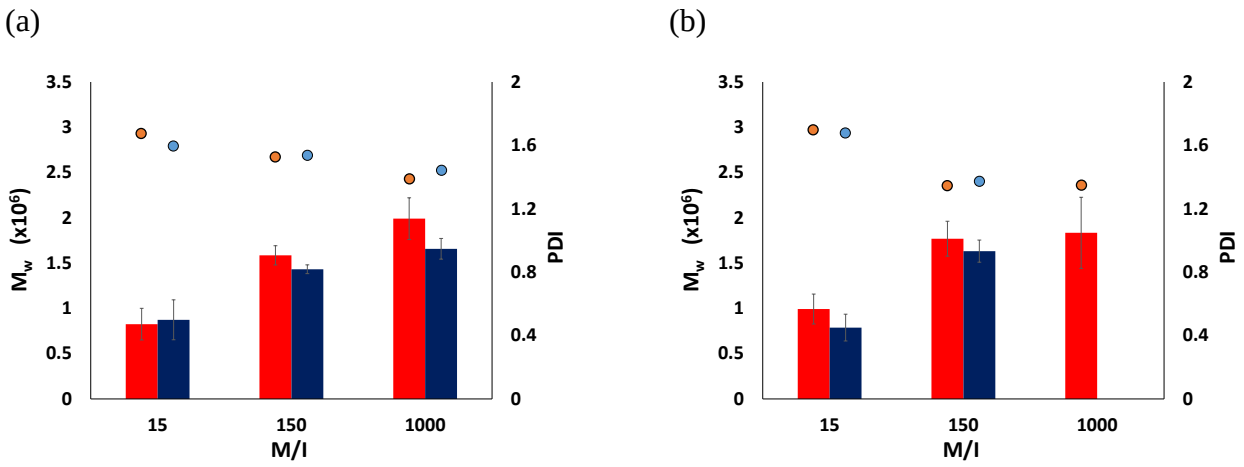

Figure A.6 Weight-averaged molecular weight (M_w) (left axis: ■ Deoxygenated ■ Control) and PDI (right-axis: ● Deoxygenated ● Control) of extracted poly-4-methylstyrene from modified silica in (a) AIBN- and (b) V-501-iniitiated deoxygenated and control admicellar polymerization at M//I values of 15, 150, and 1000.

a) b)

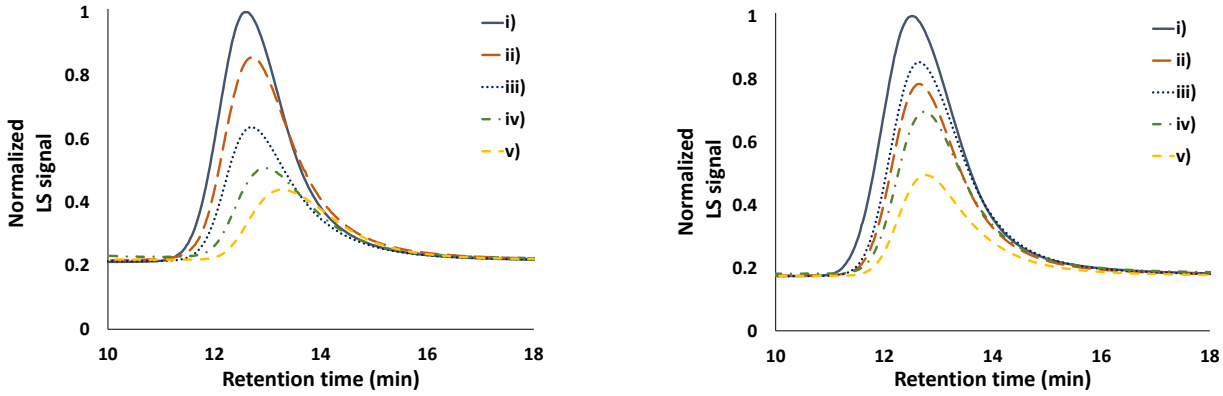

Figure A.7 GPC chromatogram of extracted polystyrene from modified silica in (a) AIBN- and (b) V-501-iniitiated admicellar polymerization at M//I values of i) 1000, deoxygenated ii) 150, deoxygenated iii) 150, control iv) 15, deoxygenated and v) 15, control.

APPENDIX B: SUPPORTING WORK

AFM of polystyrene film on mica via admicellar polymerization

B.1 Methods

Deionized water was filled into four 1 L volumetric flasks and two of the flask (2 x 1 L water) were purged with nitrogen gas for 30 mins. The purged water were used to make deoxygenated samples while another two (2 x 1 L water) were used to make control samples. 0.27 g of CTAB was added into each flask ([CTAB] ≈ 750 μM) and stirred under heat for 30 mins until dissolved. After cooling down CTAB solution, calculated amount of styrene and AIBN added into first flask. The feed concentration of styrene were calculated by taking styrene to adsorbed CTAB molar ratio of 2, assuming a complete adsorption of CTAB bilayers formed on mica disk. Mica disk was atomically smooth and the total surface area was calculated as $2\pi r(r+t)$ where r is the radius and t is the thickness of the disk. CTAB adsorbed was calculated with an area per head group of 91 $Å^2$ at air-water interfaces and styrene feed concentration of 21 nM. Due to low concentration styrene, a stock solution was made and further diluted. Firstly, solution A (1 L CTAB solution) was prepared with constant [styrene] ≈ 2126 μM and varying [AIBN] ≈ 2.1 μM, 14 μM or 142 μM to give M/I values of 1000, 150 and 15. The solution was left to stir for 1 hour. Solution A was further diluted with CTAB solution to obtain solution B with final constant [styrene] ≈ 21 nM with [AIBN] ≈ 0.021 nM, 0.14 nM and 1.4 nM to give M/I values of 1000, 150 and 15 respectively. Solution B were stirred for 30 mins. Next, solution B was poured into 40 mL vials containing mica sheet that was freshly cleaved and mounted to 12 mm metal pucks. These sample vials were left to equilibrate for an hour and later transferred into a water bath at 70 ^oC for 24 hours polymerization. After samples were cooled down, the polymerized mica disks were cleaned by dipping into deionized water for several times. Modified mica disks was then dried in the desiccator overnight and ready for AFM analysis.

Multimode AFM with Tapping Mode using 125 µm silicon tips and E-type scanners with maximum scan sizes of 10 µm (Bruker Corporation, Santa Barbara) were used. Images were analyzed with NanoScope Analysis software v1.5 to obtain the height and width data.

B.2 Preliminary results

AFM imaging of admicellar polymerized mica disks were shown in Figure B.1-B.6. Admicellar polymerization on mica sheet at the experimental condition resulting in formation of droplets with or without patches. Deoxygenated samples polymerized at constant styrene concentration and lowest initiator concentration at M/I 1000 formed droplets along with network-like patches (Figure B.1). According to the section and particle size distribution analysis, droplets have height of 2-3 nm and diameter of ~70 nm while the patches was ~6 nm height. This showed that adsolubilization of styrene and initiator in the admicelle was not distributed evenly. At very low initiator concentration, nucleation site for polymerization is believed to be limited. In previous study by See and O'Haver they explained that uneven adsolubilization can be caused by non-uniform admicelle adsorption.[I] Other than that, adsolubilization was influenced by the long-range van der Waals force between the mica substrate and polymer solution.[II,III] As a result, adsolubilized styrene is unstable and tends to coalesce forming droplets or patches. In addition, agglomeration may also take place during the drying process. Control sample at the same ratio M/I 1000 showed the formation of ultrathin patches with height of 0.7 nm (Figure B.2). Only small concentration of polymer was formed compared to the deoxygenated sample corresponds to the results reported in Chapter 4 which M/I 1000 control sample has a minimal monomer conversion.

[I] See, C. H.; O'Haver, J. *J. Appl. Polym. Sci.* **2003**, *89*, 36–46.
[II] Wyart, F. B.; Daillant, J. *Can. J. Phys.* **1990**, *68*, 1084–1088.
[III] Reiter, G. *Langmuir* **1993**, *9*, 1344–1351.

As the initiator concentration increases, deoxygenated samples at M/I 150 formed droplets on top of irregular patches or droplets (Figure B.3). A layer of patches or droplets with 2-3 nm thickness were formed on the surface. On top of that, droplets were formed with the diameter of ~100 nm and total height of ~9 nm. For M/I 150 control samples, smaller droplets with diameter of ~70 nm and height ranging from 2-3 nm were observed (Figure B.4). The larger droplets size was obtained in deoxygenated samples maybe the result of higher molecular weight polymer formation in deoxygenated samples as discussed in Chapter 4. In a previous study of admicellar polymerization formed polystyrene film on mica, See observed shrinking of polymer film but increasing film thickness as the reaction time increases.[IV] At constant monomer and initiator loading, polymer chain continues to grow and produce higher molecular weight polymer with increasing reaction time. In other word, increasing size of droplets or patches (higher diameter and height) corresponds to the formation of higher molecular weight polymer.

Further increase of initiator concentration in M/I 15 deoxygenated sample also showed increasing number of droplets (Figure B.5). Droplets measured to have diameter of ~70 nm and height of ~3 nm and patches with similar height were also observed. Meanwhile, control samples at M/I 15 showed formation of droplets with width of ~70 nm and height of ~2 nm (Figure B.6). Note that, topography of M/I 15 control sample was close to M/I 150 control sample but the latter has slightly higher thickness due to higher M_w polymer film formation (Chapter 4).

Preliminary data from this work showed us that adsolubilized styrene tends to form multilayer film and coalesce to form droplets/ patches upon admicellar polymerized on mica surface. More droplets tends to form as the initiator concentration increases may be due to increasing nucleation of polystyrene during the polymerization process. The larger the size of droplets and patches

[IV] See, C. H. Ph.D. Dissertation, *University of Mississppi*, **2004**.

(higher diameter and height) indicates the higher the molecular weight of the polymer formed. Deoxygenated admicellar polymerization produced slightly larger polymer droplets/ patches in agreement with the higher molecular weight polymer formation.

a)

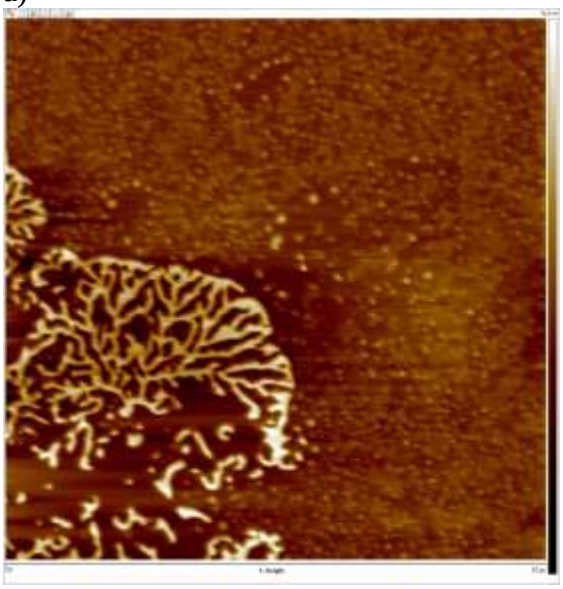

b)

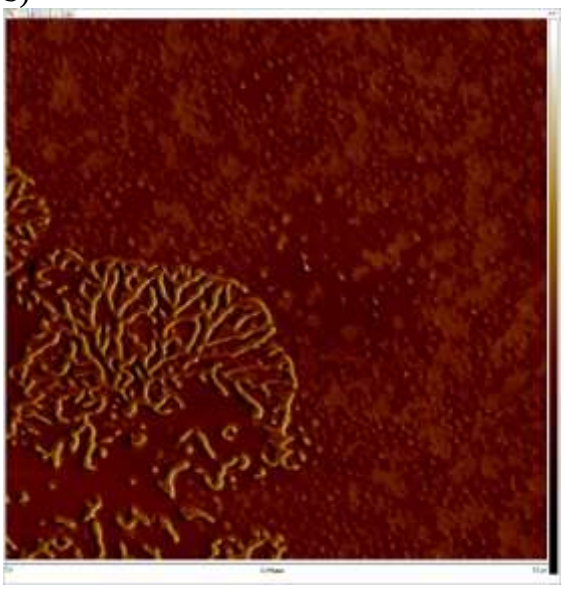

c)

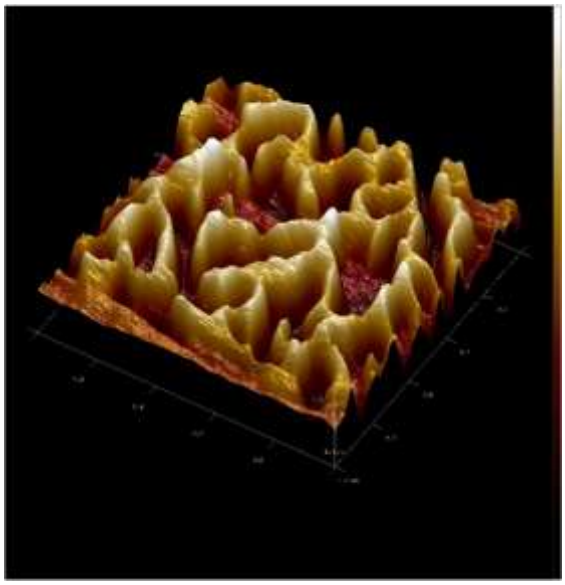

Figure B.1 Topography of polystyrene film of deoxygenated sample M/I of 1000, a) height image b) phase image with scan size 5μm x 5 μm, and c) 3D image with scan size 1 μm x 1 μm. All scaled up to z-range of 10 nm.

a)

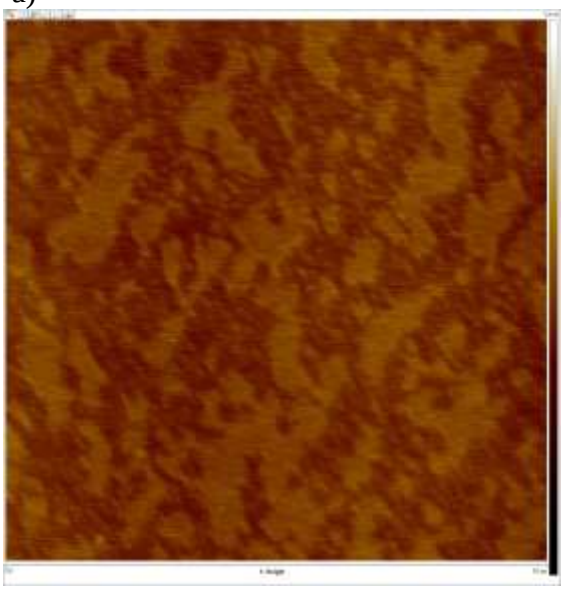

b)

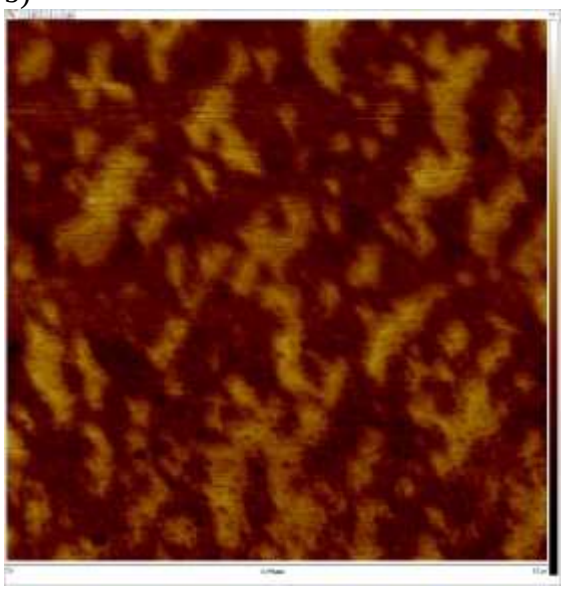

c)

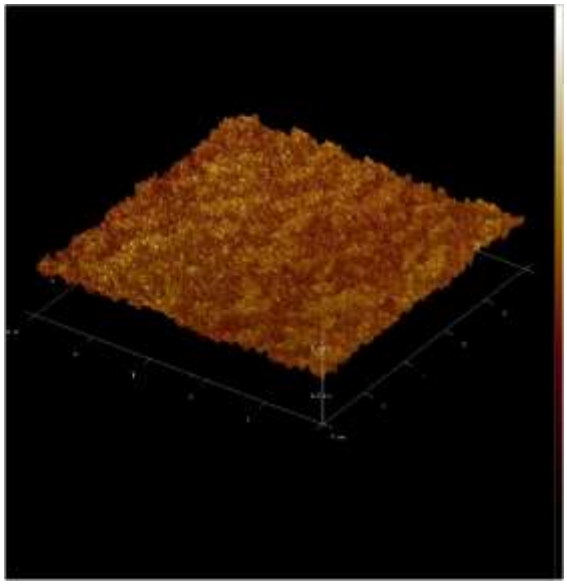

Figure B.2 Topography of polystyrene film of control sample M/I of 1000, a) height image b) phase image and c) 3D image with scan size 5µm x 5 µm. All scaled up to z-range of 5 nm.

a)

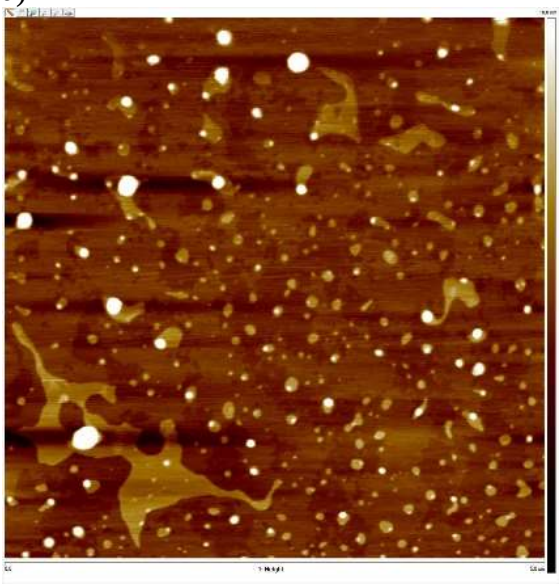

b)

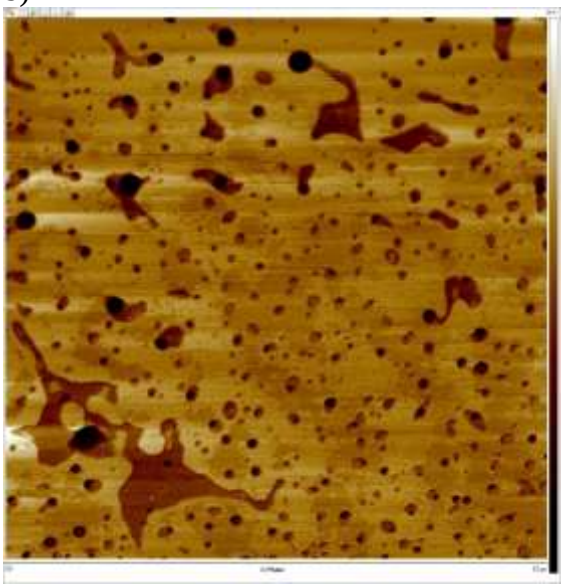

c)

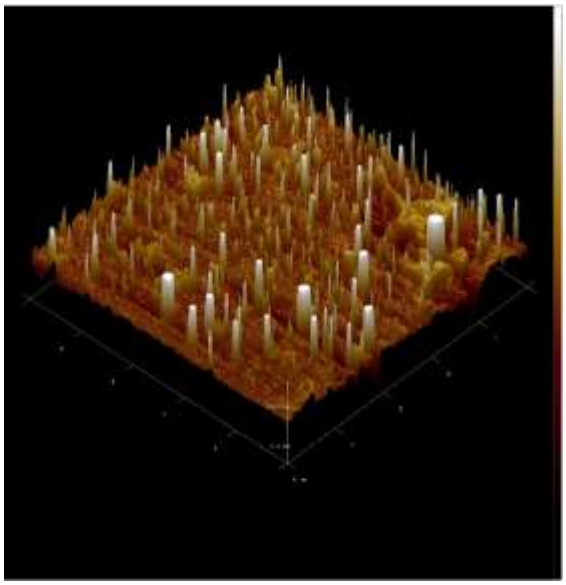

Figure B.3 Topography of polystyrene film of deoxygenated sample M/I of 150, a) height image b) phase image and c) 3D image with scan size 5µm x 5 µm. All scaled up to z-range of 5 nm.

a)

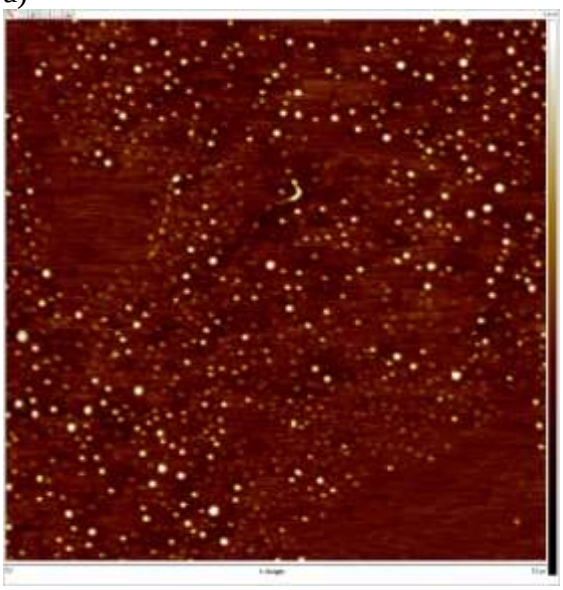

b)

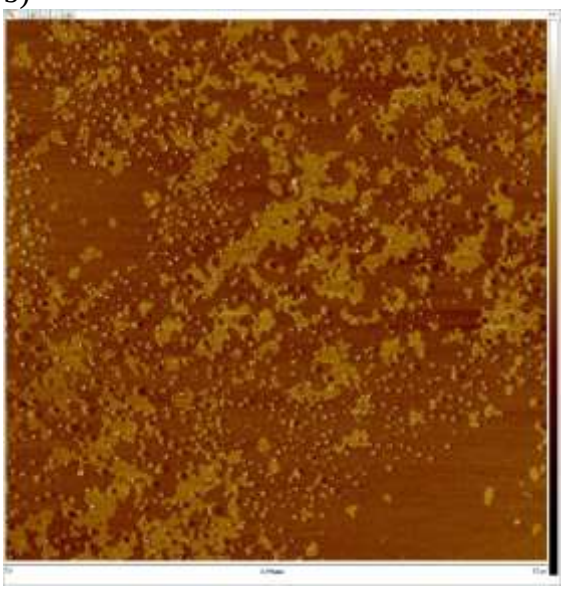

c)

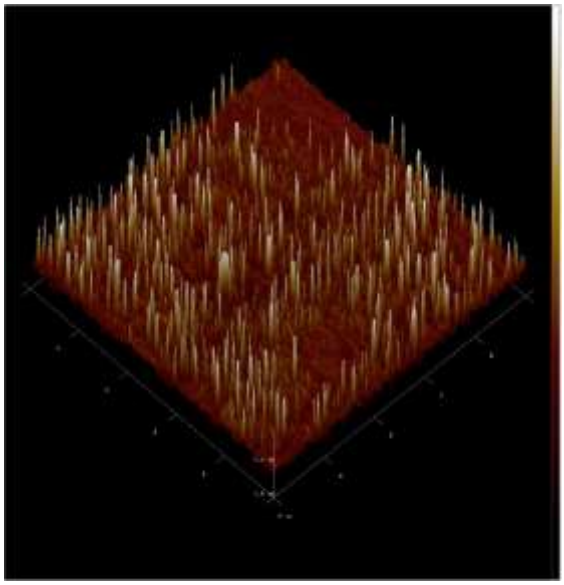

Figure B.4 Topography of polystyrene film of control sample M/I of 150, a) height image b) phase image and c) 3D image with scan size 5µm x 5 µm. All scaled up to z-range of 5 nm.

a)

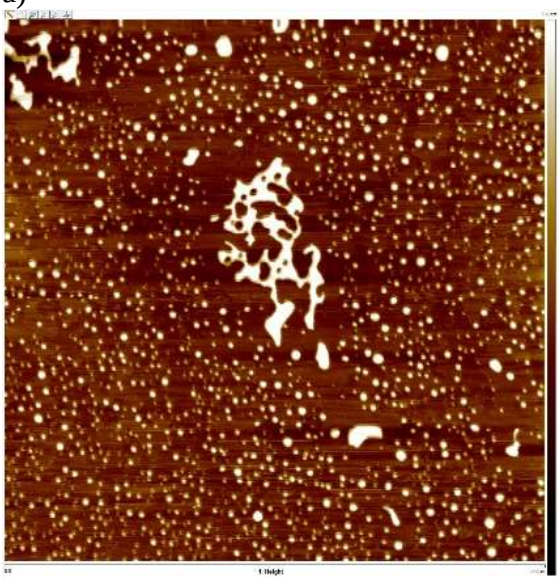

b)

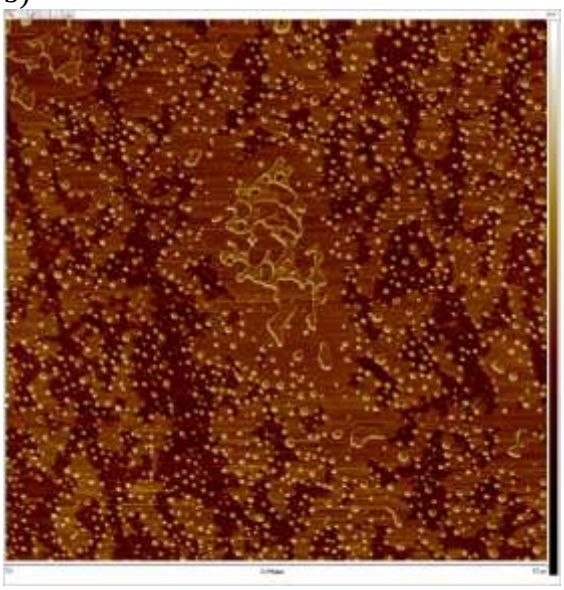

c)

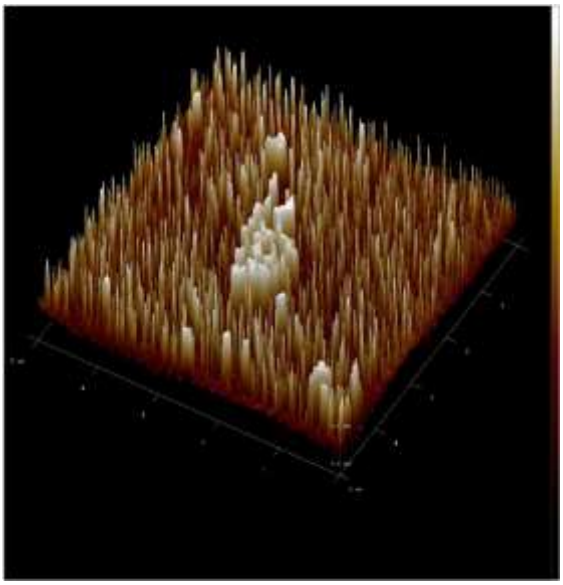

Figure B.5 Topography of polystyrene film of deoxygenated sample M/I of 15, a) 2D image b) 3D image. Scan size 5µm x 5 µm, z-range 5 nm.

a)

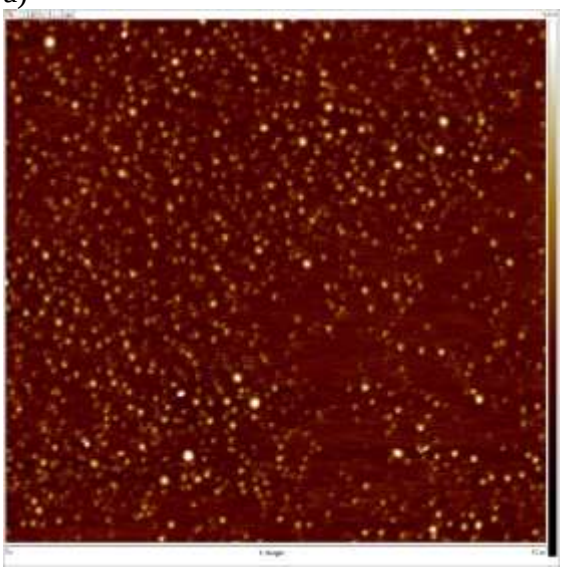

b)

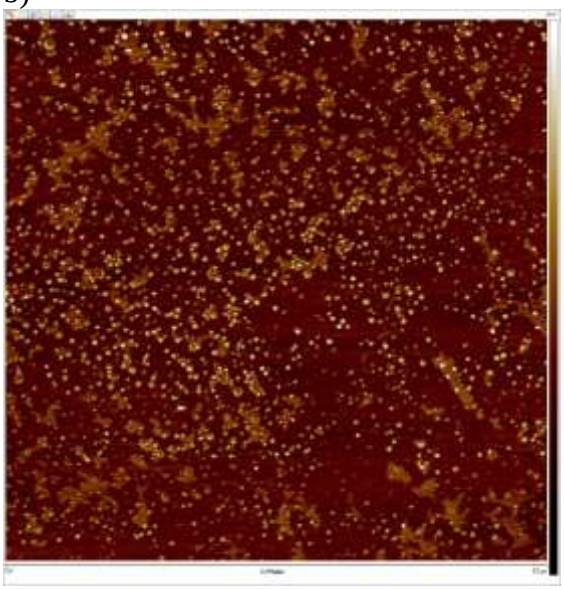

c)

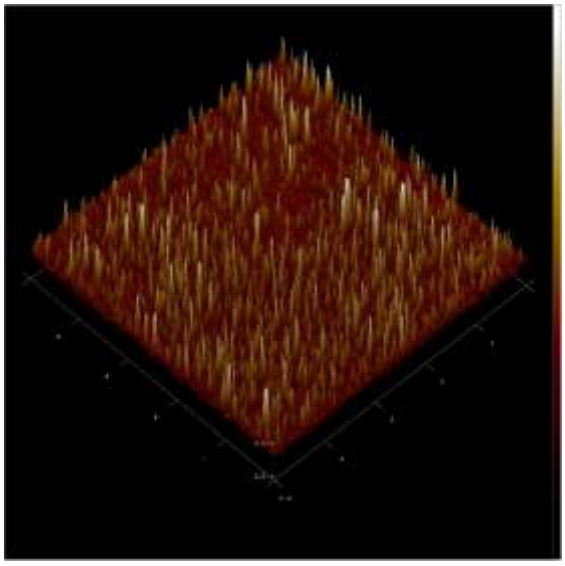

Figure B.6 Topography of polystyrene film of control sample M/I of 15, a) 2D image b) 3D image. Scan size 5µm x 5 µm, z-range 5 nm.

B.3 Challenges

Inconsistent and unreproducible results were among the challenges for this work. Polymer film consists of a distribution of different polymer chain length, randomly distributed on the surface were difficult to 'spot'. Based on the additive van der Waals model considering the interaction between the silica and air/water interface, polymer layer has to be more than 4 nm thick in order to remain stable.[I] More in-situ investigation is needed to better understanding the mechanism of the film formation.

VITA

POHLEE CHEAH

163 Garden Terrace Dr. Oxford, MS 38655 Cell: (662) 801-3206 Email: pohlee.ch@gmail.com

EDUCATION

***Ph.D Chemical Engineering*, The University of Mississippi CGPA 3.77 August 2016**

Dissertation, *"Investigation of Parameters Enabling Admicellar Reversible Addition-Fragmentation Chain Transfer (RAFT) Polymerization"*
Post Graduate Certificate, *"Hands-On Course in Tablet Technology"*

***M.S Chemical Engineering*, The University of Mississippi CGPA 3.85 August 2012**

Thesis, *"Surface Modification of Calcium Carbonate for Application in Oil-Based Drilling Mud"*

***B.S Analytical Chemistry*, University Science Malaysia CGPA 3.46 June 2008**

Thesis, *"Synthesis and Thermal Analyses of Epoxidized Natural Rubber-50/ Cyclopentylsilsesquioxanes Blends with Iodine Filler"*

WORK EXPERIENCE

Graduate Research and Teaching Assistant, *The University of Mississippi* 2009- 2016

- Design, plan and conduct research studies especially in surfactant-related projects
- Perform various analytical testing in research studies
- Prepare standard documentation for standard operating procedures
- Train and guide undergraduate research assistants

Research Officer, *BCI Chemical Corporation Sdn. Bhd.* 2008-2009, May-August 2011

- Supported research & development of new products as well as improved the existing product formulation for laundry & detergent and oil & gas specialty chemicals
- Trained with laboratory instruments and equipments focusing on oil drilling mud testing
- Conducted testing and evaluation using ASTM and API standard protocols for QC/QA
- Prepared standard documentation such as MSDS and COA

Trainee Chemist, *ALS Technichem (M) Sdn. Bhd.* May-July 2007

- Conducted analytical testing on food substance, water quality, blood & urine
- Explored the standard laboratory techniques
- Learned to report and documentation of analytical data
- Committed to professional code of conduct working in laboratory

AREA OF STRENGTH

Instrumentation:

- Surface Characterization: Atomic Force Microscopy (Tapping Mode, Contact Mode, Fluid Cell AFM), Scanning Electron Microscopy (SEM), Tensiometer
- Thermal Analyses: TGA, DSC
- Chromatography: Gel Permeation Chromatography (GPC), HPLC, GC
- Analytical: UV-VIS, TOC/TN, FTIR
- Drilling Fluids Testing Equipment: HTHP Filter Press, viscometer, hydrometer etc.

Packages/Tools: Aspen Plus, Aspen HYSYS, Aspen HTFS, Mathcad, Mathlab, C++, Microsoft Office Suite

Languages: Proficient in reading, speaking, and writing English, Chinese and Malay

RESEARCH EXPERIENCE

Investigation of Parameters Enabling Admicellar Reversible Addition-Fragmentation Chain Transfer (RAFT) Polymerization

- Formulation development for surface modification (polymer thin-film formation) via admicellar free-radical polymerization and demonstrated the first admicellar reversible addition fragmentation chain transfer (RAFT) polymerization to open a way to make advanced thin films via controlled radical polymerization technique
- Investigated the effect of oxygen on the reaction kinetics and the properties of the polymer formed with good design experiment and execution
- Addressed the reason behind the usage of tremendous high initiator concentration in traditional free-radical as compared to RAFT admicellar polymerization RAFT
- AFM studies on the polymer film formed on the surface
- Preformulation studies of the surface chemistry: cationic surfactant adsorption and organic solute adsolubilization at silica interface

Review on Adsolubilization and Admicellar Polymerization

- Addressed the important aspects in adsolubilization and admicellar polymerization studies over the years including the different substrate, surfactant/ co-surfactant, solute, solution properties, area of applications and different analytical testing

Surface Modification of Calcium Carbonate by Admicellar Polymerization for Application in Oil-based Drilling Mud

- Formulation development for surface modification (polymer thin-film formation) via free radical admicellar polymerization
- Preformulation studies of the surface chemistry: anionic surfactant adsorption and organic solute adsolubilization at calcium carbonate interface
- Studied the phase behavior of calcium ion with anionic surfactant at different temperature and experimental determined the solubility product constant K_{sp} of the cation-anionic micelle complex
- Studied the performance of the weighting agent (modified calcium carbonate) in drilling mud formulation

Synthesis and Thermal Analyses of Epoxidized Natural Rubber-50/cyclopentyl-silsesquioxanes blends with iodine filler

- Studied the effect of iodine filler incorporation in epoxidized natural rubber (ENR-50) composite blends via solvent casting technique
- Proposed a reaction mechanism for the polymer, oxidant and the inorganic filler

CONFERENCES

- 5th University of Mississippi Graduate Research Forum 2015, Oxford MS, Poster Session: ***"Deoxygenated Admicellar Polymerization"***
- 14th AIChE Annual Meeting 2014, Atlanta GA, Technical Session: Nanostructured Polymer Films, ***"Effect of Oxygen on Admicellar Polymerization"***
- 14th AIChE Annual Meeting 2014, Atlanta GA, Technical Session: Polymer Thin Films and Interfaces, ***"Formation of Ultrathin Polystyrene Films by Admicellar RAFT Polymerization"***
- 245th ACS National Meeting 2013, New Orleans LA, Poster Session: Colloid & Surface Chemistry, ***"Effect of Oxygen on Admicellar Polymerization of Silica in Forming Polystyrene Thin Film"***

PUBLICATIONS

- P. Cheah, J. H. O'Haver, A.E. Smith, "Effect of Oxygen on Admicellar Polymerization of Styrene on Silica Surfaces" – *Submitted to Journal of Polymer Science, Part A: Polymer Chemistry, 2015*
- P. Cheah, A.E. Smith, J. H. O'Haver, "Review on Adsolubilization Studies" – *Under review*